REAL-TIME EPILEPSY SEIZURE DETECTION AND BRAIN CONNECTIVITY ANALYSIS USING ELECTROENCEPHALOGRAM

A Thesis submitted by

Mingkan Shen

For the award of

Doctor of Philosophy

2023

ABSTRACT

This thesis integrates signal processing techniques, functional brain connectivity analysis, and artificial intelligence methods to address the challenges of real-time epilepsy seizure detection and provide insights into complex brain disorders, such as alcoholism and schizophrenia (ScZ). By leveraging electroencephalogram (EEG) data and advanced analysis methods, the research aims to achieve high accuracy detection and identification of biomarkers for these conditions. The real-time epilepsy seizure detection involves three main steps: pre-processing, feature extraction, and machine learning (ML) or deep learning (DL) models for classification and detection. Various signal processing methods, such as discrete wavelet transform, tunable-Q wavelet transform, and short-time Fourier transform, are applied in the pre-processing stage to decompose the EEG signals into time domain, frequency domain, and time-frequency domain data. Feature extraction techniques, such as statistical moments, entropy algorithms, and power spectrum analysis, are used to detect the sharp waves indicative of seizure activity. ML and DL models, such as support vector machines and convolutional neural networks (CNN), are employed to address the robustness challenges and provide high accuracy classification results for seizure detection. The EEG brain connectivity analysis focus on the correlations between different EEG channel signals within the complex brain network. Alcoholism and ScZ datasets are utilized in three experiments. The signal processing methods include continuous wavelet transform and multivariate autoregressive models to extract relevant features from the EEG signals. Functional brain connectivity is then calculated using mutual information and coherence algorithms. DL models, particularly CNN, are employed to classify patients and healthy control subjects based on the calculated functional connectivity. Furthermore, statistical analysis of the entire brain connectivity is conducted to identify biomarkers of abnormal connectivity patterns associated with complex brain disorders.

CERTIFICATION OF THESIS

I Mingkan Shen declare that the PhD Thesis entitled *'Real-time epilepsy seizure detection and brain connectivity analysis using electroencephalogram'* is not more than 100,000 words in length including quotes and exclusive of tables, figures, appendices, bibliography, references, and footnotes.

This Thesis is the work of Mingkan Shen except where otherwise acknowledged, with the main of the contribution to the papers presented as a Thesis by Publication undertaken by the student. The work is original and has not previously been submitted for any other award, except where acknowledged.

Date: 16/6/2023

Endorsed by:

Professor Paul (Peng) Wen

Principal Supervisor

Dr Bo Song

Associate Supervisor

Professor Yan Li

Associate Supervisor

Student and supervisors' signatures of endorsement are held at the University.

STATEMENT OF CONTRIBUTION

Mingkan Shen makes the majority contributions to the research and each of these papers

Paper 1:

[1] **Shen Mingkan**, Wen Peng, Song Bo and Li Yan, *"An EEG based real-time epilepsy seizure detection approach using discrete wavelet transform and machine learning methods."* Biomedical Signal Processing and Control, 2022. **77**: p. 103820. https://doi.org/10.1016/j.bspc.2022.103820.

Mingkan Shen contributed 90% to this paper.

Corresponding author: Mingkan Shen

Paper 2:

[2] **Shen Mingkan**, Wen Peng, Song Bo and Li Yan, "*Real-time epilepsy seizure detection based on EEG using tunable-Q wavelet transform and convolutional neural network."* Biomedical Signal Processing and Control, 2023. **82**: p. 104566. https://doi.org/10.1016/j.bspc.2022.104566.

Mingkan Shen contributed 90% to this paper.

Corresponding author: Mingkan Shen

Paper 3:

Shen Mingkan, Yang Fuwen, Wen Peng, Song Bo and Li Yan, "*A Real-time Epilepsy Seizure Detection Approach based on EEG using Short-time Fourier Transform and Google-Net Convolutional Neural Network.*" submitted to Heliyon, June 2023.

Mingkan Shen contributed 90% to this paper.

Corresponding author: Mingkan Shen

Paper 4:

[3] **Shen Mingkan**, Wen Peng, Song Bo and Li Yan, "*Detection of alcoholic EEG signals based on whole brain connectivity and convolution neural networks."* Biomedical Signal Processing and Control, 2023. **79**: p. 104242. https://doi.org/10.1016/j.bspc.2022.104242

Mingkan Shen contributed 90% to this paper.

Corresponding author: Mingkan Shen

Paper 5:

[4] **Shen Mingkan**, Wen Peng, Song Bo and Li Yan, 2023. *"Automatic identification of schizophrenia based on EEG signals using dynamic functional connectivity analysis and 3D convolutional neural network"* Computers in Biology and Medicine, 2023: p. 107022.

https://doi.org/10.1016/j.compbiomed.2023.107022

Mingkan Shen contributed 90% to this paper.

Corresponding author: Mingkan Shen

Paper 6:

Shen Mingkan, Wen Peng, Song Bo and Li Yan, 2023. "*3D convolutional neural network for identifying schizophrenia using as EEG-based brain network*" submitted to Biomedical Signal Processing and Control, May 2023.

Mingkan Shen contributed 90% to this paper.

Corresponding author: Mingkan Shen

ACKNOWLEDGEMENTS

TABLE OF CONTENTS

LIST OF TABLES

LIST OF FIGURES

ABBREVIATIONS

AVH	Auditory verbal hallucinations
CNN	Convolutional neural network
CMI	Cross mutual information
CWT	Continuous wavelet transform
DL	Deep learning
DMN	Default mode network
DT	Decision tree
DWT	Discrete wavelet transform
EEG	Electroencephalogram
EMD	Empirical mode decomposition
FT	Fourier transform
FP	False positive
HC	Health control
k-NN	k-Nearest neighbours
LMSU	Lomonosov Moscow State University
LSTM	Long short-term memory
MI	Mutual information
ML	Machine learning
MVAR	Multivariate autoregressive
PLI	Phase lag index
PLV	Phase locking value
RNN	Recurrent neural network
ROI	Region of interest
ScZ	Schizophrenia
STFT	Short time Fourier transform
SVM	Support vector machine
TQWT	Tunable-Q wavelet transform
WHO	World Health Organization
WST	Wavelet scattering transform

CHAPTER 1: INTRODUCTION

1.1. Research background and questions

Electroencephalography (EEG) research plays a significant role in understanding brain diseases and disorders. By measuring and analysing the electrical activity of the brain, EEG provides valuable insights into the underlying mechanisms and abnormalities associated with various brain conditions.

EEG has been extensively used in epilepsy research. It helps in the diagnosis and classification of epileptic seizures, as well as in localizing the epileptic focus. Long-term EEG monitoring can provide valuable information about seizure frequency, duration, and patterns, assisting in treatment planning and assessing the effectiveness of anti-epileptic medications [5].

Additionally, EEG research has provided insights into the neural abnormalities associated with complex brain disorders through functional brain network. Studies have identified specific EEG patterns, such as reduced specific frequency band activity with alcoholism and schizophrenia (ScZ) diseases. EEG can help in early detection, differential diagnosis, monitoring treatment response, and studying the impact of medications and therapeutic interventions in alcoholism and ScZ [6,7].

1.1.1. EEG background

EEG birthed by Hans Berger's pioneering work in the early 20th century, stands as an instrumental non-invasive neuroimaging tool to detect electrical patterns resultant from the brain's intricate neuronal activities [8]. Within its vast spectrum of brain activity classifications, EEG segregates waves into delta, theta, alpha, beta, and gamma bands [9]. EEG frequency bands provide insights into various cognitive and physiological states. Delta (1-4 Hz) bands are most prominent in deep sleep and may indicate brain injury during wakefulness. Theta (4-8 Hz) is associated with reduced alertness, introspection, and memory processes. Alpha (8-12 Hz) represents a relaxed, alert state and its modulation is used in biofeedback relaxation techniques. Beta (12-30 Hz) manifests during analytical thinking and heightened alertness, with excessive activity potentially indicating anxiety. Gamma (30-100 Hz), the least understood, is linked to high-level cognitive functions, including perception and consciousness, with disruptions suggesting conditions like ScZ [10]. Beyond its foundational role in epilepsy and brain connectivity research, EEG finds robust

application in sleep studies, cognitive neuroscience, brain-computer interfaces, and neurofeedback, offering insights into brain function and pathologies [11]. While EEG boasts of high temporal resolution, affordability, and accessibility, it faces challenges in spatial resolution and is often susceptible to artifacts from external and biological sources [12]. Despite these limitations, the real-time data acquisition capabilities of EEG have solidified its standing in both clinical and research settings.

1.1.2. Real-time EEG seizure detection

Epilepsy is a chronic noncommunicable brain disorder characterized by sudden abnormal synchronous activity of brain neurons [13,14]. According to a report by the World Health Organization (WHO) in 2022, approximately 50 million people worldwide are affected by epilepsy [15]. Individuals with epilepsy experience recurrent seizures, which manifest as involuntary jerks in one part of the body or the entire body [16]. To enhance the effectiveness of epilepsy treatment, the EEG technique is employed to detect the onset of seizures which can detect nerve discharges with a high time resolution at the millisecond level.

This research aims to develop a novel method for automatic identification and clinical application of EEG-based epilepsy signal detection. The study comprises four main components: EEG data collection, signal processing, feature extraction, and classification work. Figure 1.1 shows the framework for EEG seizure detection, highlighting the various stages involved.
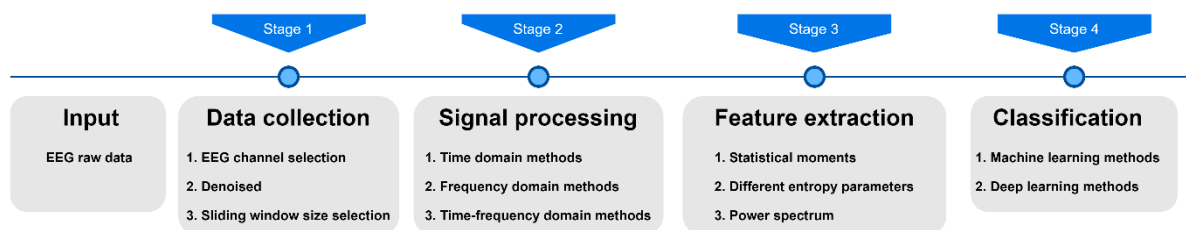
Figure 1.1: The framework of EEG seizure onset detection

In the data collection stage, EEG channel selection is performed with the objective of reducing computational costs. Since the location of epilepsy disorder in each patient may be uncertain, seizure detection faces robustness challenges. As a result, the selection of EEG channels also impacts the final detection results. Signal denoising is another important objective, aiming to eliminate noise and artifacts from the raw EEG signal. To enable real-time application, a sliding window technique is employed, and the choice of window size directly influences the performance. If the

calculation time exceeds the overlapping time, the method cannot be used in real-time clinical applications. Additionally, when detecting EEG seizure onset, the delay must be considered. A large sliding window input may lead to a significant delay, rendering the detection meaningless.

The abnormalities in EEG seizure signals are primarily observed in sharp and spike waves [17]. Analysing the signal in specific frequency bands using different signal processing methods is crucial for detecting these sharp and spike waves. Therefore, many signal processing methods are employed to extract features from time domain, frequency domain, and time-frequency domain techniques.

The feature extraction stage involves calculating the eigenvalues of the EEG features obtained through signal processing methods. This process helps reduce computational costs by transforming the decomposed signal into several eigenvalues. The eigenvalues mainly focus on statistical moments, various entropy parameters, and spectral power density, which describe the degree of oscillation in sharp and spike waves. The spectral power, representing the power density in specific frequency bands, can also be utilized in this process to capture the characteristics of sharp and spike waves.

In the classification work, artificial intelligence methods, particularly machine learning (ML) and deep learning (DL) models, play a significant role compared to traditional methods like linear discriminant method, distance discriminant method, and Bayesian classifier method. ML and DL models offer high accuracy in classifying seizure-free and seizure-active data in this research.

1.1.3. EEG brain connectivity analysis

In current research, there is significant emphasis on understanding the interaction between different brain regions to comprehend cognitive functions. By integrating the brain as a whole and conducting in-depth explorations in brain science, researchers aim to address the limitations of functional localization and gain a more comprehensive understanding of brain function [18,19]. While different areas of the human brain may have distinct functions, even a simple task requires multiple functional areas to interact and coordinate with each other, forming a network to carry out the task [20]. The functionality of brain relies on extensive interaction between multiple brain regions, highlighting the importance of interconnectedness in performing various cognitive processes.

In the analysis of complex brain networks, the region of interest (ROI) within the brain is considered as a node, and the connectivity between these nodes is represented as an edge [21]. The functional brain connectivity analysis in this thesis is centred around detecting complex brain disorders and identifying biomarkers for these diseases. Figure 1.2 illustrates the five main components or stages of the functional brain connectivity study.
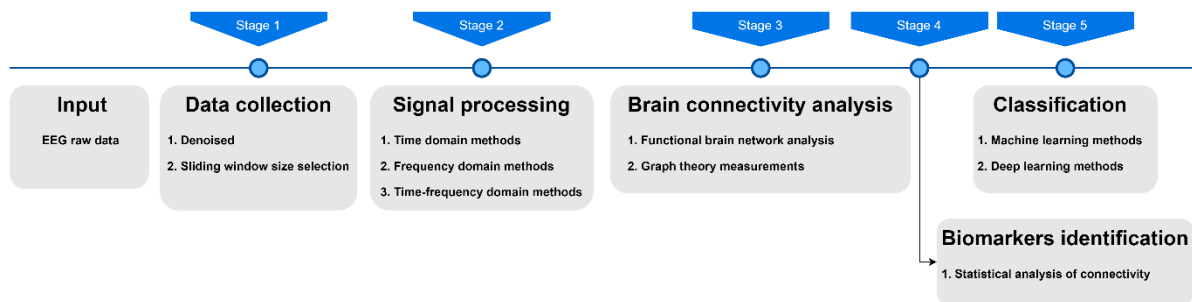
Figure 1.2: The framework of EEG brain connectivity analysis of complex brain disorders

In this study, two public EEG databases are employed for evaluation: the Archive UCI KDD database for alcoholism and the Lomonosov Moscow State University (LMSU) database for schizophrenia (ScZ). These data were collected utilizing the entire channel data to detect the functional connectivity of the entire ROI in the brain. The Butterworth algorithm's band-pass filter is applied to eliminate noise and artifacts from the raw EEG signal. To capture the dynamic changes in ScZ diseases, a sliding window technique is employed to address the time-varying nature of the functional brain network and improve research accuracy.

Signal processing methods, including time domain, frequency domain, and time-frequency domain analyses, are implemented for EEG alcoholism and EEG ScZ signals. The objective is to identify significant brain rhythms associated with the respective diseases, reducing computational costs, and enhancing detection accuracy.

Functional brain connectivity focuses on the correlations between different ROIs in the complex brain network. In EEG analysis, ROIs correspond to EEG channels. There are two main approaches to detect the connectivity matrix in functional brain network analysis. The first approach treats the connectivity matrix as a brain graph and utilizes ML or DL methods for classification. The second approach employs graph theory measurements to assess the connectivity characteristics and abilities of matrix.

To identify biomarkers for the diseases, statistical analysis of the entire brain connectivity is conducted to identify abnormal connectivity areas between patients and healthy control subjects. These biomarkers can be cross verified with medical discoveries. For example, the default mode network (DMN) may exhibit significant changes in resting-state brain activity in complex brain disorders [22].

Given the exceptional performance of ML and DL in image classification tasks, these methods are also proposed for classifying the brain graph in this study. Convolutional neural network (CNN) demonstrates high accuracy in alcoholism and ScZ detection. Additionally, ML techniques can achieve high accuracy in classifying graph theory measurements.

1.1.4. Research objectives

This research is to develop new methods to detect the EEG seizure onset in clinical detection and detect EEG complex brain disorders through brain connectivity analysis. Five objectives shown below are the focuses:

- Develop the signal processing method to extract the sharp and spike waves from epilepsy seizure EEG signal.
- Apply the ML and DL methods to classify the seizure active and seizure free EEG signals.
- Improve EEG based seizure detection performance in accuracy, sensitivity, false positive (FP) rate and delay.
- Develop and apply the brain connectivity algorithms for alcoholic and ScZ EEG signal detection.
- Provide a biomarker for alcoholic and ScZ disease, and improve detection performance in accuracy, sensitivity, and specificity.

1.2. Contributions

This thesis contains six research papers, three of them focus on the real-time EEG seizure detection and another three focus on the EEG brain connectivity analysis. The relationship between research questions, research objectives and contributions of each paper is shown in Figure 1.3 and 1.4.
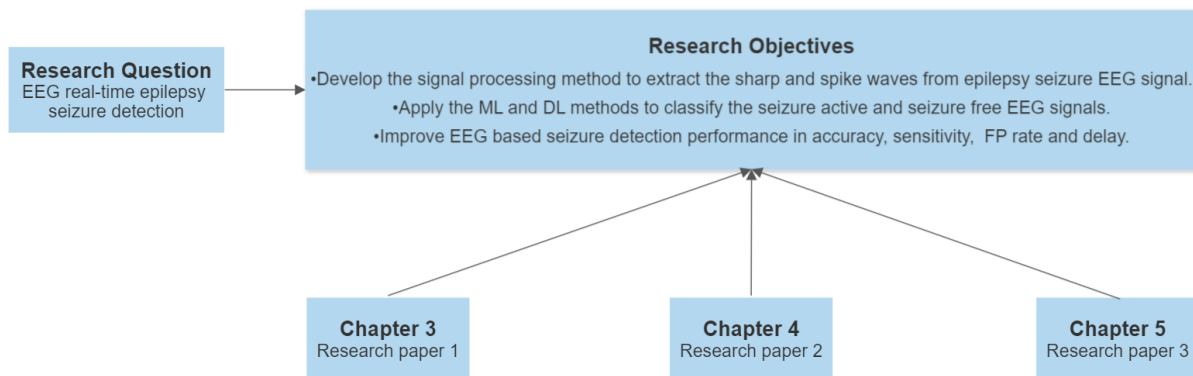
Figure 1.3: The relationship of research in EEG real-time epilepsy seizure detection
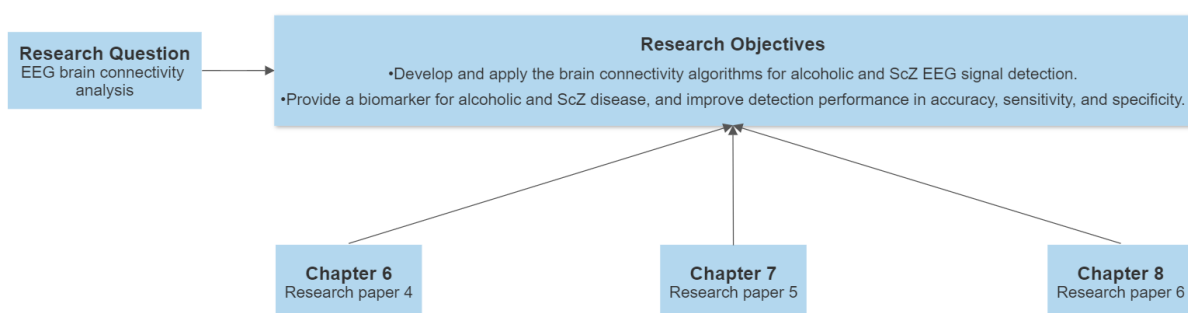
Figure 1.4: The relationship of research in EEG brain connectivity analysis

The major contributions of each paper were summarised as follow:

Paper 1: "An EEG based real-time epilepsy seizure detection approach using discrete Wavelet transform and machine learning methods".

- DB4- Discrete wavelet transform (DWT) and DB16-DWT are proposed to extract sharp and spike waves of signals and remove redundant information.

- Improve the robustness of EEG based epilepsy detection via ML methods.

- Propose a method that achieves 97% in accuracy and 96.67% in sensitivity in 3-class classification between healthy control (HC), seizure free and seizure active using Database UB, and 96.38% accuracy, 96.15% sensitivity and 3.24% false positive rate in the real-time seizure detection using Database CHB-MIT.

- Implement an automatic seizure detection approach in real-time way.

Paper 2: "Real-time Epilepsy Seizure Detection based on EEG using Tunable-Q Wavelet Transform and Convolutional Neural Network".

- Propose tunable-Q wavelet transform (TQWT) method to extract sharp and spike waves of signal and remove redundant information.
- Improve the robustness of EEG based epilepsy detection using the DL method with CNN model.
- Combine signal processing method and image classification in this experiment.
- Conduct an automatic real-time seizure detection implementation.
- Obtain excellent performance of 97.57% in accuracy, 98.90% in sensitivity, 2.10% in false positive rate and 10.46-seconds in time delay in the real-time seizure detection evaluation.

Paper 3: "A Real-time Epilepsy Seizure Detection Approach based on EEG using Short-time Fourier Transform and Google-Net Convolutional Neural Network".

- Short time Fourier transform (STFT) method is proposed to extract sharp and spike waves of the signal and remove redundant information.
- Google-Net CNN model is applied to classify the seizure-active and seizure-free EEG data and overcome the robustness problem of EEG research.
- The proposed real-time seizure detection method achieves 97.74% accuracy, 98.90% sensitivity, 1.94% false positive rate, and 9.85-second delay through STFT spectrum in CHB-MIT Database.
- The proposed method is suitable for real-time seizure detection in clinic application, the processing time is just 0.02 seconds for every 2-second EEG episode in this study.

Paper 4: "Detection of alcoholic EEG signals based on whole brain connectivity and convolution neural networks".

- A DL model enabled whole brain connectivity analysis method is applied to detect alcoholic EEG signal.
- A framework of a 3D-CNN and image classification method are developed and applied to detect EEG signal and get an accuracy of

96.25 ± 3.11% using leaving-one out training method for all the testing subjects.

- Brain rhythms factor is taken into consideration in detecting the alcoholic EEG, and the gamma band (30 – 40 Hz) is found to be the most significant rhythm.

- The results show that the Cross mutual information (CMI) adjacent connectivity between the left parietal part, the left frontal part, the right temporal part, the right frontal part and the right parietal part are found to be the fuzzy locations in determining alcoholism.

Paper 5: "Automatic identification of schizophrenia based on EEG signals using dynamic functional connectivity analysis and 3D convolutional neural network".

- The time-frequency domain functional connectivity calculated by continuous wavelet transform (CWT) and CMI is firstly used in ScZ identification, and the frequency resolution is selected in 1 Hz in this experiment.

- Sliding window technique is proposed to extend the functional connectivity to time-varying functional connectivity for exploring dynamic properties of resting-state function connectivity in EEG.

- The graph theory measures of complex brain network analysis are used to select brain rhythms and the alpha band (8-12 Hz) is found to be the significance frequency band for ScZ identification.

- The 3D-CNN models are applied to classify the ScZ subjects and HC subjects and achieved a result of 97.74 ± 1.15% accuracy, 96.91 ± 2.76% sensitivity, and 98.53 ± 1.97% specificity.

- Furthermore, the CMI values show that not only the DMN region but also the connectivity between temporal lobe and posterior temporal lobe in both right and left side has significant difference between the ScZ and HC subjects.

Paper 6: "3D convolutional neural network for identifying schizophrenia using as EEG-based brain network".

- Functional brain network calculated using multivariate autoregressive (MVAR) model and coherence algorithm is applied in ScZ detection.
- Sliding window technique is employed in this study to capture the dynamic changes of ScZ resting data.
- Brain rhythm analysis shows that the alpha band (8-12 Hz) data plays a significant role in ScZ detection.
- The self-designed 3D-CNN models achieve the $98.47 \pm 1.47\%$ accuracy, $99.26 \pm 1.07\%$ sensitivity, and $97.23 \pm 3.76\%$ specificity results of ScZ detection.
- The ScZ biomarkers of abnormal connectivity of DMN regions and temporal lobe and posterior temporal lobe in both right and left side are provided in this study.

1.3. Thesis organisation

The real-time EEG seizure detection and EEG brain connectivity analysis are the focus of this thesis, which consists of nine chapters.

Chapter 1 introduces the research background and research problems of the thesis including the EEG seizure detection, EEG brain connectivity analysis and research objectives. The contributions and the thesis organisation also presented in this chapter.

Chapter 2 provides the background and literature review of the previous works. It contains the signal processing analysis, brain connectivity analysis and ML & DL models. The research problems and gaps are summarized in this chapter as well.

Chapter 3 is the published paper "An EEG based real-time epilepsy seizure detection approach using discrete wavelet transform and machine learning methods". This paper proposed a new method to detect EEG seizure onset in real-time, and it also provided a method to classify health control, seizure free and seizure active EEG data.

Chapter 4 is the published paper "Real-time epilepsy seizure detection based on EEG using tunable-Q wavelet transform and convolutional neural network". This paper investigated the EEG real-time detection in clinical application through signal processing and deep learning method.

Chapter 5 is the submitted paper "A Real-time Epilepsy Seizure Detection Approach based on EEG using Short-time Fourier Transform and Google-net Convolutional Neural Network". This paper improved the accuracy of the detection results in EEG real-time seizure detection.

Chapter 6 is the published paper "Detection of alcoholic EEG signals based on whole brain connectivity and convolution neural networks". This paper highlighted the brain connectivity analysis in EEG alcoholic detection and provided excellent detection results.

Chapter 7 is the published paper "Automatic identification of schizophrenia based on EEG signals using dynamic functional connectivity analysis and 3D convolutional neural network." This paper reported the high identification accuracy and fuzzy localization of ScZ diseases.

Chapter 8 is the submitted paper "3D convolutional neural network for schizophrenia detection using as EEG-based functional brain network" This paper introduced several brain connectivity methods with 3D-CNN model to detect the ScZ diseases and achieved high accuracy results. The biomarkers of abnormal connectivity information also presented in this research.

Chapter 9 summarizes the main outcomes obtained and conclusions drawn from the research. In addition, it discusses the implications of the proposed studies and find the areas of future direction in EEG seizure research and EEG brain connectivity analysis.

CHAPTER 2: LITERATURE REVIEW

2.1   Significance of research problems

Real-time EEG seizure detection allows for the early identification of seizure activity as it occurs [23]. By providing immediate feedback, it enables timely intervention and treatment, which can help mitigate the impact of seizures and improve patient outcomes. Early detection is particularly crucial in cases of prolonged or repetitive seizures that may lead to status epilepticus, a medical emergency requiring immediate intervention [24]. It can trigger alerts or notifications to caregivers, family members, or healthcare professionals when a seizure is detected, enabling prompt assistance, and ensuring a safer environment for the person experiencing seizures. This can improve the quality of life for individuals with epilepsy and provide peace of mind for their caregivers. Moreover, this application can aid in the optimization of treatment strategies for individuals with epilepsy [25]. By continuously monitoring seizure activity, it provides valuable data on the frequency, duration, and patterns of seizures, allowing healthcare professionals to assess the effectiveness of medications, adjust dosages, or explore alternative treatment options. This personalized approach can lead to improved seizure control and better management of epilepsy.

EEG functional connectivity analysis plays a significant role in studying and understanding the neurological mechanisms underlying alcoholism and ScZ. This research can help identify alterations in the functional connectivity patterns of the brain in individuals with alcoholism and ScZ [26,27]. It provides insights into the disrupted communication between brain regions and the overall network organization. This information contributes to understanding the neurobiological basis of alcoholism and ScZ diseases. Additionally, functional connectivity analysis can help identify specific patterns of brain connectivity that serve as potential biomarkers for alcoholism and ScZ [28,29]. These biomarkers may aid in the early detection and diagnosis of diseases, as well as provide insights into the individual differences in susceptibility and treatment response. Furthermore, the analysis of functional brain connectivity can also be used to assess the effects of treatment interventions in alcoholism and ScZ [30,31]. By examining changes in functional connectivity patterns over time, researchers can evaluate the efficacy of different therapeutic approaches and identify neurobiological correlates of treatment response.

2.2 Signal processing of EEG signal

The main objectives of EEG signal processing are to extract the features of time-domain, frequency domain and time-frequency domain from the EEG data. The related works and methods of signal processing methods in epilepsy seizure detection, alcoholism detection and ScZ detection are reviewed and summarized discussed in this section.

2.2.1 Time domain methods

The time domain methods of EEG signal analysis are mainly focus on the wavelet transform and empirical mode decomposition (EMD) methods.

Tuncer, E. et al. utilized the DWT combined with long short-term memory (LSTM) for classifying complex partial seizures and absence seizures [32]. They reported an accuracy of 98.08%. Wijayanto, I. et al. applied the DWT as part of a compressive sensing method to detect ictal, interictal, and pre-ictal EEG seizure signals [33]. They achieved a 100% accuracy between ictal and interictal data and 95% accuracy between ictal and pre-ictal data using the support vector machine (SVM) model. Ghazali, S.M. et al. used an improved double-density DWT algorithm with Levenberg-Marquardt backpropagation classification for epilepsy seizure detection. They reported the highest accuracy of 99.45% and an average accuracy of 98.46% [34]. Chavan, P.A. et al. proposed the use of the TQWT with a hidden Markov model for detecting focal and non-focal epilepsy seizures. They obtained an accuracy of 99.158%, sensitivity of 98.086%, and specificity of 99.155% [35]. Wijayanto, I. et al. highlighted the use of EMD transform with an SVM model for detecting seizure-active, seizure-free, and HC signals from the database UB [36]. They achieved a result of 99.7% accuracy, 99.7% sensitivity, and 99.9% specificity in their study.

In addition, Patidar, S. et al. employed the TQWT in conjunction with the least squares SVM method to detect EEG signals related to alcoholism [37]. They obtained an accuracy of 97.02% in their research.

Furthermore, Sairamya, N. J. et al. utilized the DWT along with the relaxed local neighbour difference pattern (RLNDiP) technique for detecting ScZ using the database LMSU [38]. They achieved a maximum accuracy of 100% in their experiment.

2.2.2 Frequency domain methods

Power spectral density, calculated using various frequency domain algorithms, is widely used in EEG signal analysis. Researchers have applied different methods based on the Fourier transform (FT) to EEG clinical applications.

Oweis, R.J., and E.W. Abdulhay employed the Hilbert-Huang transform for seizure classification [39]. They reported a result of 94% accuracy and 96% specificity in their classification task. Hu, W., et al. proposed the mean amplitude spectrum with a CNN model for seizure prediction [40]. They achieved an 86.25% classification accuracy in their work. Baser, O. et al. proposed the use of Thomson's multi-taper power spectral density to detect spike and wave discharges in epilepsy patients and rats [41]. They suggested that their experiment could enhance the acceptance of artificial intelligence decision-making in accurate epileptic seizure detection.

Additionally, Shri, T.P. et al. introduced the calculation of spectral entropy using the Shannon entropy algorithm and FT power spectral density for detecting EEG signals related to alcoholism. They reported an accuracy of 99.6% in their research [42].

Moreover, Iglesias-Tejedor, M. et al. found that the resting-state power of FT spectral density in the theta band is related to the P300 task in ScZ [43].

2.2.3 Time-frequency domain methods

In time-frequency domain analysis of EEG signals, several popular approaches are commonly used, including STFT, CWT, and Wavelet Scattering Transform (WST).

Shayeste, H. et al. developed an STFT algorithm based on the bagging technique and decision tree (DT) model for automatic seizure detection [44]. They achieved a result of 99.56% accuracy, 99.52% sensitivity, and 99.62% specificity. Amiri, M. et al. proposed sparse common spatial pattern and adaptive STFT based synchro squeezing transform for automatic seizure detection [45], and received a result of 98.44% sensitivity, 99.19% specificity, and 98.81% accuracy.

In addition, Bajaj et al. combined STFT spectral images with a nonnegative least squares classifier to detect EEG signals related to alcoholism [46]. They achieved an accuracy result of 95.83%. Buriro, A.B. et al. applied WST time-frequency analysis in the detection of alcoholism based on EEG signals [47]. They reported excellent results with 100% accuracy, 100% sensitivity, and 100% specificity using an SVM classifier.

Furthermore, Gosala, B. et al. conducted a study on ScZ detection using time-frequency analysis and SVM [48]. They compared three signal processing methods, including DWT, CWT, and WST, and obtained the best results using WST with 97.98% accuracy, 98.2% sensitivity, 97.72% specificity, and 95.94% Kappa score.

2.3   Brain connectivity analysis

Brain connectivity analysis aims to investigate the communication and interaction between different ROIs in the brain. In EEG analysis, brain connectivity is calculated by examining the relationship between different EEG channel signals. In the context of this thesis, the focus is on the development of brain connectivity analysis methods for alcoholism and ScZ diseases.

Alcoholism and ScZ are complex brain disorders that involve dysfunctions in multiple brain regions and disrupted connectivity patterns. By studying the connectivity patterns in EEG data from individuals with these disorders, researchers can gain insights into the underlying mechanisms and identify potential biomarkers for diagnosis and treatment evaluation.

2.3.1   *Functional connectivity*

Functional brain connectivity analysis aims to construct and examine the statistical relationships between functional signals from different brain areas [49]. By studying these relationships, researchers can gain insights into the functional organization of the brain and detect patterns that are associated with specific diseases or conditions.

Mumtaz, W. et al. proposed the power coherence algorithm to calculate the frequency band functional connectivity in EEG alcoholic signal detection [50]. They reported an accuracy of 89.3% and a sensitivity of 88.5% in their study. This method analysed the coherence of power spectra between different brain regions, and investigated the functional connectivity patterns associated with alcoholism. Goksen, N. et al. utilized mutual information (MI) functional connectivity to construct time-domain functional connectivity networks for classifying alcoholism subjects [51]. They achieved an accuracy of 82.33% and a sensitivity of 85.33% in their classification task. By quantifying the statistical dependence between the signals of different brain regions, MI-based functional connectivity can capture the underlying interactions related to alcoholism. Pain, S. et al. combined the phase lag index (PLI) connectivity

feature with a graph neural network to detect alcoholism [52]. PLI measures the consistency of phase differences between different brain regions, allowing for the identification of functional connectivity disruptions associated with alcoholism. They obtained an accuracy of 93.28% using this approach.

In the context of ScZ, Wang, J. et al. investigated the left frontal-parietal/temporal networks and identified biomarkers of auditory verbal hallucinations (AVH) using the phase locking value (PLV) connectivity algorithm [53]. They achieved an accuracy of 80.95% in classifying AVH patients and non-AVH patients. PLV quantifies the phase synchronization between different brain regions, offering insights into the functional connectivity alterations associated with AVH in ScZ. Furthermore, Prieto-Alcantara, M. et al. employed EEG coherence connectivity to investigate neurophysiological differences in different cognitive states between ScZ patients and HC subjects [54]. The Coherence connectivity measures the linear relationship between the signals of different brain regions, enabling the identification of altered functional connectivity in ScZ. Their study provided evidence of distinct functional connectivity patterns between the two groups.

2.3.2   Effective connectivity

Effective connectivity analysis aims to identify and quantify the causal influences between brain regions. It goes beyond mere correlation analysis and focuses on the direction and strength of the connections. This method can also provide insights into the direction of information propagation and help uncover the underlying mechanisms of brain function and dysfunction [55]. By considering the temporal dynamics and statistical dependencies among brain signals, effective connectivity analysis can provide a more comprehensive understanding of how different brain regions interact and communicate with each other.

Khan et al. utilized the PDC algorithm in conjunction with a 3D-CNN model for alcoholism diagnosis, achieving an accuracy of 87.85 ± 4.64% [56]. This highlights the potential of effective connectivity analysis to capture the directed information flow and uncover patterns that are indicative of alcoholism.

Similarly, Zhao et al. employed the PDC connectivity measure and a SVM model to classify ScZ subjects, and reported impressive results with an accuracy of 95.16%, sensitivity of 96.15%, and specificity of 94.44% [57]. This study demonstrated the effectiveness of effective connectivity analysis in discerning patterns specific to

ScZ and differentiating between ScZ subjects and HC subjects. Moreover, Phang et al. extended the application of PDC by combining it with a vector autoregressive model and a multi-domain connectome CNN model for ScZ identification [58]. They achieved promising results with an accuracy of 91.69 ± 4.67%, sensitivity of 91.11 ± 8.31%, and specificity of 92.50 ± 10.00%. This research showed the potential of integrating effective connectivity analysis with advanced machine learning models to improve the accuracy of ScZ classification.

2.3.3   Graph theory analysis

Graph theory is a mathematical framework used to analyse functional brain network which include functional segregation and integration [59]. Five main measurements are widely used in EEG analysis which include degree, clustering coefficient, path length, small-worldness and modularity. Degree quantifies the number of connections of a node, reflecting its importance or centrality in the network. Clustering coefficient measures the extent to which nodes in a network tend to cluster together, indicating the presence of local connectivity patterns. Path length represents the average number of edges that need to be traversed to go from one node to another, reflecting the network's efficiency of information transfer. Small-worldness characterizes the balance between local clustering and global integration in a network, indicating its capacity for both specialized processing and efficient communication. Modularity assesses the presence of distinct communities or modules within a network, indicating the segregation of brain regions into functional subnetworks.

By applying graph theory measures to brain connectivity data, researchers can investigate the organization and dynamics of brain networks, identify network-level biomarkers of diseases, and understand how alterations in connectivity contribute to cognitive functions and neurological disorders. Sadiq, M.T et al. applied graph theory measures and phase space dynamics parameters to detect alcoholic EEG signals [60]. By utilizing a feedforward neural network classifier, they achieved impressive performance with 99.16% accuracy, 100% sensitivity, and 98.36% specificity. These findings demonstrate the potential of graph-based features in accurately identifying alcohol-related EEG patterns. In EEG ScZ detection, Kim, J.Y et al. utilized global and local clustering coefficients as brain network features [61]. Using a linear discriminant analysis classifier, they achieved an accuracy of 80.66%. This study underscores the

significance of graph theory measures, particularly clustering coefficients, in discerning individuals with ScZ from healthy subjects.

2.4   Artificial intelligence methods

The combination of signal processing techniques and ML or DL methods has also been widely used in EEG-based clinical applications recently. These approaches leverage the power of artificial intelligence to analyze EEG signals and extract meaningful information for classification and diagnosis purposes. In this thesis, the ML and DL methods are used in the classification of EEG seizure signal and brain connectivity features.

2.4.1   Machine learning methods

ML methods are applied to develop models that can accurately classify EEG data into different categories or classes. ML algorithms such as SVM, random forests, and k-nearest neighbours (k-NN) are utilized to construct these classification models.

Samiee, K. et al. used multivariate textural features with a gray-level co-occurrence matrix in an SVM classifier and achieved a sensitivity of 70.19% in real-time seizure detection [62]. Zarei, A. et al. utilized orthogonal matching pursuit with DWT as a pre-processing step, combined with non-linear features and an SVM classifier [63]. They reported a sensitivity of 96.81% and a false positive (FP) rate of 2.74% in seizure onset detection. Li, C. et al. proposed a method that involved EMD, Common Spatial Pattern, and an SVM model [64]. They achieved a sensitivity of 97.34% and a 2.5% FP rate. Omidvar, M. et al. used an SVM model to classify EEG data decomposed at the 5th level of DWT and obtained an accuracy of 98.7% [65]. Donos, C. et al. employed random forest methods to detect early seizures in intracranial EEG data and reported a sensitivity of 93.84% [66].

Additionally, Agarwal, S. et al. combined sliding singular spectrum analysis, independent component analysis, and the XGBoost classifier to detect alcoholic subjects. They achieved an accuracy of 98.97% [67].

Furthermore, De Miras, J.R. et al. used principal component analysis and k-NN models to distinguish patients with ScZ from healthy subjects, and achieved an accuracy of 0.87, sensitivity of 0.82, and specificity of 0.90 [68].

2.4.2   Deep learning methods

DL methods have gained significant attention in EEG analysis due to their ability to automate feature extraction and model training, eliminating the need for manual feature engineering. This advantage makes DL particularly suitable for handling complex and high-dimensional EEG data. By training DL models on large amounts of labelled EEG data, these models can automatically learn discriminative features and optimize their parameters, leading to improved performance in decoding tasks. DL models are also capable of handling common events and artifacts in EEG data, such as eye movements or background EEG, by learning to differentiate relevant features from noise. The end-to-end decoding characteristic of DL models allows them to take raw EEG signals as input and produce the desired outputs directly, such as classification labels or reconstructed signals. This eliminates the need for explicit pre-processing steps and manual feature extraction, simplifying the analysis pipeline and potentially improving performance. DL techniques, such as CNN, recurrent neural network (RNN), or LSTM networks, are also used to automatically learn discriminative features directly from the raw EEG data.

Gao, Y. et al. achieved a 90% average classification accuracy in epilepsy seizure detection using a deep CNN [69]. Cao, X. et al. utilized LSTM networks to directly detect seizure onset and achieved a 96.3% accuracy [70]. Wang, X. et al. reported an 88.14% accuracy and low FP rate using a stacked 1D-CNN model for seizure onset detection [71].

For alcoholism detection, Khan, D.M et al. combined partial directed coherence with a 3D-CNN model and achieved an 87.85% accuracy and 100% correct classification of all testing subjects [56]. Mukhtar, H. et al. applied CNN directly to normalized 8-second EEG data segments and achieved 98% accuracy in alcoholism detection [72].

In ScZ identification, Lillo, E. et al. employed a CNN model and obtained a 93% success rate, enabling computer-assisted diagnosis in a short timeframe [73]. Supakar, R. et al. proposed a deep learning model combining RNN and LSTM networks, achieving 98% accuracy on the database LMSU [74]. Hassan, F. et al. applied a CNN to extract ScZ signal features, employed logistic regression for classification, and achieved 90% and 98% accuracies on subject-based and non-subject-based testing, respectively [75].

2.5 EEG data acquisition

In this study four public EEG database are employed to develop the proposed new methods and evaluate their performance. These databases include two EEG epilepsy data, one EEG alcoholism data and one EEG ScZ data. The details of these data are listed as below:

- First EEG epilepsy database: Database UB

  Database UB was collected from the University of Bonn which includes 5 datasets named F, N, O, S and Z [76,77]. Each dataset was the single channel data with 173.61 Hz sample rate. Datasets O and Z contains 5 HC subjects which dataset O was closed eyes data and dataset Z was open eyes data. Datasets F, N and S collected from 5 epilepsy patients which datasets F and N was epilepsy seizure free state data and dataset S was epilepsy seizure active state data.

  https://www.ukbonn.de/epileptologie/arbeitsgruppen/ag-lehnertz-neurophysik/downloads/

- Second EEG epilepsy database: Database CHB-MIT

  Database CHB-MIT was collected in Boston Children's Hospital with 23 subjects (5 males between ages 3 to 22 years and 17 females of ages between 1.5 and 19 years) [78]. Each dataset was collected through International 10-20 system standard scalp of 23 bipolar channels (FP1-F7, F7-T7, T7-P7, P7-O1, FP1-F3, F3-C3, C3-P3, P3-O1, FP2-F4, F4-C4, C4-P4, P4-O2, FP2-F8, F8-T8, T8-P8, P8-O2, FZ-CZ, CZ-PZ, P7-T7, T7-FT9, FT9-FT10, FT10-T8, T8-P8) with 256 Hz sample rate. The EEG electrodes cap of this data was shown in Figure 2.1.

  https://physionet.org/content/chbmit/1.0.0/
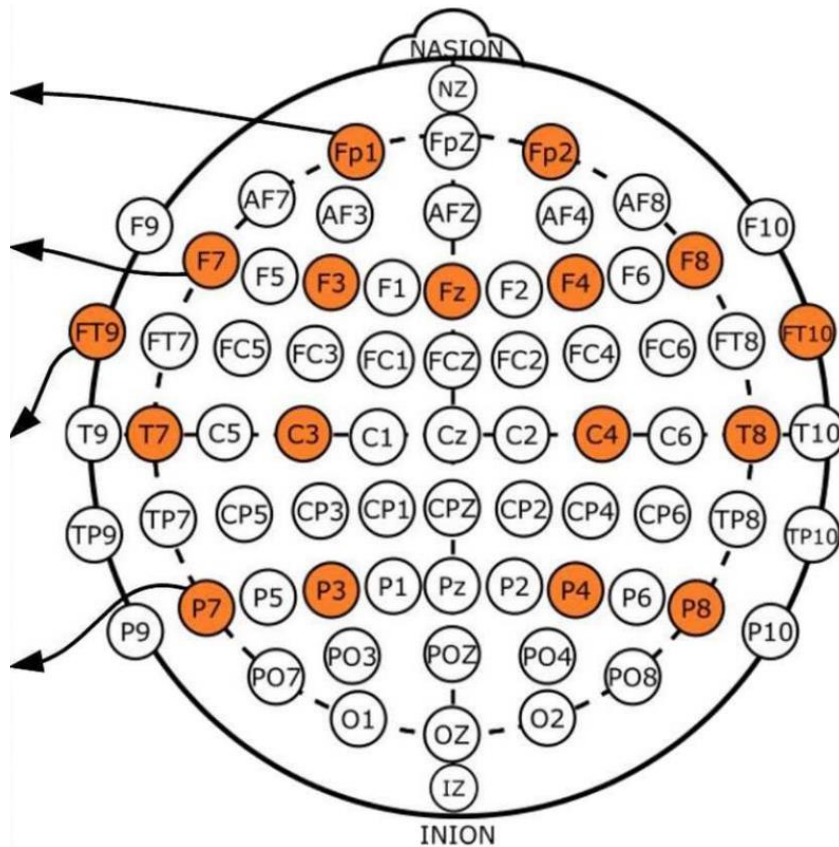
Figure 2.1: EEG electrodes position of database CHB-MIT [79].

- EEG alcoholism database: Database KDD

  Database KDD was collected from Neurodynamic Laboratory at the State University of New York [80]. It contains 122 subjects with 77 male alcoholics with an average age of 35.83 (22.3 to 49.8 ages) and 45 HC subjects. The 64-channel EEG electrodes with 256 Hz sample rate was applied to collect the EEG signal, the information of channel localization was shown in Figure 2.2.

  https://archive.ics.uci.edu/ml/datasets/eeg+database
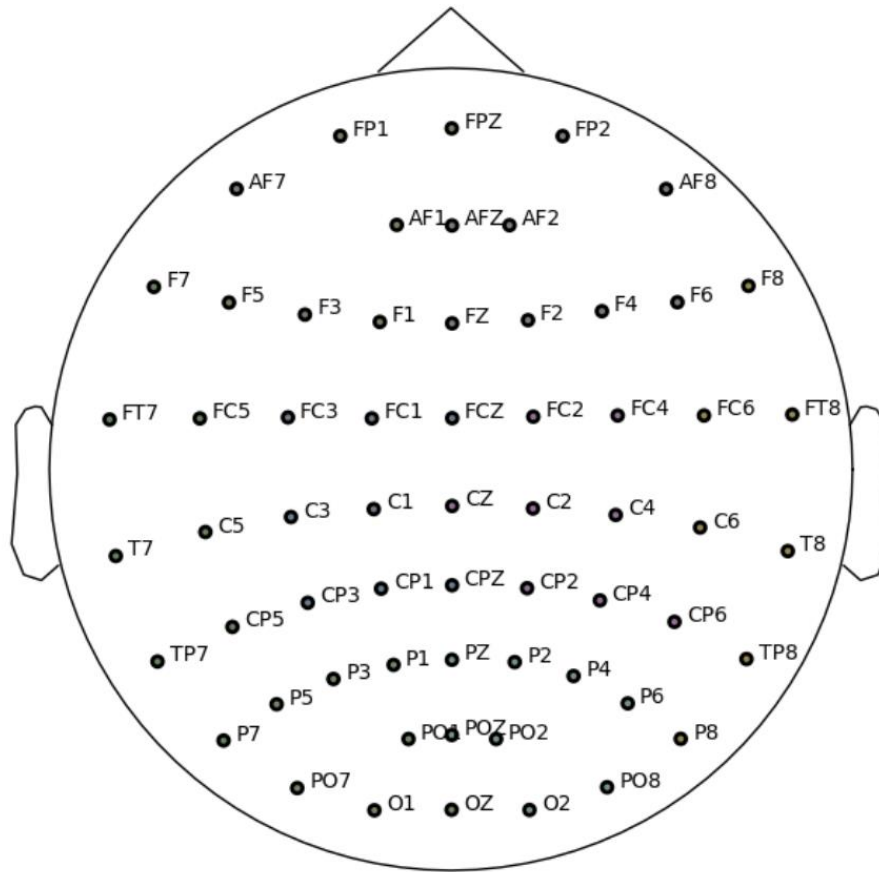
Figure 2.2: EEG electrodes position of database KDD [81].

- EEG ScZ database: Database LMSU

  The public EEG ScZ database was collected from LMSU which includes 84 subjects (45 ScZ subjects and 39 HC subjects) [82,83]. All patients with ScZ were diagnosed at the Mental Health Research Centre according to ScZ diagnostic criteria F20, F21, F25 of the ICD-10 classification of mental and behavioural disorders developed by the international statistical classification of diseases and related health problems. The data sampled in 128 Hz and collected in 16 channels (F7, F3, F4, F8, T3, C3, CZ, C4, T4, T5, P3, PZ, P4, T6, O1, O2). The details of EEG channel location of this database were shown in Figure 2.3.

  http://brain.bio.msu.ru/eeg_schizophrenia.htm
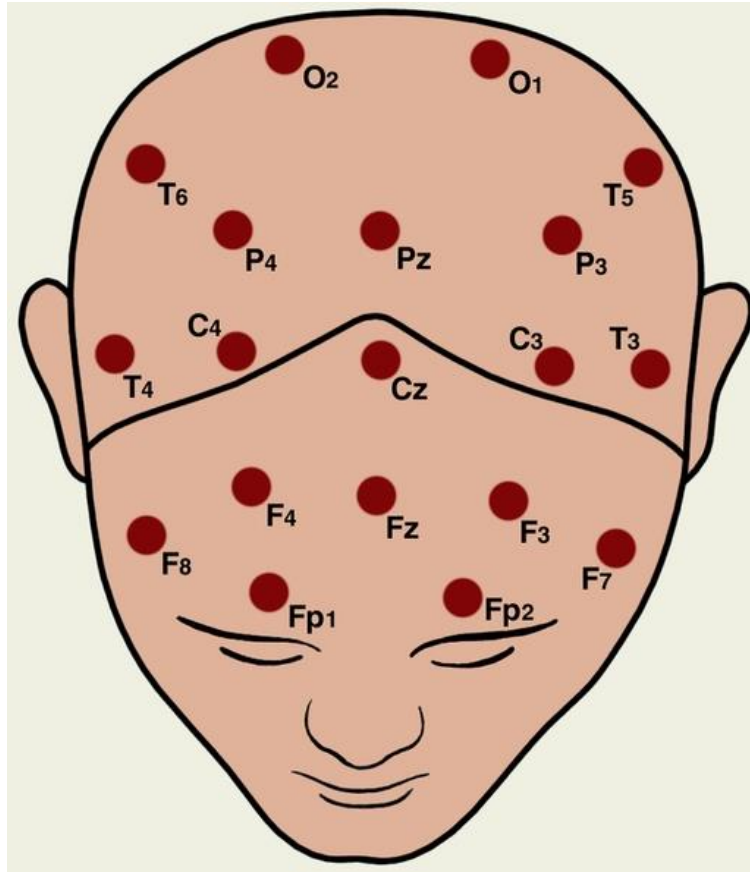
Figure 2.3: EEG electrodes position of database LMSU [84].

2.6   Research gaps of problems

The major research achievements and outcomes in the literature review of this thesis are summarized in three tables. Table 2.1 illustrates the works in EEG epilepsy seizure detection. Table 2.2 shows the works in EEG alcoholism detection. Table 2.3 describes the EEG ScZ identification.

Table 2.1: EEG based seizure detection

References	Techniques	Sen (%)	FP rate (%)	Delay (s)
Wang, X. et al. (2021) [71]	1D-CNN	88.14	0.38	Not reported
Li, C. et al. (2021) [64]	EMD + SVM	97.34	2.5	Not reported
Zarei, A. et al. (2021) [63]	DWT + SVM	96.81	2.74	Not reported

Abdelhameed, A. et al. (2021) [85]	LSTM	98.72	1.14	Not reported
Alharthi, M.K. et al. (2022) [86]	DWT + LSTM	96.85	3.02	Not reported
Amiri, M. et al. (2022) [45]	STFT + Linear SVM	98.44	0.81	Not reported
Shayeste, H. et al. (2022) [44]	STFT + DT, bagging technique	99.52	0.38	Not reported
Jiang, L. et al. (2022) [87]	Functional brain network + SVM	97.72	4.38	Not reported
Paper 1 (2022) [1]	DWT + RUS Boosted	96.15	3.24	10.42
Paper 2 (2023) [2]	TQWT + CNN	98.90	2.13	10.46
Paper 3 (2023)	STFT + Google-net CNN	98.90	1.94	9.85

* '*Sen*' is sensitivity.

From Table 2.1, three papers obtained the satisfied performance in EEG seizure onset detection. However, the previous work did not factor in clinical diagnosis in EEG seizure detection. Another three papers considered the processing time and delay of the seizure onset in clinical application. The delay refers to the time it takes for the detection algorithm to identify the onset of a seizure after it occurs. A large delay can reduce the clinical relevance of the detection method, as timely intervention or response may be compromised.

Table 2.2: EEG based alcoholism detection

References	Techniques	Acc (%)
Malar, E. et al. (2020) [88]	Wavelet decomposition + Extreme learning machine	87.6
Farsi, L. et al. (2020) [89]	LSTM	93
Agarwal, S. et al. (2021) [67]	Independent component analysis + XGBoost classifier	98.97
Mukhtar, H. et al (2021) [72]	CNN	98
Kumari, N. et al. (2022) [90]	CNN	92.7
Li, H. et al. (2022) [91]	DWT + CNN, LSTM	99.32
Paper 4 (2023) [3]	CMI + 3D-CNN	96.25 ± 3.11

* '*Acc*' is accuracy.

According to Table 2.2, work conducted in paper 4 provided a high accuracy result in EEG alcoholism detection. The related works mainly used the traditional signal processing methods and ML/DL models. Comparing the related work, Paper 4 provided the biomarkers of abnormal connectivity in the left parietal part, the left frontal part, the right temporal part, the right frontal part, and the right parietal part as well.

Table 2.3: EEG based ScZ detection

References	Technique	Acc (%)	Sen (%)	Spe (%)
Baygin, M et al (2021) [92]	Collatz pattern technique + k-NN	99.47	99.20	99.80
Akbari, H et al. (2021) [93]	Phase space dynamic features + k-NN	94.80	94.30	95.20
Lillo, E et al. (2022) [73]	CNN	93.00	-	-
Supakar, R et al. (2022) [74]	RNN - LSTM	98.00	98.00	98.00
Sairamya, N.J et al, (2022) [38]	DWT + RLNDip	100	-	-
Hassan, F et al. (2023) [75]	CNN + logistic regression	98.05 ± 1.13	99.00 ± 1.00	97.00 ± 2.00
Gosala, B et al. (2023) [48]	WST + SVM	97.98	98.20	97.72
Paper 5 [4]	CMI + 3D-CNN	97.74 ± 1.15	96.91 ± 2.76	98.53 ± 1.97
Paper 6	MVAR coherence + 3D-CNN	98.47 ± 1.47	99.26 ± 1.07	97.23 ± 3.76

* '*Acc*' is accuracy, '*Sen*' is sensitivity and '*Spe*' is specificity.

As Table 2.3 showing, based on the previous works in EEG ScZ detection, the work included in Paper 5 and Paper 6 was conducted and achieved excellent results. Furthermore, these two papers also provided the biomarkers of ScZ abnormal connectivity in DMN region, the temporal and posterior temporal lobes of both right and left hemispheres.

2.7 Summary of literature review

This chapter provides a comprehensive literature review on the recent advancements in EEG-based clinical applications leveraging signal processing, brain connectivity and artificial intelligence methodologies. The focus has been on the integration of signal processing techniques with ML and DL models to enhance EEG data classification, specifically in the domains of seizure detection. Additionally, this chapter also summarize the method in combining brain connectivity analysis and artificial intelligence techniques to develop the alcoholism detection, and ScZ identification. Various studies employing techniques such as SVM, CNN, LSTM, and more, have been systematically presented. These works achieved notable accuracy, sensitivity, and specificity rates. Moreover, the materials of EEG database have shared in this chapter which encourage readers to do the further research. Furthermore, significant research gaps are listed which include EEG seizure detection, alcoholism detection and ScZ identification in recent years. Overall, while strides have been made in the EEG analysis using artificial intellgence, areas of improvement remain, underlining the need for continued exploration and innovation in the fields.

CHAPTER 3: PAPER 1 – An EEG based real-time epilepsy seizure detection approach using discrete wavelet transform and machine learning methods

3.1 Overview of Paper 1

The details of the Paper 1 are given below:

- Paper title: "An EEG based real-time epilepsy seizure detection approach using discrete wavelet transform and machine learning methods."
- Paper length: 8 pages
- Journal: Biomedical signal processing and control
  - Rank: Q1 (Biomedical Engineering)
  - Impact factor: 5.1 (2022-2023)
  - Cite Score: 8.2 (2022)
  - SJR: 1.071 (2022)
  - SNIP: 1.552 (2022)
- DOI: https://doi.org/10.1016/j.bspc.2022.103820
- First author: Mingkan Shen
- Corresponding author: Mingkan Shen

HDR thesis author's declaration

☒ The authors declare that they have no known competing financial   interests or personal relationships that could have appeared to influence the work reported in this paper.

☐ The authors declare the following financial interests/personal relationships which may be considered as potential competing interests:

Table 3.1: Authorship contributions of Paper 1

Conception and design of study	Mingkan Shen, Peng Wen, Bo Song, Yan Li
Analysis and interpretation of data	Mingkan Shen
Drafting the manuscript	Mingkan Shen

Revising the manuscript critically for important intellectual content	Mingkan Shen, Peng Wen, Bo Song, Yan Li
Approval of the version of the manuscript to be published	Mingkan Shen, Peng Wen, Bo Song, Yan Li

3.2   Summary of Paper 1

In the endeavour to develop effective real-time systems for epilepsy seizure detection, the utilization of EEG signals has emerged as a pivotal tool. The unpredictability and sudden onset of epileptic seizures not only disrupt daily activities but can also lead to grave complications. Immediate detection, thus, becomes crucial for timely intervention. This paper introduces a novel approach that combines the prowess of the DWT with cutting-edge machine learning methods to detect seizures using EEG data.

Traditionally, EEG signals have been challenging to interpret due to their intricate nature. However, the DWT, known for its capability to decompose signals into various frequency bands, provides a solution. By applying DWT, we extracted salient features from segmented EEG signals, distinguishing between seizure and non-seizure activities. Following this, a series of machine learning algorithms were employed to classify these segments, leading to an effective real-time seizure detection mechanism.

The findings from this research, which encompass data from 16 epilepsy-diagnosed patients, not only highlight the potential of the combined DWT and machine learning approach but also emphasize its potential application in wearable technologies for continuous monitoring. Through this, we seek to usher in a new age in epilepsy management, ensuring safer environments for patients by minimizing risks associated with undetected seizures.

3.3   Paper file
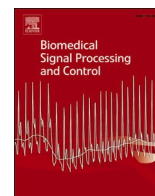
An EEG based real-time epilepsy seizure detection approach using discrete wavelet transform and machine learning methods

Mingkan Shen [a,1], Peng Wen [a], Bo Song [a], Yan Li [b]

[a] *School of Mechanical and Electrical Engineering, University of Southern Queensland, Toowoomba, QLD 4350, Australia*
[b] *School of Science, University of Southern Queensland, Toowoomba, QLD 4350, Australia*

A R T I C L E   I N F O

A B S T R A C T

Epilepsy is one of the most common complex brain disorders which is a chronic non-communicable disease caused by paroxysmal abnormal super-synchronous electrical activity of brain neurons. This paper proposed an electroencephalogram (EEG) based real-time approach to detect epilepsy seizures. Discrete wavelet transform and eight eigenvalues' algorithms are applied to extract features in different sub-frequency bands. Then support vector machine is employed for three-classes classification of health control, seizure free and seizure active, and finally RUSBoosted tree Ensemble method is used for real-time seizure onset detection. The proposed algorithm is evaluated using two public datasets: one short-term dataset named UB and one long-term dataset named CHB-MIT. The results show that the algorithm achieves 97% accuracy and 96.67% sensitivity in the three-classes classification of health control, seizure-free and seizure-active groups in UB dataset, and 96.38% accuracy, 96.15% sensitivity, 3.24% false positive rate for the real time seizure onset detection in CHB-MIT Dataset.

1. Introduction

Epilepsy is a chronic non-communicable disease caused by the abnormal synchronous electrical activity of brain neurons [1,2]. It is also one of the most common neurological diseases in the world, and affects approximately 50 million people [2,3]. Due to the differences in the starting region and propagation mode of abnormal electrical activity in the brain, the clinical manifestations of epilepsy are diversified and complicated [4]. Repeated seizures can cause persistent negative effects on patients' mental and cognitive functions, and bring life-threatening risks [5]. Therefore, research on the diagnosis and treatment of epilepsy has very important clinical significance. Automatic identification of epilepsy seizures from electroencephalogram (EEG) signals and its real-time implementation can provide an objective reference basis for the diagnosis and in time evaluation of epilepsy, thereby reducing the workload of doctors and improving the efficiency of treatment [6]. Majority of the recent papers have set the ultimate objective of developing automated EEG monitoring system to detect epileptic seizures. Bhattacharyya et al. highlighted a real-time seizure detection through empirical Wavelet transform method [7]. Disruptive EEG networks for epileptic seizures in real-time application reported by Bomela et al. [8]. Harmonic Wavelet packet transform with relevance vector machine

method were proposed by Vidyaratne et al. [2].

EEG is a microvolt level electrical signal generated by synchronized neuronal activity in the brain collected by electrodes placed at a specific position on the scalp [9,10]. EEG abnormalities in epileptic seizures are mainly manifested as spike waves and sharp waves [11]. Therefore, using feature extraction methods to find the eigenvalues which can divide the normal waves and spike or sharp waves in different seizure state should be thoroughly investigated. So far many methods in time, frequency, and time–frequency domains have been developed such as discrete wavelet transform (DWT), empirical mode decomposition (EMD), Q-wavelet transformation, Hilbert-Huang transform (HHT), mean amplitude spectrum (MAS), etc [7,12–15]. Another important progress of epilepsy seizure detection is the development of machine learning based classification methods. The main objective of machine learning methods is to overcome the robustness of EEG individuals in epilepsy detection. Specifically, support vector machine (SVM), linear discriminant analysis (LDA), naive Bayes, logistic regression (LR), random forest were used to classify the different seizure states in previous studies [12,16–19]. Currently, automatic epilepsy detection can be divided into two types: offline seizure detection and real-time seizure detection. The purpose of offline seizure detection is to identify epileptic seizure signals as accurately as possible from EEG signal [20]. The

E-mail addresses: Mingkan.Shen@usq.edu.au (M. Shen), Paul.Wen@usq.edu.au (P. Wen), Bo.Song@usq.edu.au (B. Song), Yan.Li@usq.edu.au (Y. Li).
[1] 0000-0002-6770-4366

purpose of real-time seizure detection is to identify seizures onsite with the shortest possible delay when the patient has a seizure during continuous EEG monitoring [21].

Two public datasets are available in EEG seizure detection. Dataset UB is a short-term dataset from the University of Bonn, which is used to do seizure event detection through the classifications of two classes (seizure free and seizure active) and three classes (health control, seizure free and seizure active). In the studies of two-classes classification, fractional linear prediction and SVM were used by Joshi et al. and achieved 95.33% accuracy [22]. Fast Fourier transform with k-nearest neighbor (k-NN) model proposed by Ghaderyan et al. could result in 98.72% accuracy [23]. In addition, The Dual-tree complex wavelet and the nearest neighbor (NN) model was reported to have 95.5% accuracy by Chen et al. [24]. Meanwhile, in the three classes classification studies, Acharya et al. discussed four entropy parameters (approximate entropy, sample entropy, two phase entropies) combined with fuzzy classifier, and achieved 98.1 % accuracy [25]. Omidvar et al. used the DB4-DWT method based on the artificial neural network and SVM models, and got 98.7% accuracy [12]. Currently, feature extraction based on machine learning classification is one of the most researched approaches in seizure event detection using EEG signal. Tunable-Q wavelet transform based multiscale entropy measure proposed by Bhattacharyya, A., et al. is used to classifier 3-classes between normal, seizure-free and seizure EEG signals and achieve 98.6% accuracy results [26]. Gupta, V. and R.B. Pachori stated that Fourier-Bessel series expansion (FBSE) and weighted multiscale Renyi permutation entropy (WMRPE) for EEG rhythms and get 97.3% accuracy results [27]. Empirical wavelet transform (EWT) with FBSE method highlighted by Anuragi, A., et al. can also achieved 97.7% accuracy classification [28].

Dataset CHB-MIT is a long-term dataset from Boston Children's Hospital, which is used by many researchers to do the real-time automatic seizure detection. Samiee et al. used multivariate textural features with gray-level co-occurrence matrix (GLCM) in SVM and reported 70.19% sensitivity in the real-time seizure detection [29]. As a contrast, time delay embedding method proposed by Zabihi et al. was reported to have 89.01% sensitivity [30]. In particularly, graph theory analysis, function connectivity analysis and effective connectivity analysis were used in the seizure detection [16,31,32]. Bomela et al. constructed the network connectivity using Fourier transform to detect the seizure onset and reported 93.6 % sensitivity and a false positive rate of 0.16 per hour (FP/h) result [8]. A stactked 1D-CNN model is presented via Wang, X., et al. to detect seizure onset automatically and achieved 88.14% accuracy and 0.38% false positive (FP) result [33]. Orthogonal matching pursuit with DWT as pre-processing progress with non-linear features and SVM classifier can also detect the seizure onset in same dataset, Zarei, A. and B.M. Asl, used this method reported 96.81% sensitivity and 2.74% FP result [34]. Li, C., et al. proposed EMD, common spatial pattern and SVM model get 97.34% sensitivity, 2.5% FP output as well [35].

In this study, the proposed real time EEG based seizure detection method includes four major steps using the aforementioned both datasets (UB and CHB-MIT) in two experiments. Specifically, in the first experiment using Dataset UB, DWT analysis with DB4 mother wavelet was used to decompose the raw EEG signal data. After feature extraction and selection, 12 eigenvalues were evaluated as the input of the SVM model to classify health control, seizure-free and seizure-active subjects. Based on the first experiment, real-time seizure detection was implemented using Dataset CHB-MIT. Similarly, DB16 DWT analysis with 7 eigenvalues were fed into the SVM and RUSBoosted tree Ensemble model to obtain the final results. All the experiments in this study were carried out in a Dell workstation with dual Intel Xeon E5-2697V3 CPUs using MATLAB 2019b. The main contributions and innovations of this study are: (1) DB4-DWT and DB16-DWT were proposed to extract approximate and details of signals and remove redundant information. (2) Improved the robustness of EEG based epilepsy detection via machine learning methods. (3) Proposed a method that can achieve 97%

accuracy and 96.67% sensitivity in 3-class classification (health control, seizure free and seizure active) using Dataset UB, and 96.38% accuracy, 96.15% sensitivity and 3.24% false positive rate in the real-time seizure detection using Dataset CHB-MIT. (4) Implemented an automatic seizure detection approach in real-time way.

The first section of the paper provided a brief introduction of the work. Section II described the details of the short-term dataset (Dataset UB) and long-term dataset (Dataset CHB-MIT). The pre-processing, feature extraction, classification and real-time application are also introduced in this section. Section III reported the work in our experiments and results obtained using the proposed method. Comparisons of previous work using the same datasets were conducted and evaluated in Section IV. Section V concluded the paper.

2. Methodology

The proposed methodology utilized DWT for the data pre-processing, and calculated nine eigenvalues via entropy-based and statistical measures to extract features. SVM and RUSBoosted tree Enemble methods were used to train and test Dataset UB and Dataset CHB-MIT. The framework of the proposed method is described as follow Fig. 1:

2.1. Datasets

Dataset UB is collected from the University of Bonn which consists of the sets F, N, O, S and Z [36]. Each set contains 100 single channel segments with 23.6 s duration in 173.61 Hz sample rate. Sets Z and O were collected from 5 healthy control subjects via surface EEG standard 10–20 system caps, which Set Z is open eyes EEG data and Set O is closed eyes EEG data [37]. Sets N and Sets F were collected from 5 epileptic patients through seizure-free state via intracranial EEG (iEEG) signals. Sets S involves 5 epileptic patients in seizure active state by iEEG signals as well [36,37]. According to the Dataset UB has three different classes that health control, seizure free and seizure active respectively, thus, the first experiment in this study is to do the 3 classes' classification detection.

Dataset CHB-MIT is collected from Boston Children's Hospital with 23 subjects (5 males between ages 3 to 22 years and 17 females of ages between 1.5 and 19 years) [38]. All CHB-MIT database was sampled at 256 Hz, and it collected in 23 bipolar channels by scalp EEG standard 10–20 system caps. Here, Channel FT10 - T8 is used to detect the seizure onset in real-time applications. This study used 16 patents from the CHB-MIT database, and excluded patients that had seizures characterized by amplitude depression [15]. Furthermore, case'Chb24′ was not used in the real-time seizure detection due to the insufficient specific real-time information. The details of the CHB-MIT used in this study is shown in Table 1.

2.2. Pre-processing

One of the most challenging parts in epilepsy seizure detection is to detect the sharp waves and spike waves. However, not all features in all frequency bands are significantly different among seizure active, seizure free and health control states. Thus, DWT is proposed to decompose an EEG signal in different frequency sub-bands into frequency components, and the formula of DWT is shown as follow [39,40]:

$$C(a, b) = \frac{1}{\sqrt{a}} \int \overline{\psi}(\frac{t - b}{a}) x(t) dt \tag{1}$$

where ψ is the analyzing wavelet method, 'a' and 'b' are the parameters of time dilation and time translation, respectively.

After DWT decomposition, two style coefficients the detail coefficients and approximation coefficients of each sub-bands are calculated in Eqs. (2) and (3).
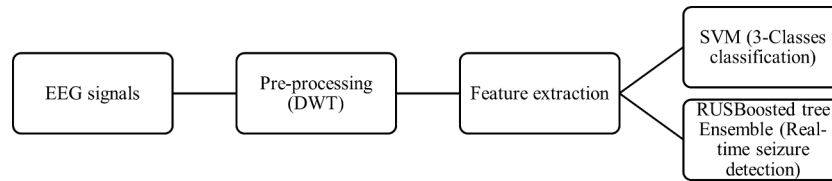
Fig. 1. The framework of DWT and machine learning methods for seizure detection.

Table 1
Long term EEG data (Dataset CHB-MIT).

Patient	EEG used (h)	Number of seizures	Seizure duration (s)
Chb01	25	7	40,27,40,51,90,93,101
Chb02	16	3	82,81,9
Chb03	36	7	52,65,69,52,47,64,53
Chb04	25	4	49,111,102,116
Chb05	14	5	115,110,96,120,117
Chb07	28	3	86,96,143
Chb08	16	5	171,190,134,160,264
Chb09	34	4	64,79,71,62
Chb10	20	7	35,70,65,58,76,89,54
Chb11	12	3	22,32,752
Chb17	15	3	90,115,88
Chb18	18	6	50,30,68,55,68,46
Chb19	14	3	78,77,81
Chb20	15	8	29,30,39,38,35,49,35,39
Chb22	15	3	58,74,72
Chb23	14	7	113,20,47,71,62,27,84

$$A_j(n) = \sum_{l=-\infty}^{+\infty} g(l - 2n)A_{(j-1)}(l), j = 1, 2, ..., J \quad (2)$$

$$D_j(n) = \sum_{l=-\infty}^{+\infty} h(l - 2n)A_{(j-1)}(l), j = 1, 2, ..., J \quad (3)$$

where $A_j(n)$ and $D_j(n)$ are the approximation coefficients and detail coefficients at level j respectively.

The sample rate of Dataset UB is 173.61 Hz, 5-level DWT with 'DB4' wavelet technique is used to decompose the data. D_1, D_2, D_3, D_4 and A_4 coefficients are used to represent the EEG sub-bands described in Table 2. The pre-processing method used in Dataset CHB-MIT was slightly changed to accommodate the different sampling rates. 6-level DWT with 'DB16' wavelet method was applied to decompose the components and the details are shown as Table 3.

2.3. Feature extraction

Nine features were calculated to assess the time-domain signal correspond to sub-band j to find the difference in different seizure states. The features include the standard deviation (SD), mean band power (BP), Shannon entropy (SE), log-energy entropy (LE), fuzzy entropy (FE), maximum, kurtosis, and median.

The SD can describe the degree of dispersion of the signal, is defined as.

Table 2
5-level DWT decomposition (DB4) in Dataset UB.

Sub-band j	Decomposed signal	Frequency band (Hz)
1	D1	43.4–86.8
2	D2	21.7–43.4
3	D3	10.8–21.7
4	D4	5.4–10.8
4	A4	0–5.4

Table 3
6-level DWT decomposition (DB16) in Dataset CHB-MIT.

Sub-band j	Decomposed signal	Frequency band (Hz)
1	D1	64–128
2	D2	32–64
3	D3	16–32
4	D4	8–16
5	D5	4–8
5	A5	0–4

$$SD = \sqrt{\frac{1}{N} \sum_{n=0}^{N} (S_n - \mu)^2} \quad (4)$$

where μ is the mean value of the EEG segments.

$$\mu = \frac{1}{N} \sum_{i=1}^{N} S_n \quad (5)$$

The BP of the signal is calculated to assess the power of time-domain amplitude.

$$BP = \frac{1}{N} \sum_{i=1}^{N} S_i^2 \quad (6)$$

Entropy is the parameter to define the confusion of the signal. In particular, SE, LE and FE are calculated to detect seizures [41,42].

$$SE = -\sum_{i=1}^{N} p_i \log_2 p_i \quad (7)$$

$$LE = -\sum_{i=1}^{N} (\log_2 p_i)^2 \quad (8)$$

$$FE(m, n, r, N) = \ln\phi^m(n, r) - \ln\phi^{m+1}(n, r) \quad (9)$$

where p_i is the probability of occurrence in the EEG segments, and.

$$\phi(n, r) = \frac{1}{N - m} \sum_{i=1}^{N-m} \left[\frac{1}{N - m - 1} \sum_{j=1, j \neq i}^{N-m} D_{ij}^m \right] \quad (10)$$

where m is the embedding dimension, r is the threshold which equals to $0.15 \times SD$ and n is the fuzzy power. Empirically, values like $m = 2, n = 2$ produced the best performance.

Kurtosis is a measure of the peak of the probability distribution of a random variable. High kurtosis means that the increase in variance is caused by extreme differences in low frequencies that are greater than or less than the average.

$$Max = \max(S_n) \quad (11)$$

$$M = median(S_n) \quad (12)$$

$$K = \frac{1}{N - 1} \sum_{i=1}^{N} \frac{(S_i - \mu)^4}{\sigma^4} \quad (13)$$

where μ is the mean value and σ is the SD of the EEG segments.

There are nine features for each sub-band's signal, and total 45 eigenvalues for the 5 sub-bands from Dataset UB. Similarly, nine features for each sub-band's signal, total 54 eigenvalues from Dataset CHB-MIT.

2.4. Classification

In Dataset UB, SVM was applied in the 3-classe classifications (health control, seizure free and seizure active). The leaving one out training method and RUSBoosted tree Ensemble were used to detect seizure onset based on Dataset CHB-MIT.

2.4.1. Three -class classification for Dataset UB

Polynomial function of SVM helps the model to improve the accuracy in classification. Two key parameters of SVM model, γ and c, were selected, where γ is the inverse of the radius of influence of samples selected by the model as support vectors, and c parameter trades off correct classification of training examples against maximisation of the decision function's margin. Here, $\gamma = 0.1$, and $c = 1$.

In Dataset UB, 80% data (segment 1 to segment 80, all 400 segments) of each set (Set Z, O, N, F, S) is used to training in SVM model while the remaining 20% (segment 81 to segment 100, all 100 segments) were used to test the performance of the proposed method.

2.4.2. Leaving one out experiment for Dataset CHB-MIT

Sixteen patients' data from dataset CHB-MIT (detail shown in Table 1) was used in this study. In leaving one out training method, one subject data is used for testing and the other 15 subjects were used for training. As a result, 16 models have been trained. The same SVM model constructed in Dataset UB was re-used in Dataset CHB-MIT. But in Dataset CHB-MIT, it is a two-class classification problem in seizure free and seizure active, thus the RUSBoosted tree Ensemble model function with 5-fold cross validation in MATLAB Classification Learner toolbox was applied to conduct the seizure detection and comparisons with the SVM model.

In this study, the EEG data was segmented into 30 s epoch with 256 Hz sample rate, which resulted 7680 sampling points in each epoch. In all 16 subjects, the EEG raw data of 30 min before seizure epochs and 30 min after seizure epochs for each subject data were used to train.

2.5. Real time implementation

The real-time application is implemented and evaluated in Dataset CHB-MIT, as the Dataset UB is not a continuous real-time data. In particular, a 30-second sliding window was developed and data within the moving window was considered as the input data, and the sliding window overlap was selected as 1 s in the real-time detection. The features of $BP-D_5$, $SD-D_4$, $SD-D_5$, $SE-D_4$, $SE-D_5$, $LE-D_4$, $LE-D_5$ with the EEG raw data of Channel FT10 - T8 for case 'Chb01' first seizure is shown in Fig. 2.

Obviously, the eigenvalues have changed significantly before and after the seizure onset (the 2996 s). Thus, these eigenvalues were selected to train in the machine learning model. Using leaving one out training method, 16 models have been trained, the left one subject as the test data is used to test by corresponding models.

3. Experiments and results

Accuracy and sensitivity were used to evaluate the 3-class classification for Dataset UB, while accuracy, sensitivity, false positive rate and seizure onset detection delay were used to evaluate the proposed method for Dataset CHB-MIT.

Accuracy is a direct parameter in method evaluation which is define as follow:

$$Acc = \frac{TP + TN}{TP + TN + FP + FN} \tag{14}$$

where, TP is the true positive, TN is the true negative, FP is the false positive and FN is the false negative.

Sensitivity is another parameter for evaluation which is defined as:

$$Sen = \frac{TP}{TP + FN} \tag{15}$$

However, the sensitivity of Dataset UB and Dataset CHB-MIT is different because this parameter is focus on how much seizure times has
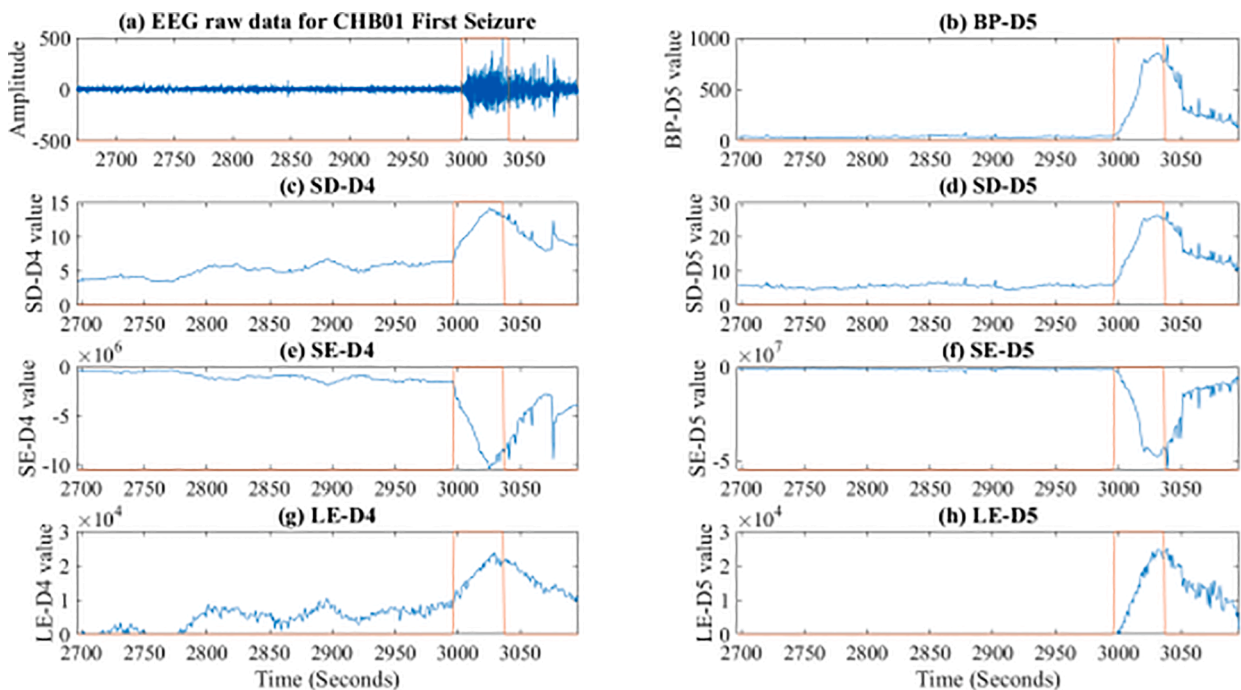

Fig. 2. (a) Raw EEG signal of Chb01, FT10 – T8 Channel, (b) BP of D5 level, (c) SD of D4 level, (d) SD of D5 level, (e) SE of D4 level, (f) SE of D5 level, (g) LE of D4 level, (h) LE of D5 level, orange line is the seizure states labelled by the doctor from the 2996 s to 3036 s.

been detected in real-time detection. The sensitivity of this part is calculated as:

$$Sen_{real-time} = \frac{TP}{NS} \qquad (16)$$

where *NS* means the number of the seizures.

3.1. Three-class classification results using Dataset UB

There are 45 eigenvalues for these EEG signals. However, the performance of those features was quite different. Empirically, 12 eigenvalues were selected to train the model, and their details are shown in Table 4(a). The last 20% data (segment 81 to segment 100 for each Set, all 100 segments) were used to test, and the classification results of 97% accuracy, 96.67% sensitivity were received for Dataset UB.

3.2. Real-time seizure onset detection results using Dataset CHB-MIT

About 7 eigenvalues from 53 eigenvalues were selected in the real-time implementation using Dataset CHB-MIT, and the details of features selection is shown in Table 4(b). SVM and RUSBoosted tree Ensemble machine method were applied to evaluate the model using leaving one training method. As a result, RUSBoosted tree Ensemble achieved results of 96.15% sensitivity, 96.38% accuracy and 3.24% false positive rate (Tables 5 and 6).

4. Discussion

We used DWT to decompose EEG raw signal into different frequency bands, after that nine eigenvalues are calculated in each sub-band. However, not every sub-band's features are obviously different between seizure active state and seizure free state. Thus, we studied the level of decompositions, mother wavelet selection, and sliding window size selection to get the best performance. The work and results are presented below:

4.1. Level of decompositions and mother wavelet selection

To extract features from EEG raw signal, we compared several eigenvalues in 3 different states in Dataset UB, and before and after seizure onset in Dataset CHB-MIT. After computing all 9 eigenvalues of different seizure state, 5 levels for Dataset UB and 6 levels for Dataset CHB-MIT are selected as they show a significant difference between different seizure states. The performance of BP in different levels is shown in Fig. 3, which clearly shows that the eigenvalues of BP in D_4 and D_5 have a better performance. Therefore, the parameter of the level of decompositions was selected as 6.

There is no standard method to choose the best wavelet. Omidvar et al. reported a method using 5-level DB4 DWT to the seizure

Table 4

Selected features for Dataset UB and CHB-MIT.

(a) Features selection for Dataset A		(b) Features selection for Dataset B	
Decomposition level	Features	Decomposition level	Features
D3	SD	D5	BP
A4	SD	D4	SD
D3	Mean	D5	SD
D4	Mean	D4	SE
D2	LE	D5	SE
D3	LE	D4	LE
D3	FE	D5	LE
D2	Max		
D3	Max		
D3	Median		
D2	Kurtosis		
D3	Kurtosis		

Table 5

Real time detection using Dataset CHB-MIT and SVM method.

Patient	NS	TP	FP (%)	Sen (%)	Delay (s)	Acc (%)
Chb01	7	7	0.0	100	20.7	99.60
Chb02	3	3	0.0	100	19.0	99.76
Chb03	7	4	0.2	57.1	25.8	99.30
Chb04	4	3	0.1	75	60.0	99.62
Chb05	5	5	16.3	100	16.4	83.59
Chb07	3	3	0.2	100	18.7	99.64
Chb08	5	5	0.1	100	19.6	98.60
Chb09	4	3	11.4	75	−171.0	88.40
Chb10	7	7	0.7	100	23.6	98.83
Chb11	3	1	0.1	33.3	91.0	98.16
Chb17	3	2	0.0	66.7	43.0	99.53
Chb18	6	3	0.0	50	30.3	99.57
Chb19	3	3	0.0	100	46.0	99.66
Chb20	8	0	0.0	0	–	99.41
Chb22	3	3	0.0	100	39.7	99.66
Chb23	7	6	0.7	85.7	29.0	98.60
Total	78	58				
Mean			1.86		20.79	97.62
Sen		74.36				

Table 6

Real time detection using Dataset CHB-MIT and RUSBoosted tree Ensemble method.

Patient	NS	TP	FP (%)	Sen (%)	Delay (s)	Acc (%)
Chb01	7	7	0.0	100	3.1	99.70
Chb02	3	3	6.1	100	−52.7	93.86
Chb03	7	7	2.3	100	18.6	97.32
Chb04	4	4	8.3	100	38.5	91.49
Chb05	5	5	7.0	100	−4.2	92.75
Chb07	3	3	4.6	100	4.3	95.41
Chb08	5	5	3.0	100	1.8	96.50
Chb09	4	4	0.0	100	13.6	98.72
Chb10	7	7	5.6	100	18.3	94.09
Chb11	3	1	0.6	33.3	19.0	98.14
Chb17	3	3	0.5	100	22.7	99.27
Chb18	6	5	1.2	83.3	27.0	98.42
Chb19	3	3	0.4	100	15.7	99.48
Chb20	8	8	3.4	100	27.8	96.10
Chb22	3	3	0.2	100	14.7	99.68
Chb23	7	7	8.6	100	−1.5	91.13
Total	78	75				
Mean			3.24		10.42	96.38
Sen		96.15				

'*NS*' is the number of seizures, '*TP*' is true positive, '*FP*' is false positive rate, '*Sen*' is sensitivity, and '*Acc*' is accuracy. 'delay' represents the difference between the detected seizure onset time and the doctor's marker. Delay is negative if detected the seizure active signal early.

classification using the Set Z, Set F and Set S of Dataset UB, and they got 98.7 % accuracy [12]. Following the same mother wavelet technique DB4, this study achieved a satisfying result as well using Dataset UB. However, in another real-time experiment of Dataset CHB-MIT, DB4 is not the best mother wavelet because of different sample rate of two datasets and different level of decompositions. After increasing the DB value from 4 to 6, 8, …20 while calculate 7 eigenvalues, we found DB16 mother wavelet can distinguish seizure active and seizure free states more accurately.

4.2. Length of the sliding window

The sliding window size selection also directly affects the results. If the sliding window size is too small, the eigenvalues do not change before and after seizure. If the size is too big, the results may cause big delay in seizure onset detection. The performance of eigenvalue LE are provided as the results of two sliding window size (10 s and 30 s). According to the performance described in Fig. 4, the sliding window size was selected as 30 s in this study for seizure onset detection in Dataset
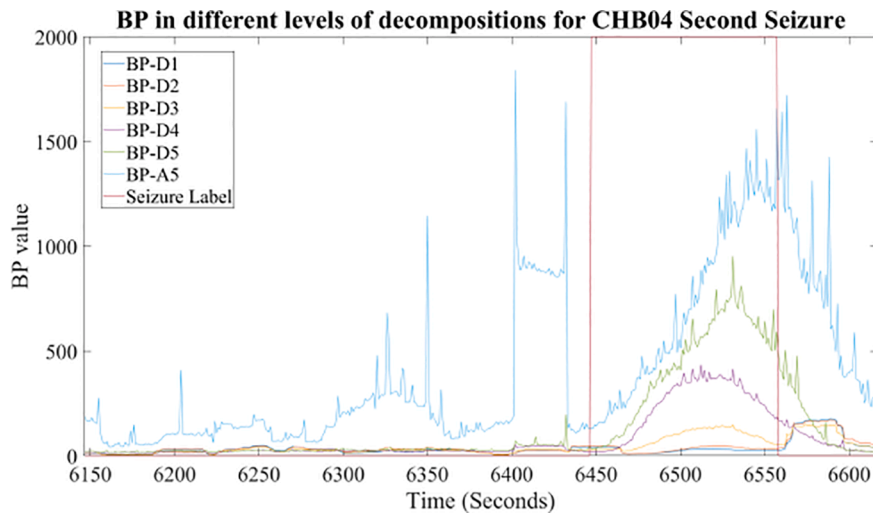
Fig. 3. BP in different levels of decompositions for Chb04 Second Seizure, seizure label line is the seizure state labelled by the doctor from the 6446 s to 6557 s.
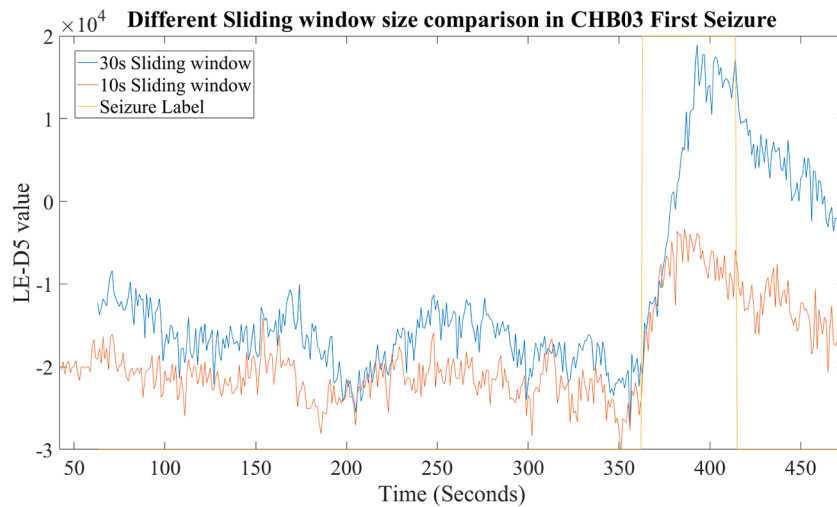
Fig. 4. LE-D5 in different sliding window size for Chb03 First Seizure, seizure label line is the seizure state labelled by the doctor from the 362 s to 414 s.

CHB-MIT because there are more significant differences in eigenvalue LE before and after seizure onset.

4.3. Training data and training method selection

Through the real-time sliding window analysis, 12 eigenvalues of Dataset UB and 7 eigenvalues of Dataset CHB-MIT were selected as the input of SVM and RUSBoosted tree Ensemble technique of the machine learning methods respectively, according to their performance in different seizure states and before and after seizure onset. The raw EEG data was segmented into 30 s epochs as the input for training. This work could avoid the confusing data, because in epilepsy onset detection the raw EEG signal wave will begin to change drastically in pre-seizure state which always appear before seizure onset several seconds. In addition, it significantly reduced the cost of training time as well.

Leaving one out training method based on SVM and RUSBoosted tree Ensemble models was used to analysis Dataset CHB-MIT. Leaving one out training method can be evaluated more objectively and compared with the random subject allocations for training and test. In addition, in seizure detection, the proportion of seizure free and seizure active differs significantly. Thus, the sensitivity of results is a very important parameter to assess the proposed method, and here RUSBoosted tree Ensemble model can provide a better result than SVM model (detail in Tables 5 and

6).

4.4. DWT and other methods in seizure detection

Tunable-Q wavelet transform (TQWT) as an advanced wavelet transform method has been used in epileptic EEG signals analysis. Bhattacharyya et al. proposed the TQWT with the entropy measure and achieved 98.6% accuracy results in Dataset UB [26]. Three parameters need to be defined in this experiment, which are the quality factor 'Q', the redundancy parameter 'r' and the number of decomposition levels 'J'. To compare the performance of TQWT and DWT in this experiment, parameter 'J' was selected as J = 5 in Dataset UB and J = 6 in Dataset CHB-MIT to replace the proposed DWT using the same eigenvalues and process. Thus, these TQWT were extracted with the same amounts of sub-bands as the DWT in this work. The redundancy parameter 'r' will be sufficient if r ≥ 3. For r ≈ 1, the wavelet will resemble the 'sinc' wavelet. When r ≥ 3, the passband of the level-J frequency response will not have a 'flat top' (where the frequency response is equal to a constant over a sub-interval of its passband). The parameter 'r' was selected as r = 3 in this experiment. The specified Q-factor should be chosen from the range of Q ≥ 1. Setting Q = 1 leads to a wavelet transform for which the wavelet resembles the second derivative of a Gaussian. Higher values of Q lead to more oscillatory wavelets. In this experiment, we select Q =

1,2,3,4 with r = 3, J = 5 in Dataset UB and Q = 1,2,3,4 with r = 3, J = 6 in Dataset CHB-MIT. Comparing the results with different values of quality factor 'Q', the best performance was observed when Q = 2. To compare the TQWT with the proposed DWT in this case, we selected the parameters of TQWT as Q = 2, r = 3, J = 5 for dataset UB and Q = 2, r = 3, J = 6 for dataset CHB-MIT to ensure the same decomposition levels in DWT. Using the same features and machine learning models, the TQWT achieved 79% accuracy in the three classes classification of health control, seizure free and seizure active groups in Dataset UB, and 74.36% sensitivity in Dataset CHB-MIT during the real time simulation.

This study focused more on the features' performance in each decomposition level for seizure detection than the wavelet methods. EEG is often described in terms of rhythmic activity, so that different frequency bands in DWT correspond to various EEG rhythms. As shown in Table 3, Dataset CHB-MIT, each decomposition level can correspond to the defined frequency band such as delta band (0–4 Hz), theta band (4–8 Hz), alpha–beta band (8–16 Hz), low-gamma band (16–32 Hz), high gamma band (64–128 Hz). We found the features in theta band and alpha–beta band had more significant difference before and after seizure onset. In Dataset UB, because of the different sample rate from the Dataset CHB-MIT, we divided the dataset in five frequency bands as shown in Table 2. In addition, it still can correspond to various EEG rhythms just a little difference which are delta band (0–5.4 Hz), theta band (5.4–10.8 Hz), alpha–beta band (10.8–21.7 Hz), low gamma band (21.7–43.4 Hz) and high gamma band (43.4–86.8 Hz) respectively. Therefore, using DWT in EEG analysis can provide more insights from the clinic detection perspective and we can focus on the specific frequency bands rather than the whole frequency band to reduce the computational load during the calculation.

4.5. Performance comparison with Dataset UB

Table 7 summarizes the performance of the proposed method and other peer works in the three-class classification using Dataset UB. Comparing with the previous works, this study used the whole data of 5 Sets and achieved a promising result (97% accuracy and 96.67% sensitivity). In this study, 80% data (segment 1 to segment 80, all 400 segments) of each set (Set Z, O, N, F, S) is used to training and the remaining 20% (segment 81 to segment 100, all 100 segments) were used to test the performance of the proposed method.

4.6. Performance comparison with previous work using Dataset CHB-MIT

A similar method is used to implement the real-time detection in Dataset CHB-MIT. Table 8 summarizes the results of the proposed real-time method and previous offline works in seizure detection using Dataset CHB-MIT. The proposed method achieved 96.38% accuracy, 96.15% sensitivity and 3.24% false positive rate in real-time seizure onset detection.

5. Conclusion

This study proposed an EEG based real-time epilepsy seizure detection approach using DWT, SVM and RUSBoosted tree Ensemble models of machine learning, and evaluated its performance by comparison. Using the 12 eigenvalues in corresponding decomposition levels extracted by DB4-DWT, and SVM models, our study achieved a 97% accuracy and 96.67% sensitivity in the three classes classification (health control, seizure-free and seizure-active) of Dataset UB. Experiments show the proposed method can classify the seizure free, health control and the seizure active states. In addition, our study also implemented the real-time seizure detection using DB16-DWT in seven eigenvalues with RUSBoosted tree Ensemble method, and obtained a 96.38% accuracy, 96.15% sensitivity and 3.24% false positive rate in Dataset CHB-MIT. The proposed method is also suitable for real-time seizure detection.

Table 7

Comparison of the proposed method and previous works using Dataset UB.

References	Feature extraction	Classifier	Datasets	Acc (%)
Kumar et al. (2014) [44]	DWT + fuzzy approximate entropy	SVM	Z, F, S	95.67
Acharya et al. (2012) [25]	Four entropy parameters	Fuzzy classifier	Z, F, S	98.1
Kaya and Ertuğrul (2018) [45]	One-dimensional ternary patterns	Random Forest	Z, F, S	95.7
Zhang et al. (2018) [46]	Generalized Stockwell Transform, singular value decomposition	Random Forest	Z, F, S	99
Omidvar et al. (2021) [12]	DWT + 11 features	ANN, SVM	Z, F, S	98.7
Bhattacharyya, A., et al. (2017) [26]	Tunable-Q wavelet transform, K-NN entropy	SVM	Z, F, N, O, S	98.6
Gupta, V. and R.B. Pachori (2019) [27]	Fourier-Bessel series expansion (Morelet wavelet)	Least squares SVM	Z, F, S	97.3
Anuragi, A., et al. (2022) [28]	Fourier-Bessel series expansion, EWT	Ensemble classifiers	Z, F, N, O, S	97.7
Proposed method	DWT + 12 features	SVM	Z, F, N, O, S	97

Table 8

Comparison of the proposed method and previous works using Dataset CHB-MIT.

Reference	Sen (%)	FP (%)	Delay (s)
Ahammad et al. (2014) [20]	98.50	14.4	1.76
Samiee et al. (2015) [29]	70.19	2.26	Not reported
Zabihi et al. (2015) [30]	88.27	6.79	Not reported
Bhattacharyya and Pachori (2017) [7]	97.91	0.43	Not reported
Fan and Chou (2018) [47]	97	8.61	6–7
Bomela et al. (2020) [8]	93.6	0.16 per hour	10.06
Wang, X., et al. (2021) [33]	88.14	0.38	Not reported
Li, C., et al. (2021) [35]	97.34	2.5	Not reported
Zarei, A. and B.M. Asl (2021) [34]	96.81	2.74	Not reported
Proposed method	96.15	3.24	10.42

Declaration of Competing Interest

The authors declare that they have no known competing financial interests or personal relationships that could have appeared to influence the work reported in this paper.

References

[1] A.S. Zandi, M. Javidan, G.A. Dumont, R. Tafreshi, Automated real-time epileptic seizure detection in scalp EEG recordings using an algorithm based on wavelet packet transform, IEEE Trans. Biomed. Eng. 57 (7) (2010) 1639–1651.

[2] L.S. Vidyaratne, K.M. Iftekharuddin, Real-time epileptic seizure detection using EEG, IEEE Trans. Neural Syst. Rehabil. Eng. 25 (11) (2017) 2146–2156.

[3] R.B. Yaffe, P. Borger, P. Megevand, D.M. Groppe, M.A. Kramer, C.J. Chu, S. Santaniello, C. Meisel, A.D. Mehta, S.V. Sarma, Physiology of functional and effective networks in epilepsy, Clin. Neurophysiol. 126 (2) (2015) 227–236.

[4] J. Xiang, C. Li, H. Li, R. Cao, B. Wang, X. Han, J. Chen, The detection of epileptic seizure signals based on fuzzy entropy, J. Neurosci. Methods 243 (2015) 18–25.

[5] D.C. Bergen, Do seizures harm the brain? Epilepsy Curr. 6 (4) (2006) 117–118.

[6] R. Rosch, T. Baldeweg, F. Moeller, G. Baier, Network dynamics in the healthy and epileptic developing brain, Network Neurosci. 2 (1) (2018) 41–59.

[7] A. Bhattacharyya, R.B. Pachori, A multivariate approach for patient-specific EEG seizure detection using empirical wavelet transform, IEEE Trans. Biomed. Eng. 64 (9) (2017) 2003–2015.

[8] W. Bomela, S. Wang, C.-A. Chou, J.-S. Li, Real-time inference and Detection of Disruptive eeG networks for epileptic Seizures, Sci. Rep. 10 (1) (2020).

[9] Y.i. Liang, C. Chen, F. Li, D. Yao, P. Xu, L. Yu, J.T. Cao, Altered Functional Connectivity after Epileptic Seizure Revealed by Scalp EEG, Neural Plasticity 2020 (2020) 1–8.

[10] H. Yu, L. Zhu, L. Cai, J. Wang, J. Liu, N. Shi, J. Liu, Variation of functional brain connectivity in epileptic seizures: an EEG analysis with cross-frequency phase synchronization, Cogn. Neurodyn. 14 (1) (2020) 35–49.

[11] J. Wu, T. Zhou, T. Li, Detecting epileptic seizures in EEG signals with complementary ensemble empirical mode decomposition and extreme gradient boosting, Entropy 22 (2) (2020) 140.

[12] M. Omidvar, A. Zahedi, H. Bakhshi, EEG signal processing for epilepsy seizure detection using 5-level Db4 discrete wavelet transform, GA-based feature selection and ANN/SVM classifiers, J. Ambient Intell. Hum. Comput. 12 (11) (2021) 10395–10403.

[13] K. Jindal, R. Upadhyay, H.S. Singh, Application of tunable-Q wavelet transform based nonlinear features in epileptic seizure detection, Analog Integr. Circ. Sig. Process 100 (2) (2019) 437–452.

[14] R.J. Oweis, E.W. Abdulhay, Seizure classification in EEG signals utilizing Hilbert-Huang transform, Biomed. Eng. Online 10 (1) (2011) 1–15.

[15] W. Hu, et al., Mean amplitude spectrum based epileptic state classification for seizure prediction using convolutional neural networks, J. Ambient Intell. Hum. Comput. (2019) 1–11.

[16] B. Akbarian, A. Erfanian, A framework for seizure detection using effective connectivity, graph theory, and multi-level modular network, Biomed. Signal Process. Control 59 (2020) 101878.

[17] Y. Gao, Z. Zhao, Y. Chen, G. Mahara, J. Huang, Z. Lin, J. Zhang, Automatic epileptic seizure classification in multichannel EEG time series with linear discriminant analysis, Technol. Health Care 28 (1) (2020) 23–33.

[18] Y.L. Niriayo, A. Mamo, T.D. Kassa, S.W. Asgedom, T.M. Atey, K. Gidey, G. T. Demoz, S. Ibrahim, Treatment outcome and associated factors among patients with epilepsy, Sci. Rep. 8 (1) (2018).

[19] C. Donos, M. Dümpelmann, A. Schulze-Bonhage, Early seizure detection algorithm based on intracranial EEG and random forest classification, Int. J. Neural Syst. 25 (05) (2015) 1550023.

[20] N. Ahammad, T. Fathima, P. Joseph, Detection of epileptic seizure event and onset using EEG, BioMed. Res. Int. 2014 (2014) 1–7.

[21] M. Qaraqe, M. Ismail, E. Serpedin, H. Zulfi, Epileptic seizure onset detection based on EEG and ECG data fusion, Epilepsy Behav. 58 (2016) 48–60.

[22] V. Joshi, R.B. Pachori, A. Vijesh, Classification of ictal and seizure-free EEG signals using fractional linear prediction, Biomed. Signal Process. Control 9 (2014) 1–5.

[23] P. Ghaderyan, A. Abbasi, M.H. Sedaaghi, An efficient seizure prediction method using KNN-based undersampling and linear frequency measures, J. Neurosci. Methods 232 (2014) 134–142.

[24] G. Chen, Automatic EEG seizure detection using dual-tree complex wavelet-Fourier features, Expert Syst. Appl. 41 (5) (2014) 2391–2394.

[25] U.R. Acharya, F. Molinari, S.V. Sree, S. Chattopadhyay, K.-H. Ng, J.S. Suri, Automated diagnosis of epileptic EEG using entropies, Biomed. Signal Process. Control 7 (4) (2012) 401–408.

[26] A. Bhattacharyya, et al., Tunable-Q wavelet transform based multiscale entropy measure for automated classification of epileptic EEG signals, Appl. Sci. 7(4) (2017) 385.

[27] V. Gupta, R.B. Pachori, Epileptic seizure identification using entropy of FBSE based EEG rhythms, Biomed. Signal Process. Control 53 (2019) 101569.

[28] A. Anuragi, D.S. Sisodia, R.B. Pachori, Automated FBSE-EWT based learning framework for detection of epileptic seizures using time-segmented EEG signals, Comput. Biol. Med. 136 (2021) 104708.

[29] K. Samiee, S. Kiranyaz, M. Gabbouj, T. Saramäki, Long-term epileptic EEG classification via 2D mapping and textural features, Expert Syst. Appl. 42 (20) (2015) 7175–7185.

[30] M. Zabihi, S. Kiranyaz, A.B. Rad, A.K. Katsaggelos, M. Gabbouj, T. Ince, Analysis of high-dimensional phase space via Poincaré section for patient-specific seizure detection, IEEE Trans. Neural Syst. Rehabil. Eng. 24 (3) (2016) 386–398.

[31] G. Wang, D. Ren, K. Li, D. Wang, M. Wang, X. Yan, EEG-based detection of epileptic seizures through the use of a directed transfer function method, IEEE Access 6 (2018) 47189–47198.

[32] H. Rajaei, M. Adjouadi, M. Cabrerizo, P. Janwattanapong, A. Pinzon, S. Gonzales-Arias, A. Barreto, J. Andrian, N. Rishe, I. Yaylali, Dynamics and Distant Effects of Frontal/Temporal Epileptogenic Focus Using Functional Connectivity Maps, IEEE Trans. Biomed. Eng. 67 (2) (2020) 632–643.

[33] X. Wang, X. Wang, W. Liu, Z. Chang, T. Kärkkäinen, F. Cong, One dimensional convolutional neural networks for seizure onset detection using long-term scalp and intracranial EEG, Neurocomputing 459 (2021) 212–222.

[34] A. Zarei, B.M. Asl, Automatic seizure detection using orthogonal matching pursuit, discrete wavelet transform, and entropy based features of EEG signals, Comput. Biol. Med. 131 (2021) 104250.

[35] C. Li, W. Zhou, G. Liu, Y. Zhang, M. Geng, Z. Liu, S. Wang, W. Shang, Seizure Onset Detection Using Empirical Mode Decomposition and Common Spatial Pattern, IEEE Trans. Neural Syst. Rehabil. Eng. 29 (2021) 458–467.

[36] R.G. Andrzejak, K. Lehnertz, F. Mormann, C. Rieke, P. David, C.E. Elger, Indications of nonlinear deterministic and finite-dimensional structures in time series of brain electrical activity: Dependence on recording region and brain state, Phys. Rev. E 64 (6) (2001) 061907.

[37] U. Herwig, P. Satrapi, C. Schönfeldt-Lecuona, Using the international 10–20 EEG system for positioning of transcranial magnetic stimulation, Brain Topogr. 16 (2) (2003) 95–99.

[38] A.L. Goldberger, L.A.N. Amaral, L. Glass, J.M. Hausdorff, P.C. Ivanov, R.G. Mark, J. E. Mietus, G.B. Moody, C.-K. Peng, H.E. Stanley, PhysioToolkit, and PhysioNet: components of a new research resource for complex physiologic signals, Circulation 101 (23) (2000).

[39] M. Stephane, A wavelet tour of signal processing, Elsevier, 1999.

[40] M. Vetterli, C. Herley, Wavelets and filter banks: Theory and design, IEEE Trans. Sign. Process. 40(ARTICLE) (1992) 2207–2232.

[41] C.E. Shannon, A mathematical theory of communication, Bell Syst. Techn. J. 27 (3) (1948) 379–423.

[42] A. Ishikawa, H. Mieno, The fuzzy entropy concept and its application, Fuzzy Sets Syst. 2 (2) (1979) 113–123.

[44] Y. Kumar, M. Dewal, R. Anand, Epileptic seizure detection using DWT based fuzzy approximate entropy and support vector machine, Neurocomputing 133 (2014) 271–279.

[45] Y. Kaya, Ö.F. Ertuğrul, A stable feature extraction method in classification epileptic EEG signals, Australas. Phys. Eng. Sci. Med. 41 (3) (2018) 721–730.

[46] Y. Zhang, et al., Integration of 24 feature types to accurately detect and predict seizures using scalp EEG signals, Sensors 18 (5) (2018) 1372.

[47] M. Fan, C.-A. Chou, Detecting abnormal pattern of epileptic seizures via temporal synchronization of EEG signals, IEEE Trans. Biomed. Eng. 66 (3) (2018) 601–608.

CHAPTER 4: PAPER 2 –Real-time epilepsy seizure detection based on EEG using tunable-Q wavelet transform and convolutional neural network

4.1 Overview of Paper 2

The details of the Paper 2 are given below:

- Paper title: "Real-time epilepsy seizure detection based on EEG using tunable-Q wavelet transform and convolutional neural network."
- Paper length: 9 pages
- Journal: Biomedical signal processing and control
    - Rank: Q1 (Biomedical Engineering)
    - Impact factor: 5.1 (2022-2023)
    - Cite Score: 8.2 (2022)
    - SJR: 1.071 (2022)
    - SNIP: 1.552 (2022)
- DOI: https://doi.org/10.1016/j.bspc.2022.104566
- First author: Mingkan Shen
- Corresponding author: Mingkan Shen

HDR thesis author's declaration

☒ The authors declare that they have no known competing financial   interests or personal relationships that could have appeared to influence the work reported in this paper.

☐ The authors declare the following financial interests/personal relationships which may be considered as potential competing interests:

Table 4.1: Authorship contributions of Paper 2

Conception and design of study	Mingkan Shen, Peng Wen, Bo Song, Yan Li
Analysis and interpretation of data	Mingkan Shen
Drafting the manuscript	Mingkan Shen
Revising the manuscript critically for important intellectual content	Mingkan Shen, Peng Wen, Bo Song, Yan Li

| Approval of the version of the manuscript to be published | Mingkan Shen, Peng Wen, Bo Song, Yan Li |

4.2   Summary of Paper 2

Epileptic seizures, unpredictable in nature and abrupt in onset, pose significant risks if not identified and managed immediately. The challenge lies in the real-time detection of these seizures to provide prompt intervention. The utilization of EEG data has been at the forefront of attempts to address this challenge. This paper pioneers an innovative methodology that amalgamates the advantages of the TQWT and the computational depth of CNN to detect seizures using EEG signals in real time.

EEG signals, with their complex and multifaceted characteristics, demand an advanced analytical approach for efficient interpretation. The TQWT, with its capacity to analyse non-stationary signals and adjust its Q-factor, permits the extraction of pertinent features from segmented EEG signals. Subsequent to this feature extraction, we introduced these segments into a convolutional neural network. The CNN, renowned for its ability to handle intricate patterns in image and signal processing, was optimized to classify these segments as seizure or non-seizure events.

Based on a study encompassing EEG data from 16 patients diagnosed with epilepsy, our methodology exhibited promising results in the real-time detection of seizures. Beyond the sheer accuracy of detection, this paper also sheds light on the potential of integrating the TQWT-CNN approach into next-generation wearable devices.

4.3   Paper file

Real-time epilepsy seizure detection based on EEG using tunable-Q wavelet transform and convolutional neural network

Mingkan Shen [a,*], Peng Wen [a], Bo Song [a], Yan Li [b]

[a] School of Mechanical and Electrical Engineering, University of Southern Queensland, Toowoomba, QLD 4350, Australia
[b] School of Science, University of Southern Queensland, Toowoomba, QLD 4350, Australia

ARTICLE INFO

ABSTRACT

Epilepsy is a chronic disease caused by sudden abnormal discharge of brain neurons, leading to transient brain dysfunctions. This paper proposed an EEG based real-time approach to detect epilepsy seizures using tunable-Q wavelet transform and convolutional neural network (CNN). Statistical moments and spectral band power were used to reveal the time domain and frequency domain features in EEG, and then were converted into imaged-like data fed into CNN. The proposed approach was evaluated using the database CHB-MIT. The proposed algorithm achieved 97.57% in accuracy, 98.90% in sensitivity, 2.13% in false positive rate and 10.46-second delay. In addition, the proposed method is suitable in real-time implementation. The outcomes indicate that the proposed method can applied to real-time seizure detection in clinical applications.

1. Introduction

Epilepsy is a chronic non-communicable disease caused by the abnormal synchronous electrical activity of brain neurons [1,2]. It is one of the most common neurological diseases, which affects approximately 50 million people in the world [2,3]. Repeated seizures can cause persistent adverse effects on patients' mental and cognitive functions, and bring life-threatening risks [4]. Therefore, research on the diagnosis and treatment of epilepsy has important clinical significance. Automatic identification of epilepsy seizures from electroencephalogram (EEG) signals and its real-time implementation can provide an objective reference basis for the diagnosis and in time evaluation of epilepsy, thereby reducing the workload of doctors and improving the efficiency of treatment [5]. Bhattacharyya et al. introduced a real-time seizure detection approach through the empirical Wavelet transform method [6]. Disruptive EEG networks for epileptic seizures in real-time application was reported by Bomela et al. [7]. Harmonic Wavelet packet transform with relevance vector machine method was proposed by Vidyaratne et al [2]. Automatic seizure detection based on imaged-EEG signals through fully convolutional networks research was reported by Gómez, C., et al., and they achieved 98.0% in accuracy and 98.3% in specificity result [8]. A deep learning method via two-dimensional deep convolutional autoencoder method was developed by Abdelhameed, A. and M. Bayoumi, and they achieved 98.79% in accuracy and 98.72% in sensitivity [9].

EEG abnormalities in epileptic seizures are mainly manifested as spike waves and sharp waves [10]. Many methods in time, frequency, and time–frequency domains have been developed, such as discrete wavelet transform (DWT), empirical mode decomposition (EMD), Q-wavelet transformation, Hilbert-Huang transform (HHT), mean amplitude spectrum (MAS), tunable-Q wavelet transform (TQWT), etc. [6,11–15]. An important progress in epilepsy seizure detection is the development of machine learning based classification methods. The support vector machine (SVM), linear discriminant analysis (LDA), naive Bayes, logistic regression (LR) and random forest were used to classify the different seizure states in previous studies [11,15–19]. Traditional machine learning methods require manual feature extraction and model matching, while deep learning methods greatly simplify the preprocessing process, which can automatically extract features and complete decoding at the same time. Deep convolutional neural network (CNN) was proposed by Gao et al. and achieved an average classification accuracy of 90% in epilepsy detection [20]. Long short-term memory networks (LSTM) deep learning method was reported by Cao et al., in their experiment, they achieved an 96.3% accuracy [21]. Currently, automatic epilepsy detection can be divided into two types: offline seizure detection and real-time seizure detection. The purpose of offline seizure detection is to identify epileptic seizure signals as accurately as possible from EEG signal [22]. The purpose of real-time seizure
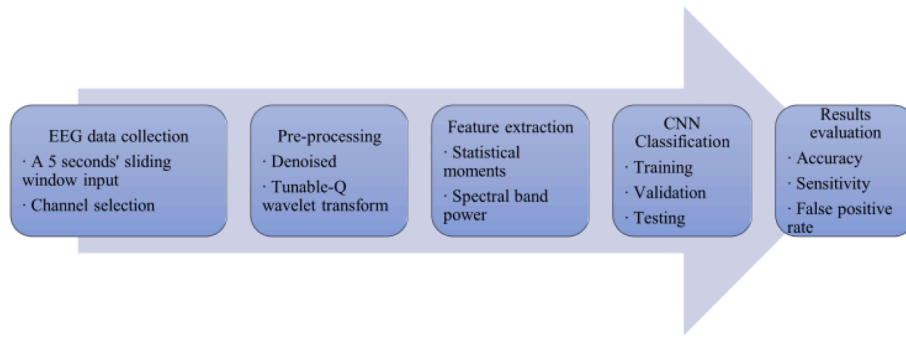

Fig. 1. The framework and main procedures.

Table 1
Data collection from Long-term EEG data Dataset CHB-MIT.

Patient	EEG used (h)	Number of seizures	Seizure duration (s)
Chb01	25	7	40,27,40,51,90,93,101
Chb02	16	3	82,81,9
Chb03	36	7	52,65,69,52,47,64,53
Chb04	25	4	49,111,102,116
Chb05	14	5	115,110,96,120,117
Chb07	28	3	86,96,143
Chb08	16	5	171,190,134,160,264
Chb09	34	4	64,79,71,62
Chb10	20	7	35,70,65,58,76,89,54
Chb17	15	3	90,115,88
Chb18	18	6	50,30,68,55,68,46
Chb19	14	3	78,77,81
Chb20	15	8	29,30,39,38,35,49,35,39
Chb22	15	3	58,74,72
Chb23	14	7	113,20,47,71,62,27,84
Chb24	12	16	25,25,29,25,32,27,19,24,22,19,70,16,27,17,66,68

detection is to identify seizures onsite with the shortest possible delay when the patient has a seizure during continuous EEG monitoring [23].

Samiee et al. used multivariate textural features with gray-level co-occurrence matrix (GLCM) in SVM and reported a 70.19% sensitivity in the real-time seizure detection [24]. As a contrast, time delay embedding method proposed by Zabihi et al. obtained an 89.01% sensitivity [25]. In particularly, graph theory analysis, function connectivity analysis and effective connectivity analysis were used in the seizure detection [15,26–27]. Bomela et al. constructed the network connectivity using Fourier transform to detect the seizure onset and reported 93.6 % sensitivity and a false positive (FP) rate of 0.16 per hour (FP/h) result [7]. A stacked 1D-CNN model is presented via Wang, X., et al. to detect seizure onset automatically and achieved 88.14% accuracy and 0.38% FP rate result [28]. Orthogonal matching pursuit with DWT as pre-processing progress with non-linear features and SVM classifier can also detect the seizure onset in the same dataset. Zarei, A. and B.M. Asl used this method and reported 96.81% sensitivity and 2.74% FP result [29]. Li, C., et al. proposed EMD, common spatial pattern and SVM model get 97.34% sensitivity, 2.5% FP output as well [30]. In our previous work, we achieved 96.15% sensitivity, 96.38% accuracy and 3.24% false positive rate for the real-time seizure onset detection via DWT and RUSBoosted tree Ensemble method [31].

With the recent high-speed development of artificial intelligence techniques in graph classification, research combining signal processing and image classification are used widely in EEG based clinical applications. Chen et al. constructed the imaged-like data via mutual information (MI) brain network matrix based on the EEG attention-deficit/hyperactivity disorder (ADHD) signal as the input of CNN model, and they reported an accuracy of 94.67% on the test data [32]. Ozcan, A.R. and S. Erturk, using 3D-CNN model with an imaged-based approach in

seizure prediction work [33]. They converted the statistical moments, Hjorth parameters and spectral band power into 3Dimaged-like data and achieved 85.7% sensitivity and a false prediction rate of 0.096/h in their study. Considering the good performance of this method in other EEG research areas, we applied it in this study by combining the signal processing and image classification in EEG real-time epilepsy seizure detection.

This study aims to develop a seizure detection approach which can be implemented in real-time. In this study, the Butterworth zero-phase filter denoised method and TQWT method were used for the data pre-processing. Statistical moments and spectral band power were calculated to reveal the time domain and frequency domain features to distinguish the seizure-free and seizure active states. The features were then converted into imaged-like data as the input of the CNN models for training and testing using Database CHB-MIT. Finally, the approached is implemented using a 5-second sliding window. All the experiments in this study were carried out in a Dell workstation with dual Intel Xeon E5-2697 V3 CPUs using MATLAB 2021b.

The first section of the paper provides a brief introduction of this study. Section II describes the details of the EEG long-term epilepsy patients' Database CHB-MIT. The pre-processing, feature extraction and CNN model classification are also introduced in this section. Section III reported the work in our experiments and results obtained using the proposed method. Comparisons of previous work using the same datasets were conducted and evaluated in Section IV. Section V concluded the paper.

2. Methodology

In this study, the proposed real-time EEG based seizure detection method includes four major steps using CHB-MIT Database. EEG data from eight channels was selected in this study and the moving sliding window size was selected as 5 s. The Butterworth algorithm was applied to denoise the EEG raw data and TQWT analysis was used to decompose the EEG signal data. After feature extraction, 30 eigenvalues from both time domain and frequency domain features of each EEG channel data were converted into 8*30 imaged-like data as the input of the CNN model to classify seizure free and seizure active subjects for real-time epilepsy seizure detection. The framework of the proposed method is described in Fig. 1.

2.1. EEG data collection

Database CHB-MIT was collected by Boston Children's Hospital with 23 subjects (5 males in age 3–22 years and 17 females in age 1.5–19 years) [34]. The CHB-MIT data was sampled at 256 Hz from 23 bipolar channels by scalp EEG standard 10–20 system caps. In this experiment, 8 electrodes closer to both sides of frontal and temporal regions, such as channel FP1 - F7, F7 - T7, T7 - P7, T7 - FT9, FP2 - F8, F8 - T8, T8 - P8 and FT10 - T8, were used to detect the seizure onset in real-time applications. This study used 16 patients from the CHB-MIT Database, which

Table 2
Extra details of the CHB-MIT Database.

Patient	Gender	Age (y)	Seizure type	Seizure onset zone
Chb01	F	11	SP, CP	Temporal
Chb02	M	11	SP, CP, GTC	Frontal
Chb03	F	14	SP, CP	Temporal
Chb04	M	22	SP, CP, GTC	Temporal, Occipital
Chb05	F	7	CP, GTC	Frontal
Chb07	F	14.5	SP, CP, GTC	Temporal
Chb08	M	3.5	SP, CP, GTC	Temporal
Chb09	F	10	CP, GTC	Frontal
Chb10	M	3	SP, CP, GTC	Temporal
Chb17	F	12	SP, CP, GTC	Temporal
Chb18	F	18	SP, CP	Temporal, Occipital
Chb19	F	19	SP, CP, GTC	Frontal
Chb20	F	6	SP, CP, GTC	Temporal
Chb22	F	9	Not reported	Temporal, Occipital
Chb23	F	6	Not reported	Frontal
Chb24	F	13.5	SP, CP	Temporal

Here, '*GTC*' is generalized tonic-clonic seizures, '*CP*' is complex partial seizures, '*SP*' is simple partial seizures.

excluded patients that had seizures characterized by amplitude depression [14]. The selected subject details are shown in Table 1.

The extra details of CHB-MIT database are summarized in Table 2.

2.2. Pre-processing

In this work, EEG signals were firstly segmented into a 5-second sliding window size with 1-second overlap. A six order Butterworth zero-phase filter between 1 and 50 Hz was used to denoise the raw EEG data. One of the most challenging parts of the EEG based epilepsy seizure detection is to detect the sharp waves and spike waves. However, in different brain rhythms, the features perform differently between different seizure states. TQWT is extensively to decompose an EEG signal into different frequency sub-bands. In TQWT analysis, three adjustable parameters are needed for different signal, which are quality factor '*Q*', the redundancy parameter '*r*' and the number of levels of decomposition '*j*'. The selection of appropriate TQWT parameters significantly affects classification of seizure free and seizure active EEG. The formula of

TQWT is shown in formula (1) and (2):

$$
G_0^j = \begin{cases} \Pi_{m=0}^{j-1} G_0\left(\dfrac{\omega}{\alpha^m}\right), |\omega| \leqslant \alpha^j \pi \\ 0, \alpha^j \pi \leqslant |w| \leqslant \pi \end{cases} \tag{1}
$$

$$
G_1^j = \begin{cases} G_1\left(\dfrac{\omega}{\alpha^{j-1}}\right) \Pi_{m=0}^{j-2} G_0\left(\dfrac{\omega}{\alpha^m}\right), (1-\beta)\alpha^{j-1} \leqslant |\omega| \langle \alpha^{j-1} \pi \\ 0, \omega \in [-\pi, \pi] \end{cases} \tag{2}
$$

where 'α' is the low-pass scaling of low-pass frequency response '$G_0(\omega)G_0(\omega)$', 'β' is the high pass scaling of high-pass frequency response '$G_1(\omega)G_1(\omega)$' (the conditions $0 < \alpha < 1$, $0 < \beta \leq 1$, and $\alpha + \beta > 1$ is selected to avoid redundancy in signal reconstruction progress), and 'j' is the decomposition level.

The Quality factor 'Q' affects the oscillation behaviour of wavelets and the extent to which the wavelet oscillations are maintained, and expressed as:

$$
Q = \frac{2-\beta}{\beta} \tag{3}
$$

The redundancy parameter 'r' is the oversampling rate calculated as:

$$
r = \frac{\beta}{1-\alpha} \tag{4}
$$

In this study, the redundancy parameter 'r' was selected as 3. The redundancy parameter 'r' will be sufficient if $r \geq 3$. For $r \approx 1$, the wavelet will resemble the '$sinc$' wavelet. When $r \geq 3$, the passband of the level-J frequency response will not have a 'flat top' (where the frequency response is equal to a constant over a sub-interval of its passband) [35]. The Quality factor 'Q' was adjusted as 2 and the specified Q-factor should be chosen from $Q \geq 1$. Setting $Q = 1$ leads to a wavelet transform for which the wavelet resembles the second derivative of a Gaussian, and higher values of 'Q' lead to more oscillatory wavelets [35]. In addition, we divided the EEG raw signal into 6 sub-bands when selected $j = 5$, because j levels decomposition corresponds to into $j + 1$ sub-bands [36]. Then, the first 1280 samples of sub-band 2, the first 640 samples of sub-bands 3, 4, 6 and 320 samples of sub-band 5 were selected respectively, which demonstrate significant differences between seizure free and
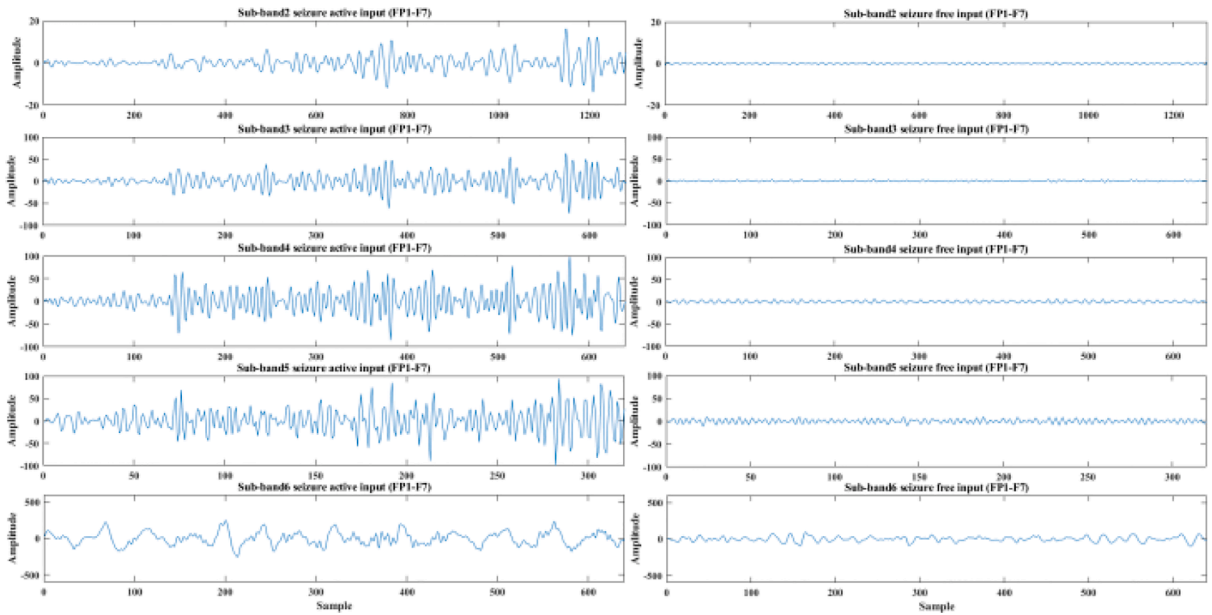
Fig. 2. (a) Sub-band 2 seizure active data, (b) Sub-band 3 seizure active data, (c) Sub-band 4 seizure active data, (d) Sub-band 5 seizure active data, (e) Sub-band 6 seizure active data, (f) Sub-band 2 seizure free data, (g) Sub-band 3 seizure free data, (h) Sub-band 4 seizure free data, (i) Sub-band 5 seizure free data, (j) Sub-band 6 seizure free data. The seizure active input is collected from Chb01_03 from 3006 s to 3011 s data of Channel FP1 – F7, the seizure free input is collected from Chb01_03 from 55 s to 60 s data of Channel FP1 – F7.
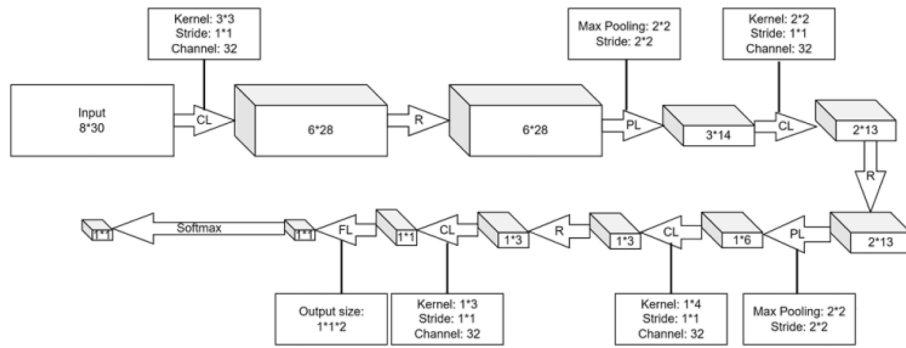
Fig. 3. Diagram of 11-layer CNN architecture, '*CL*' is convolution layer, '*R*' is ReLU, '*PL*' is max pooling layer and '*FL*' is fully connected layer.

Table 3
The architecture of CNN for training and test of the seizure detection.

Layer	Input size	Output size	Trainable parameters
Imaged-data input	8*30*1		
Convolution layer	8*30*1	6*28*32	Kernel size: 3*3 Stride: 1*1 Channel: 32
ReLU	6*28*32	6*28*32	
Max Pooling layer	3*14*32	3*14*32	Pooling size: 2*2 Stride: 2*2
Convolution layer	3*14*32	2*13*32	Kernel size: 2*2 Stride: 1*1 Channel: 32
ReLU	2*13*32	2*13*32	
Max Pooling layer	2*13*32	1*6*32	Pooling size: 2*2 Stride: 1*1
Convolution layer	1*6*32	1*3*32	Kernel size: 1*4 Stride: 1*1 Channel: 32
ReLU	1*3*32	1*3*32	
Convolution layer	1*3*32	1*1*32	Kernel size: 1*3 Stride: 1*1
Fully Connected layer	1*1*32	1*1*2	Channel: 32
Softmax	1*1*2		

Table 4
The validation accuracy of 16 CNN training models.

| Subject for CNN training model	Validation Acc (%)
Chb01	97.38
Chb02	97.29
Chb03	97.50
Chb04	97.51
Chb05	97.43
Chb07	97.20
Chb08	97.10
Chb09	97.10
Chb10	97.06
Chb17	97.63
Chb18	97.65
Chb19	97.27
Chb20	96.91
Chb22	97.27
Chb23	97.08
Chb24	95.74
Mean ± SD	97.20 ± 0.44

'*Acc*' is accuracy.

seizure active states. Detail is shown in the Fig. 2.

2.3. Feature extraction

Five time domain statistical moments from each sub-band were calculated to assess and find the differences in different seizure states.

The time domain features contain the standard deviation (SD), mean value, variance, skewness and kurtosis. Furthermore, the frequency domain features were considered in this study as well, we calculated the spectral band power from the denoised EEG data and divided it into five frequency bands, which are δ δ band (1–4 Hz), θ band (4–8 Hz), α band (8–12 Hz), β band (12–30 Hz) and γ band (30–50 Hz) respectively. As a result, 25 time domain eigenvalues and 5 frequency domain eigenvalues were derived for each 5-second sliding window data.

Both SD and variance can be used to describe the degree of dispersion of the signal, and can be obtained as below in formula (5) and (6)

$$SD = \sqrt{\frac{1}{N} \sum_{n=0}^{N} (S_n - \mu)^2} \tag{5}$$

$$Variance = SD^2 = \frac{1}{N} \Sigma_{n=0}^{N} (S_n - \mu)^2 \tag{6}$$

$H(F_i, F_j)$ Kurtosis is a measure of the peak of the probability distribution of a real random variable. High kurtosis means that the increase in variance is caused by extreme differences in low frequencies that are greater than or less than the average. Skewness describes the measure of the asymmetry of a probability distribution function. The formula of kurtosis and skewness is described in formula (7) and formula (8).

$$Kurtosis = \frac{E(x - \mu)^4}{\sigma^4} \tag{7}$$

$$Skewness = \frac{E(x - \mu)^3}{\sigma^3} \tag{8}$$

where 'μ' is the mean value and 'σ' is the SD of the EEG segments, and E(.) is the expectation operator.

In addition, we calculate the percentage of the total power in a specified frequency interval.

$$SpectrualBP(\delta, \theta, \alpha, \beta, \gamma) = \frac{\text{Power}(\delta, \theta, \alpha, \beta, \gamma)}{\text{Power}(1 - 50Hz)}\% \tag{9}$$

Eight channels were selected in this study, and each channel included 30 eigenvalues. Thus, we construct the imaged-like data into an 8*30 matrix as the input of CNN model.

2.4. Classification via convolutional neural networks

Following the approach based on the VGGNet, a 11-layer CNN was constructed in this study which shown in Fig. 3 [37]. The leaving one out training method and CNN deep learning method were applied to detect seizure onset using Database CHB-MIT.

1) *Leaving one out experiment for Database CHB-MIT*

Sixteen patients' data from Database CHB-MIT (detail shown in Table 1) was used in this part. In leaving one out training method, one subject
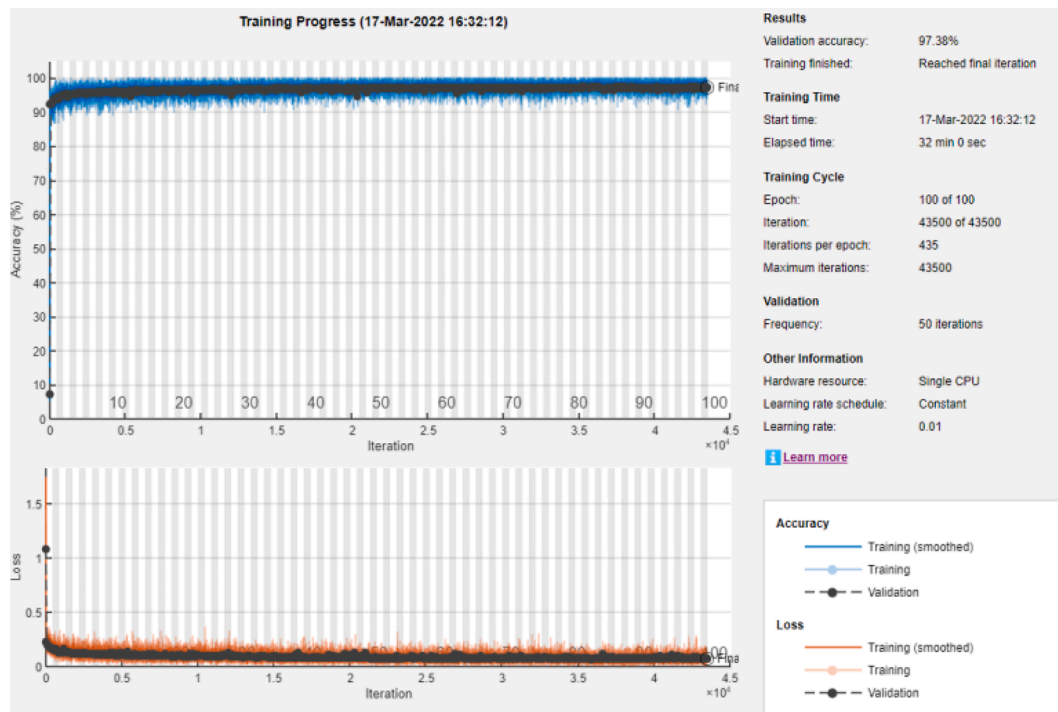
Fig. 4. Training progress for case 'Chb01' based on MATLAB 2021b software.
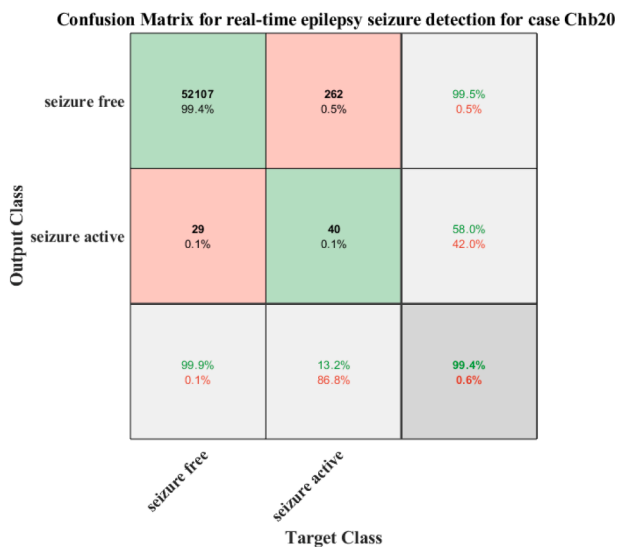
Fig. 5. Confusion matrix for real-time epilepsy seizure detection for case 'Chb20'.

Table 5
Real time detection for Database CHB-MIT using CNN method.

Patient	NS	TP	FP (%)	Sen (%)	Delay (s)	Acc (%)
Chb01	7	7	0.13	100	12.60	99.59
Chb02	3	3	3.74	100	7.36	96.13
Chb03	7	7	0.64	100	6.88	98.97
Chb04	4	4	7.73	100	38.53	91.86
Chb05	5	5	7.96	100	1.03	91.99
Chb07	3	3	4.73	100	3.03	95.22
Chb08	5	5	0.27	100	9.23	98.53
Chb09	4	4	1.50	100	−3.97	98.49
Chb10	7	7	2.71	100	8.32	97.11
Chb17	3	3	0.59	100	15.36	98.98
Chb18	6	5	0.30	83.33	19.43	99.42
Chb19	3	3	0.17	100	10.36	99.65
Chb20	8	8	0.50	100	24.78	99.45
Chb22	3	3	0.58	100	6.03	99.32
Chb23	7	7	1.64	100	−0.97	97.68
Chb24	16	16	0.86	100	9.41	98.70
Total	91	90				
Mean			2.13		10.46	97.57
Sen		98.90				

'*NS*' is the number of seizures, '*TP*' is true positive, '*FP*' is false positive rate, '*Sen*' is sensitivity, and '*Acc*' is accuracy.

data was used for testing, and the other 15 subjects were used for training. As a result, 16 models have been trained.

In this part, the EEG data was segmented into 5-second epoch with a 256 Hz sample rate, which resulted in 1280 sampling points in each epoch. In all 16 subjects, the EEG raw data of 10 min before seizure epochs and 5 min after seizure epochs for each subject data were used to train. The 1-minute interval between the preictal period and the seizure was considered an intervention time and excluded from the training data.

2) *Convolutional neural network*

In this study, the 8*30 size imaged-like data is the input of the CNN

model. In CNN model analysis, the training progress selects the learning rate as 0.01, and epochs as 100.

The CNN model includes four convolution layers with batch normalization, two max pooling layers, three ReLU layers and one fully connected layer. The six convolution layers all use 32 filters with convolution kernels of 3*3, 2*2, 1*4, and 1*3, respectively. Batch normalization of each convolution layer is to reduce the internal covariance shift, which can improve training speed and reduce the over-fitting phenomenon. Two Max pooling layers of this architecture are to reduce the cost of training calculation with 2*2 size and 2*2 stride. The activation function ReLU is defined as f(x) = tanh(x) which is used to activate or deactivate a node based on mapped value. The last part is the fully connected layer followed by a Softmax classifier for the identification using the concatenated outputs of the last layers. Table 3
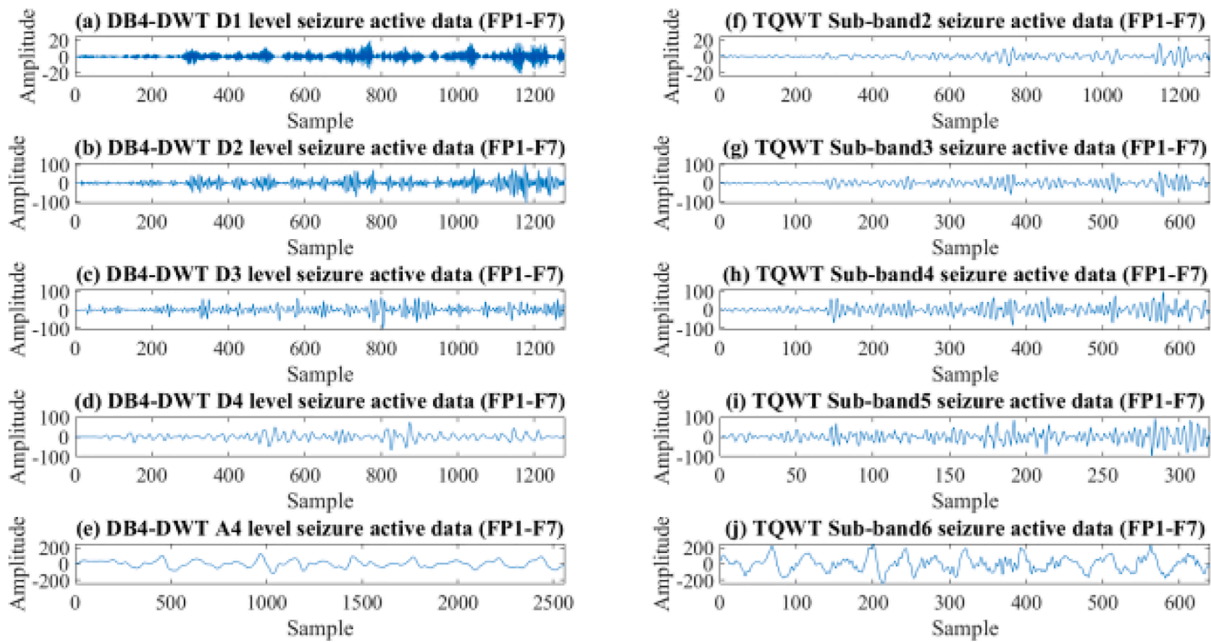
Fig. 6. (a) DB4-DWT D1 level seizure active data, (b) DB4-DWT D2 level seizure active data, (c) DB4-DWT D3 level seizure active data, (d) DB4-DWT D4 level 5 seizure active data, (e) DB4-DWT A4 level seizure active data, (f) TQWT sub-band 2 seizure active data, (g) TQWT sub-band 3 seizure active data, (h) TQWT sub-band 4 seizure active data, (i) TQWT sub-band 5 seizure active data, (j) TQWT sub-band 6 seizure active data. The seizure active input is collected from Chb01_03 from 3006 s to 3011 s data of Channel FP1 – F7.

Table 6
Statistical analysis in TQWT method.

State	Eigenvalue	TQWT decomposition levels				
		Sub-2	Sub-3	Sub-4	Sub-5	Sub-6
Seizure-free	SD	1.3619 ± 2.2613	6.5784 ± 10.3294	10.4072 ± 13.2264	15.0327 ± 17.3020	39.1627 ± 28.2774
	Var	8.0975 ± 64.3944	173.8810 ± 1273.8478	325.4521 ± 1443.8094	609.1218 ± 2319.7164	2790.4187 ± 12547.2178
	Mean	0.0001 ± 0.0015	0.8034 ± 1.5672	-0.0001 ± 0.0069	0.0001 ± 0.0121	-0.0027 ± 0.2678
	SK	0.0011 ± 0.2146	-0.0002 ± 0.0827	-0.0006 ± 0.0870	0.0001 ± 0.0950	0.0936 ± 0.2188
	Kur	6.2395 ± 5.3059	5.3712 ± 4.3218	5.4932 ± 4.4805	5.3152 ± 4.2003	4.7753 ± 2.2624
Seizure-active	SD	3.2849 ± 2.5685	16.3514 ± 12.9003	27.2736 ± 21.5849	40.5403 ± 32.2915	128.3645 ± 82.9969
	Var	19.4455 ± 35.8182	485.7264 ± 893.4722	1357.5774 ± 2472.6776	3016.4642 ± 5510.5715	$26905.3477 \pm 35389.4594$
	Mean	0.0001 ± 0.0032	1.6878 ± 1.2154	-0.0002 ± 0.0149	-0.0003 ± 0.0300	-0.0054 ± 0.7251
	SK	0.0017 ± 0.1900	0.0019 ± 0.0977	-0.0005 ± 0.1015	0.0013 ± 0.1066	0.0635 ± 0.1745
	Kur	7.2427 ± 5.3358	6.5474 ± 4.3414	6.7001 ± 4.6037	6.4038 ± 4.3846	4.1248 ± 1.7769

'*Var*' is variance, '*SK*' is skewness and '*Kur*' is kurtosis.

Table 7
Statistical analysis in DWT method.

State	Eigenvalue	DWT decomposition levels				
		D1	D2	D3	D4	A4
Seizure-free	SD	2.0692 ± 3.0851	9.2324 ± 12.2004	10.9351 ± 11.5218	9.2463 ± 8.8087	16.5965 ± 11.9710
	Var	15.9233 ± 105.9836	267.2654 ± 1373.9836	294.0855 ± 1184.4718	185.0976 ± 1366.8678	517.8911 ± 2067.3266
	Mean	0.0000 ± 0.0008	1.0804 ± 1.7132	0.0002 ± 0.0068	0.0001 ± 0.0149	0.0003 ± 0.6136
	SK	0.0025 ± 0.0666	0.0044 ± 0.0391	-0.0147 ± 0.0924	0.0194 ± 0.1082	0.0891 ± 0.2362
	Kur	5.7845 ± 5.1579	7.1305 ± 5.7376	6.8999 ± 5.2255	6.1760 ± 2.7626	4.6424 ± 1.7191
Seizure-active	SD	5.2033 ± 4.0940	24.2633 ± 19.1757	32.3770 ± 26.2264	35.4194 ± 31.9827	53.2343 ± 31.8316
	Var	49.0374 ± 89.7095	971.2714 ± 1963.0377	1932.0716 ± 3436.5237	2588.6643 ± 5024.4247	4356.7395 ± 5314.4662
	Mean	0.0001 ± 0.0013	2.4564 ± 1.8062	-0.0001 ± 0.0228	0.0002 ± 0.0635	0.0100 ± 1.4412
	SK	0.0003 ± 0.0724	0.0039 ± 0.0450	0.0022 ± 0.0893	0.0171 ± 0.0901	0.0558 ± 0.1651
	Kur	7.1263 ± 5.1789	8.8929 ± 6.0805	8.0551 ± 5.4553	6.0060 ± 2.8144	3.7751 ± 1.1979

'*Var*' is variance, '*SK*' is skewness and '*Kur*' is kurtosis.

summarizes the details of the architecture and gives the details of hyperparameter settings in each layer.

In this study, 20% training data is used to validate the CNN model via hold-out validation method and the validation frequency was selected as 50 iterations. In addition, the validation accuracy is listed in Table 4 for

16 CNN models, which shows the performance for each imaged CNN model.

All CNN analysis is implemented using MATLAB 2021b with a single CPU in a Dell workstation of dual Intel Xeon E5-2697 V3 CPUs. The loss and accuracy of training models and validation accuracy were

Table 8
Results of 3 Machine learning methods and proposed methods.

Machine learning methods	Sen (%)	Acc (%)	FP rate (%)
DWT	98.90	96.71	3.02
TQWT	98.90	97.57	2.13

'*Sen*' is sensitivity, and '*Acc*' is accuracy.

summarized in Fig. 4 in the progress of the training data for case 'Chb01′.

The accuracy, sensitivity, FP rate and seizure onset detection delay used to evaluate the proposed method in Database CHB-MIT are defined as below.

Accuracy is a direct parameter in method evaluation, and is defined in formula (10).

$$Acc = \frac{TP + TN}{TP + TN + FP + FN} \tag{10}$$

'*TP*' is the true positive, '*TN*' is the true negative, '*FP*' is the false positive and '*FN*' is the false negative.

Sensitivity is the parameter to measure the ability to recognize the patient cases correctly. In EEG real-time detection, this parameter is used to evaluate the active seizure detection performance.

$$Sen = \frac{TP}{NS} \tag{11}$$

where '*NS*' means the number of seizures.

The seizure onset detection delay represents the difference between the detected seizure onset time and the doctor's marker. Delay is negative if detected the seizure active signal early.

3. Results

3.1. The confusion matrix of real-time seizure detection

The confusion matrix describes all the measures for evaluation in epilepsy seizure detection, which includes the '*TP*', '*TN*', '*FP*', and '*FN*'. The confusion matrix for case '*Chb20′* detection is shown in Fig. 5.

According to the confusion matrix information, we calculated the accuracy as 99.45% and the false rate as 0.50%. There are 8 seizure active states in this case, and all the seizure active states were detected correctly, so the sensitivity of this case is 100%, and their detection delays were 19.03, 27.03, 33.03, 29.03, 22.03, 19.03, 18.03 and 31.03 s, respectively.

3.2. Real-time seizure onset detection results for Database CHB-MIT

In the real-time application, 240 eigenvalues from 8*30 matrix imaged-like data were selected, and the details of the features selected are shown in Fig. 3 and Fig. 4. CNN model of deep learning method was applied to evaluate the model using leaving one training method. As a result, we received 98.90% sensitivity, 97.57% accuracy, 2.13% FP rate and 10.46 s delay (Table 5).

4. Discussion

4.1. Comparison with other decomposition methods

To compare the performance between TQWT, DB4-DWT and EMD,

Table 9
Results of 3 Machine learning methods and proposed methods.

Machine learning methods	Sen (%)	Acc (%)	FP rate (%)
SVM	76.92	97.83	1.75
KNN	79.12	97.25	2.26
RUSBoosted tree Ensemble	95.60	96.53	3.12
CNN	98.90	97.57	2.13

'*Sen*' is sensitivity, and '*Acc*' is accuracy.

Table 10
Comparison of the proposed method and previous works using CHB-MIT Database.

Reference	Sen (%)	FP (%)	Delay (s)
Bhattacharyya and Pachori (2017) [6]	97.91	0.43	Not reported
Fan and Chou (2018) [40]	97	8.61	6–7
Bomela et al. (2020) [7]	93.6	0.16 per hour	10.06
Wang, X., et al. (2021) [28]	88.14	0.38	Not reported
Li, C., et al. (2021) [30]	97.34	2.5	Not reported
Zarei, A. and B.M. Asl (2021) [29]	96.81	2.74	Not reported
Abdelhameed, A. and M. Bayoumi (2021) [9]	98.72	1.14	Not reported
Our previous work (2022) [31]	96.15	3.24	10.42
Proposed method	98.90	2.13	10.46

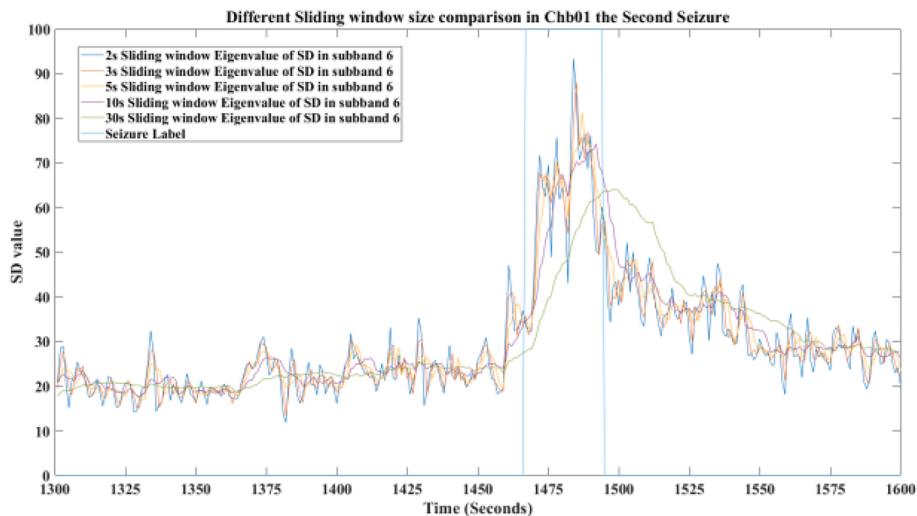'*Sen*' is sensitivity, and '*Acc*' is accuracy.

Fig. 7. The eigenvalue SD of the sixth sub-band of TQWT from Channel T7 – P7 in different sliding window sizes for Chb01 second seizure, seizure label line is the seizure active state labelled by doctor from the 1467 s to 1494 s.

the number of decomposition level were all selected as 5. However, the EMD method cannot decompose all 5-sliding window size data into 5 levels. In EMD analysis, parts of seizure-free data can just decompose into 4 levels. Thus, we just compare the performance between TQWT and DWT. In DWT analysis, 5 decomposition levels correspond to 64–128 Hz, 32–64 Hz, 16–32 Hz, 8–16 Hz and 0–8 Hz, respectively. The details of TQWT and DWT were shown in Fig. 6.

To compare performance of TQWT and DWT in this study, the statistical analysis between seizure free and seizure active of training data is conducted. The details of eigenvalues in TQWT and DWT decomposition levels are summarized in Table 6 and Table 7.

The statistical comparison between seizure free and seizure active in this experiment shows that the SD and variance of sub-band 6 in TQWT and A4 level in DWT has most significant difference. Compare with the TQWT and DWT, the difference between seizure free and seizure active in TQWQ of eigenvalue SD and variance is greater but not in eigenvalue mean, skewness and kurtosis. So, we used the CNN model with same architecture to test the performance of the DWT method and the results show in the Table 8.

It is evident that, from Table 8, the TQWT provides a better performance in real-time epilepsy seizure detection which can provide lower FP rate and higher accuracy.

4.2. EEG channel selection and real-time implementation

Channel selection is essential in EEG epilepsy detection, as it can improve accuracy and reduce the computation time. In previous studies, researchers used algorithms, such as the typical spatial pattern, permutation entropy and non-dominated sorting genetic algorithm (NSGA), to select the most significant channels [30,38,39]. After analysing the previous works and the information listed in Table 2 that recorded the details of seizure onset zone in Database CHB-MIT, we found that the electrodes located in the lateral border of the brain have a better performance in epilepsy seizure detections. In this study, we selected eight channels, which are FP1-F7, F7-T7, T7-P7, T7-FT9, FP2-F8, F8-T8, T8-P8 and FT10-T8. Considering the random nature of the epilepsy seizure onset zone for each patient, the aforementioned eight channels were selected to cover the pre-frontal lobe, inferior frontal lobe, temporal lobe and posterior temporal lobe area in both right and left side of the brain.

If the calculation time of each sliding size data is greater than a sliding window overlap (1 s in this study), the real-time implementation would not be possible. The intervention time includes the progress of Butterworth filter denoised, TQWT analysis, eigenvalues calculation and CNN classifier in each 5-second sliding window is 0.03 s. If the sliding window size is too small, the false positive rate will increase. If the size is too large, the results may cause a long-time delay in seizure onset detection due to the increased computational workload. The performance of eigenvalue SD (the sixth sub-band of TQWT from Channel T7 – P7 data) is provided under five sliding window sizes (2 s, 3 s, 5 s, 10 s and 30 s). According to the performance described in Fig. 7, the sliding window is selected as 5 s in this study because of the time delay.

4.3. Performance comparison

We compared three machine learning methods with the proposed CNN model in test data. In the epilepsy seizure detection via TQWT, CNN models, we get 97.57% accuracy, 98.90% sensitivity, and 2.13% FP rate. SVM, KNN and RUSBoosted tree Ensemble methods with random 20% hold-out validation were applied to conduct the EEG epilepsy signal detection and compared with the results of the CNN models. In CNN model, we used 8*30 matrix imaged-like data as input, thus, in these machine learning methods we use the same 240 features as input. The results of these three machine learning methods are summarized in Table 9.

It is obvious in Table 9, the CNN models provide a better

performance in real-time EEG epilepsy seizure onset detection than these three machine learning methods. The SVM provides better accuracy and less FP rate, but it just detects 70 of 91 seizures.

Table 10 summarizes the performance of the proposed method and other peer works in the epilepsy seizure onset detection using CHB-MIT Database. The proposed method achieved 97.57% accuracy, 98.90% sensitivity, 2.13% FP rate and 10.46-second delay in real-time seizure onset detection.

5. Conclusion

This study proposed an EEG based real-time epilepsy seizure detection approach using TQWT and CNN models of deep learning method, and evaluated its performance by comparison. In this paper, our proposed method can achieve 97.57% accuracy, 98.90% sensitivity, 2.10% false positive rate and 10.46-second delay in automatic real-time seizure detection implementation in CHB-MIT Database. In addition, we combined signal processing and image classification methods in this experiment. We firstly proposed TQWT method to extract approximate and details of signal and remove redundant information. Furthermore, the comparison also showed that the TQWT is better than DWT in this study which can provide less FP rate. Secondly, we improved the robustness of EEG based epilepsy detection using the deep learning method with CNN model. We also compared the designed CNN model with three machine learning models (SVM, KNN and RUSBoostred tree Ensemble), and find the CNN model can achieve better performance in classifying imaged-like data in this study. At last, the proposed method is suitable for real-time seizure detection in clinical applications as well.

Declaration of Competing Interest

The authors declare that they have no known competing financial interests or personal relationships that could have appeared to influence the work reported in this paper.

Data availability

No data was used for the research described in the article.

References

[1] A.S. Zandi, et al., Automated real-time epileptic seizure detection in scalp EEG recordings using an algorithm based on wavelet packet transform, IEEE Trans. Biomed. Eng. 57 (7) (2010) 1639–1651.
[2] L.S. Vidyaratne, K.M. Iftekharuddin, Real-time epileptic seizure detection using EEG, IEEE Trans. Neural Syst. Rehabil. Eng. 25 (11) (2017) 2146–2156.
[3] R.B. Yaffe, et al., Physiology of functional and effective networks in epilepsy, Clin. Neurophysiol. 126 (2) (2015) 227–236.
[4] D.C. Bergen, Do seizures harm the brain? Epilepsy Curr. 6 (4) (2006) 117–118.
[5] R. Rosch, et al., Network dynamics in the healthy and epileptic developing brain, Network Neurosci. 2 (1) (2018) 41–59.
[6] A. Bhattacharyya, R.B. Pachori, A multivariate approach for patient-specific EEG seizure detection using empirical wavelet transform, IEEE Trans. Biomed. Eng. 64 (9) (2017) 2003–2015.
[7] W. Bomela, et al., Real-time inference and detection of disruptive eeG networks for epileptic seizures, Sci. Rep. 10 (1) (2020) 1–10.
[8] C. Gómez, et al., Automatic seizure detection based on imaged-EEG signals through fully convolutional networks, Sci. Rep. 10 (1) (2020) 1–13.
[9] A. Abdelhameed, M. Bayoumi, A deep learning approach for automatic seizure detection in children with epilepsy, Front. Comput. Neurosci. 15 (2021) 29.
[10] J. Wu, T. Zhou, T. Li, Detecting epileptic seizures in EEG signals with complementary ensemble empirical mode decomposition and extreme gradient boosting, Entropy 22 (2) (2020) 140.
[11] M. Omidvar, A. Zahedi, H. Bakhshi, EEG signal processing for epilepsy seizure detection using 5-level Db4 discrete wavelet transform, GA-based feature selection and ANN/SVM classifiers, J. Ambient Intell. Hum. Comput. (2021) 1–9.
[12] K. Jindal, R. Upadhyay, H.S. Singh, Application of tunable-Q wavelet transform based nonlinear features in epileptic seizure detection, Analog Integr. Circ. Sig. Process 100 (2) (2019) 437–452.
[13] R.J. Oweis, E.W. Abdulhay, Seizure classification in EEG signals utilizing Hilbert-Huang transform, Biomed. Eng. Online 10 (1) (2011) 1–15.

[14] W. Hu, et al., Mean amplitude spectrum based epileptic state classification for seizure prediction using convolutional neural networks, J. Ambient Intell. Hum. Comput. (2019) 1–11.

[15] A. Bhattacharyya, et al., Tunable-Q wavelet transform based multiscale entropy measure for automated classification of epileptic EEG signals, Appl. Sci. 7 (4) (2017) 385.

[16] B. Akbarian, A. Erfanian, A framework for seizure detection using effective connectivity, graph theory, and multi-level modular network, Biomed. Signal Process. Control 59 (2020), 101878.

[17] Y. Gao, et al., Automatic epileptic seizure classification in multichannel EEG time series with linear discriminant analysis, Technol. Health Care (2020(Preprint):) 1–11.

[18] Y.L. Niriayo, et al., Treatment outcome and associated factors among patients with epilepsy, Sci. Rep. 8 (1) (2018) 1–9.

[19] C. Donos, M. Dümpelmann, A. Schulze-Bonhage, Early seizure detection algorithm based on intracranial EEG and random forest classification, Int. J. Neural Syst. 25 (05) (2015) 1550023.

[20] Y. Gao, et al., Deep convolutional neural network-based epileptic electroencephalogram (EEG) signal classification, Front. Neurol. 11 (2020) 375.

[21] X. Cao, et al., Automatic seizure classification based on domain-invariant deep representation of EEG, Front. Neurosci. (2021) 1313.

[22] N. Ahammad, T. Fathima, P. Joseph, Detection of epileptic seizure event and onset using EEG, Biomed Res. Int. (2014. 2014.).

[23] M. Qaraqe, et al., Epileptic seizure onset detection based on EEG and ECG data fusion, Epilepsy Behav. 58 (2016) 48–60.

[24] K. Samiee, et al., Long-term epileptic EEG classification via 2D mapping and textural features, Expert Syst. Appl. 42 (20) (2015) 7175–7185.

[25] M. Zabihi, et al., Analysis of high-dimensional phase space via Poincaré section for patient-specific seizure detection, IEEE Trans. Neural Syst. Rehabil. 24 (3) (2015) 386–398.

[26] G. Wang, et al., EEG-based detection of epileptic seizures through the use of a directed transfer function method, IEEE Access 6 (2018) 47189–47198.

[27] H. Rajaei, et al., Dynamics and distant effects of frontal/temporal epileptogenic focus using functional connectivity maps, IEEE Trans. Biomed. Eng. 67 (2) (2019) 632–643.

[28] X. Wang, et al., One dimensional convolutional neural networks for seizure onset detection using long-term scalp and intracranial EEG, Neurocomputing 459 (2021) 212–222.

[29] A. Zarei, B.M. Asl, Automatic seizure detection using orthogonal matching pursuit, discrete wavelet transform, and entropy based features of EEG signals, Comput. Biol. Med. 131 (2021), 104250.

[30] C. Li, et al., Seizure onset detection using empirical mode decomposition and common spatial pattern, IEEE Trans. Neural Syst. Rehabil. Eng. 29 (2021) 458–467.

[31] M. Shen, et al., An EEG based real-time epilepsy seizure detection approach using discrete wavelet transform and machine learning methods, Biomed. Signal Process. Control 77 (2022), 103820.

[32] H. Chen, Y. Song, X. Li, A deep learning framework for identifying children with ADHD using an EEG-based brain network, Neurocomputing 356 (2019) 83–96.

[33] A.R. Ozcan, S. Erturk, Seizure prediction in scalp EEG using 3D convolutional neural networks with an image-based approach, IEEE Trans. Neural Syst. Rehabil. Eng. 27 (11) (2019) 2284–2293.

[34] A.L. Goldberger et al., PhysioBank, PhysioToolkit, and PhysioNet: components of a new research resource for complex physiologic signals, Circulation 101 (23) (2000) e215–e220.

[35] I. Bayram, I.W. Selesnick, Frequency-domain design of overcomplete rational-dilation wavelet transforms, IEEE Trans. Signal Process. 57 (8) (2009) 2957–2972.

[36] I.W. Selesnick, Wavelet transform with tunable Q-factor, IEEE Trans. Signal Process. 59 (8) (2011) 3560–3575.

[37] K. Simonyan, A. Zisserman, Very deep convolutional networks for large-scale image recognition. arXiv preprint arXiv:1409.1556, 2014.

[38] J.S. Ra, T. Li, Y. Li, A novel permutation entropy-based EEG channel selection for improving epileptic seizure prediction, Sensors 21 (23) (2021) 7972.

[39] L.A. Moctezuma, M. Molinas, EEG channel-selection method for epileptic-seizure classification based on multi-objective optimization, Front. Neurosci. 14 (2020).

[40] M. Fan, C.-A. Chou, Detecting abnormal pattern of epileptic seizures via temporal synchronization of EEG signals, IEEE Trans. Biomed. Eng. 66 (3) (2018) 601–608.

CHAPTER 5: PAPER 3 – A Real-time Epilepsy Seizure Detection based on EEG using Short-time Fourier Transform and Google-net Convolutional Neural Network

5.1 Overview of Paper 3

The details of the Paper 3 are given below:

- Paper title: "A Real-time Epilepsy Seizure Detection based on EEG using Short-time Fourier Transform and Google-net Convolutional Neural Network."

- Paper length: 16 pages

- Journal: Heliyon
    - Rank: Q1 (Multidisciplinary)
    - Impact factor: 4.0 (2022-2023)
    - Cite score: 5.6 (2022)
    - SJR: 0.609 (2022)
    - SNIP: 1.332 (2022)

- First author: Mingkan Shen

- Corresponding author: Mingkan Shen

HDR thesis author's declaration

☒ The authors declare that they have no known competing financial   interests or personal relationships that could have appeared to influence the work reported in this paper.

☐ The authors declare the following financial interests/personal relationships which may be considered as potential competing interests:

Table 5.1: Authorship contributions of Paper 3

Conceptualization	Mingkan Shen, Fuwen Yang, Peng Wen, Bo Song, Yan Li
Methodology	Mingkan Shen
Software	Mingkan Shen
Validation	Mingkan Shen, Peng Wen, Bo Song
Formal analysis	Mingkan Shen

Writing – original draft preparation	Mingkan Shen
Writing – review and editing	Mingkan Shen, Fuwen Yang, Peng Wen, Bo Song, Yan Li
Supervision	Fuwen Yang, Peng Wen, Bo Song, Yan Li
Project administration	Mingkan Shen

5.2 Summary of Paper 3

This paper introduces an advanced approach to real-time epilepsy seizure detection, merging the capabilities of signal processing techniques with deep learning methodologies. Using the Scalp EEG standard from the CHB-MIT Database, the study employs the STFT to refine EEG signals, emphasizing essential features. This refinement not only enhances data clarity but also bolsters the reliability of epilepsy detection.

At the heart of the methodology stands the Google-Net CNN model, adapted expressly for image-like data derived from EEG readings. To ascertain its efficacy, the performance of the Google-Net CNN was juxtaposed with renowned models like the Squeeze-net and VGG-net CNNs. The outcomes were notable, with the Google-Net CNN demonstrating superior accuracy and sensitivity in data classification.

Key findings include an impressive accuracy rate of 97.74% and a sensitivity rate of 98.90%, underscoring the method's viability for clinical settings. The paper concludes by spotlighting potential future explorations, focusing on the integration of seizure prediction using portable EEG devices and brainwave monitors, forging a pathway for significant real-world applications in healthcare.

5.3 Paper file

Heliyon

A Real-time Epilepsy Seizure Detection Approach based on EEG using Short-time Fourier Transform and Google-Net Convolutional Neural Network

--Manuscript Draft--

Manuscript Number:	
Article Type:	Original Research Article
Section/Category:	Physical and Applied Sciences
Keywords:	Epilepsy seizure detection; EEG; real-time; STFT; Google-net CNN
Manuscript Classifications:	20.140.100.140: Machine Learning; 20.190: Signal Processing; 30.250: Biomedical engineering
Corresponding Author:	Mingkan Shen AUSTRALIA
First Author:	Mingkan Shen
Order of Authors:	Mingkan Shen
	Fuwen Yang
	Peng Wen
	Bo Song
	Yan Li
Abstract:	Epilepsy is one of the common brain disorders, and seizures of epilepsy have severe adverse effects on patients. Real-time epilepsy seizure detection using electroencephalography (EEG) signals is an important area of research aimed at improving the diagnosis and treatment of epilepsy. This paper proposed a real-time approach based on EEG signal for detecting epilepsy seizures using the STFT and Google-net convolutional neural network (CNN). CHB-MIT database was evaluated in this study, and received the results of 97.74% accuracy, 98.90% sensitivity, 1.94% false positive rate. Additionally, the proposed method was implemented in a real-time manner using the sliding window technique. In this research, the processing time of this study is just 0.02 seconds for every 2-second EEG episode and achieved average 9.85- second delay in each seizure onset.
Suggested Reviewers:	Abhijit Bhattacharyya pachori@iiti.ac.in
	Abdulhamid Zahedi zahedi@kut.ac.ir
	Chun-An Chou ch.chou@northeastern.edu
Opposed Reviewers:	

A Real-time Epilepsy Seizure Detection Approach based on EEG using Short-time Fourier Transform and Google-Net Convolutional Neural Network

Mingkan Shen[1] **, Fuwen Yang**[2] **, Peng Wen**[1] **, Bo Song**[1] **and Yan Li**[3]

[1] *School of Engineering, University of Southern Queensland, Toowoomba, Australia*

[2] *School of Engineering and Built Environment, Griffith University, Gold coast, Australia*

[3] *School of Mathematics, Physics and Computing, University of Southern Queensland, Toowoomba, Australia*

Corresponding Author: Mingkan Shen, Mingkan.Shen@usq.edu.au

Abstract

Epilepsy is one of the common brain disorders, and seizures of epilepsy have severe adverse effects on patients. Real-time epilepsy seizure detection using electroencephalography (EEG) signals is an important area of research aimed at improving the diagnosis and treatment of epilepsy. This paper proposed a real-time approach based on EEG signal for detecting epilepsy seizures using the STFT and Google-net convolutional neural network (CNN). CHB-MIT database was evaluated in this study, and received the results of 97.74% accuracy, 98.90% sensitivity, 1.94% false positive rate. Additionally, the proposed method was implemented in a real-time manner using the sliding window technique. In this research, the processing time of this study is just 0.02 seconds for every 2-second EEG episode and achieved average 9.85-second delay in each seizure onset.

Keywords: Epilepsy seizure detection, EEG, real-time, STFT, Google-net CNN.

1. Introduction

Epilepsy is indeed a neurological disorder characterized by abnormal synchronous electrical activity in the brain [1]. It affects a significant number of people worldwide, with an estimated 50 million individuals living with epilepsy [2]. Given the high prevalence of epilepsy and the impact of seizures on patients, there is a growing need to improve the efficiency of diagnosis and treatment. One approach to address this is by developing real-time automatic detection systems that utilize electroencephalogram (EEG) signals [3].

The main features of EEG seizure active signals are the spikes waves and sharp waves. To distinguish the spike waves, sharp waves with the normal waves, majority of the signal processing methods were proposed in recent years. The study by Alharthi, M.K et al. focused on EEG seizure onset detection using a combination of the discrete wavelet transform (DWT) and a deep learning model consisting of a 1D-Convolutional Neural Network (CNN) with bidirectional long short-term memory (Bi-LSTM) [4]. They achieved the results of 96.87% accuracy, 96.85% sensitivity and 96.98% precision in their experiment. Zarei, A et al. explored the use of orthogonal matching pursuit (OMP) combined with a support vector machine (SVM)

classifier for detecting seizure onsets [5]. Their study reported a sensitivity of 96.81% and a false positive (FP) rate of 2.74%. In another study by Bhattacharyya, A. et al., they proposed the use of tunable-Q wavelet transform (TQWT) to decompose EEG epilepsy signals [6]. They then calculated entropy measures based on the decomposed signals. Their approach achieved an accuracy of 98.6%. Li, C. et al. proposed the use of common spatial pattern (CSP) to select relevant EEG channels for seizure onset detection [7]. They combined CSP with empirical mode decomposition (EMD) and an SVM model and obtained the result of a sensitivity of 97.34% and a false positive rate of 2.5%. In the research conducted by Oweis, R.J. et al., they utilized the Hilbert-Huang transform (HHT) in the frequency domain for seizure detection [8]. Their method achieved an accuracy of 94% and specificity of 96%. Hu, W. et al. highlighted the use of mean amplitude spectrum (MAP) combined with a CNN model for classifying the seizure active and seizure free data [9]. Their approach reported a classification accuracy of 86.25%. Bomela, W. et al. developed a complex brain connection method for real-time seizure detection [10]. They supported the result of a sensitivity of 93.6% and a false positive rate of 0.16 per hour in their study. Shayeste, H. et al. developed a short-time Fourier transform (STFT) algorithm based on the bagging technique and a decision tree model for automatic seizure detection [11]. Their approach received high accuracy, sensitivity, and specificity, with reported values of 99.56%, 99.52%, and 99.62%, respectively. Amiri, M. et al. utilized Sparse CSP combined with an adaptive STFT-based synchro squeezing transform for automatic seizure detection [12]. Their method achieved a sensitivity of 98.44%, specificity of 99.19%, and accuracy of 98.81%. In our previous work, DWT and RUSBoosted tree Ensemble methods were combined to detect EEG epilepsy seizure onset in real-time application, and achieved 96.15% sensitivity, 96.38% accuracy, 3.24% FP rate and 10.42 seconds delay results [13]. Furthermore, TQWT and CNN model were also applied our seizure detection work, the results received 97.57% in accuracy, 98.90% in sensitivity, 2.13% in FP rate and 10.46-second delay [14].

To address the robustness issue in EEG-based epilepsy detection, researchers have focused on developing machine learning and deep learning methods. Omidvar, M. et al. proposed the use of a SVM model to classify EEG signals decomposed at the 5th level using the 5-db DWT [15]. They reported an accuracy of 98.7% as the result in their paper. Donos, C. et al. employed the random forest algorithm to detect early seizures using intracranial EEG data [16]. Their method can obtain a result of 93.84% sensitivity. Gao, Y. et al. focused on deep learning and utilized a deep CNN to classify seizure activity in EEG data [17]. Their approach achieved an average classification accuracy of 90% in epilepsy seizure detection. Cao, X. et al. used LSTM networks to directly detect seizure onset [18]. They provided the result with an accuracy of 96.3% in their experiment. Wang, X et al. proposed a stacked 1D-CNN model for automatic seizure onset detection [19]. Their approach obtained an accuracy of 88.14% and a false positive rate of 0.38%.

Combining signal processing and image classification techniques using CNN models has shown promising results in EEG research. Chen, H et al. utilized mutual information (MI) algorithm to calculate brain graph data and combined it with a graph CNN model for detecting subjects with attention-deficit/hyperactivity disorder (ADHD) using EEG signals [20]. In their study, they received an accuracy of 94.67% on the test data. Ozcan, A.R. et al. employed a 3D-CNN model to classify features extracted from EEG signals, including statistical parameters and band power spectrum, in the context of seizure prediction. Their method achieved a

sensitivity of 85.7% and a false positive rate of 0.096 per hour [21]. In our previous work, 3D-CNN classifier was proposed to classify the EEG alcoholic brain connectivity data and received the results of $96.25 \pm 3.11\%$ accuracy [22]. Moreover, this kind of method also employed in our previous research focused on EEG schizophrenia identification work [23]. 3D-CNN provided the $97.74 \pm 1.15\%$ accuracy, $96.91 \pm 2.76\%$ sensitivity, and $98.53 \pm 1.97\%$ results in this study. By integrating signal processing techniques with deep learning models can support good performance in classifying other EEG diseases data, leveraging this kind of methods in EEG seizure onset detection is proposed in this study. Signal processing methods can be used to pre-process and extract relevant features from EEG signals, while the image classification capabilities of CNN models enable the learning of complex patterns and representations.

In this study, a bandpass filter using a 6th-order Butterworth zero-phase algorithm is used to denoise the raw EEG data within the frequency range of 1-60 Hz. To extract features from the EEG signals, STFT spectrums can provide a time-frequency representation of the data. The obtained spectrums were then transformed into graph data, which serves as the input for the Google-Net CNN models. To implement the approach in real-time, a sliding window technique with a duration of 1.35 seconds and a 1-second overlap is utilized. The experiments of this study were conducted on a Dell workstation equipped with an Intel I9-10900K CPU, 64 GB memory, and an Nvidia 2080ti GPU. MATLAB 2021b, along with the Deep Network Designer toolbox, was used for the deep learning work and model development.

Section 1 brief introduced the background and literature review of this paper. Section 2 described the methodology and list the algorithm of this study which include the signal processing, feature extraction and CNN model classification. Section 3 reported the results obtained using the proposed method. Section 4 discussed the statistical analysis in time-frequency spectrum analysis, brain rhythms selection, and evaluation of different CNN models. Moreover, the previous works of the database CHB-MIT were also listed and evaluated in Section 4. Section 5 concluded the paper.

2. Material

The CHB-MIT database, collected by Boston Children's Hospital, consists of EEG data from 23 subjects [24]. The database included 5 males ranging in age from 3 to 22 years and 17 females ranging in age from 1.5 to 19 years. The EEG data in the CHB-MIT database was recorded using scalp EEG standard 10-20 system caps, with a sampling rate of 256 Hz. The data was collected from 22 bipolar channels. In this experiment, six specific electrodes located closer to the frontal and temporal regions were used for detecting seizure onset in real-time applications. These electrodes are P3 - O1, FP2 - F8, P8 - O2, P7 - T7, T7 - FT9, and FT10 - T8. For this study, a subset of the CHB-MIT Database was selected, consisting of 16 patients. Patients who had seizures characterized by amplitude depression were excluded from the analysis [10]. The details of the selected subjects can be found in Table 1 of the study.

TABLE 1

INFORMATION ABOUT DATABASE CHB-MIT OF THIS STUDY

Case	Data collected (hour)	Number of seizures	Seizure duration (second)
Patient 1	26	7	40,27,40,51,90,93,101
Patient 2	17	3	82,81,9
Patient 3	37	7	52,65,69,52,47,64,53

Patient 4	24	4	49,111,102,116
Patient 5	16	5	115,110,96,120,117
Patient 7	29	3	86,96,143
Patient 8	18	5	171,190,134,160,264
Patient 9	32	4	64,79,71,62
Patient 10	22	7	35,70,65,58,76,89,54
Patient 17	17	3	90,115,88
Patient 18	17	6	50,30,68,55,68,46
Patient 19	16	3	78,77,81
Patient 20	17	8	29,30,39,38,35,49,35,39
Patient 22	17	3	58,74,72
Patient 23	15	7	113,20,47,71,62,27,84
Patient 24	13	16	25,25,29,25,32,27,19,24,22,19,70,16,27,17,66,68

3. Methodology

Figure 1 in this proposed study illustrates the progression of the method, highlighting the four major steps involved. To reduce computational costs, six specific channels are selected for analysis. These channels include P3 - O1, FP2 - F8, P8 - O2, P7 - T7, T7 - FT9, and FT10 - T8. To enable real-time application, a sliding window technique is employed. The sliding window has a size of 1.35 seconds, which corresponds to 345 samples of EEG data. This approach allows for continuous analysis of the EEG signals by processing them in overlapping segments. The EEG raw data is subjected to band-pass filtering using a 6th-order Butterworth algorithm. This filtering process helps to remove unwanted noise and artifacts from the EEG signals, focusing on frequency components within the range of interest. Time-frequency analysis is performed on the filtered EEG data to extract specific frequency bands of interest. This analysis provides information on how the frequency content of the EEG signals changes over time, capturing transient characteristics such as those seen during seizure activity. The resulting time-frequency spectra are converted into a graph representation with dimensions of 120×344, which serves as the input for the Google-net CNN model.
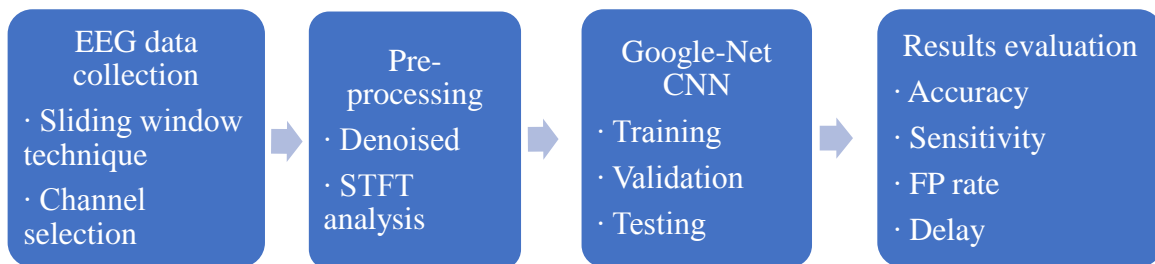
Figure. 1. The framework of STFT spectrum and Google-Net CNN models for seizure detection.

3.1 Pre-processing

A 6th-order Butterworth algorithm is applied as a band-pass filter to the raw EEG data in this study. The purpose of this filtering process is to selectively retain frequency components within the range of interest while attenuating frequencies outside this range. By applying the 6th-order Butterworth filter, frequencies outside the desired range from 1 to 60 Hz are attenuated, reducing the impact of noise and artifacts on the EEG signals. The filtered EEG signals

primarily contain frequency components within the specified range, which is important for subsequent analysis and feature extraction steps in the proposed method.

3.2 Short-time Fourier transform

In this paper, STFT is utilized as a time-frequency analysis technique to decompose the EEG signal into different frequency sub-bands and components. Specifically, the STFT is used to construct the time-frequency domain spectrum of the EEG signal within the frequency range of 20-60 Hz. This frequency range is of interest in this study, because it contains relevant information related to the detection of epilepsy seizures. The STFT provides a representation of the signal in both the time and frequency domains by applying a series of Fourier transforms to overlapping segments of the signal. Based on the Fourier transform, STFT analysis considers the window function of time varying EEG fragments which are converted into frequency and time axes. The formula of Fourier transforms and STFT analysis are shown in equations (1) and (2).

$$S(\omega) = \sum_t \bar{s}(t)e^{j\omega t} \tag{1}$$

$$S(\omega) = \sum_t \bar{s}(t)g(t-u)e^{j\omega t} \tag{2}$$

where ω is the selected frequency band, $g(t\text{-}u)$ is the window function. Here, the window is selected as hamming 2 samples, and the number of overlapped samples is selected as 1. The input data from the K domains are donated by $\bar{x} = [\bar{x}^1, ..., \bar{x}^K]^T \in R^{K \times d}$, where $\bar{x} \in R^{d \times 1}$, and the epoch with the time index t is given as $\bar{x}(t)$.

In this study, the frequency resolution for the STFT is chosen as 2 Hz. After the STFT analysis, one channel EEG data is converted into a 20×344 image-like data. Detail is shown in Figure. 2. After obtaining the STFT spectra for the six selected channels, the next step in the proposed approach is to combine them together. The spectra from each channel are combined to create a single input matrix with a size of 120×344 per epoch.

(a) STFT analysis of seizure-free input (P3-O1) (b) STFT analysis of seizure-active input (P3-O1)
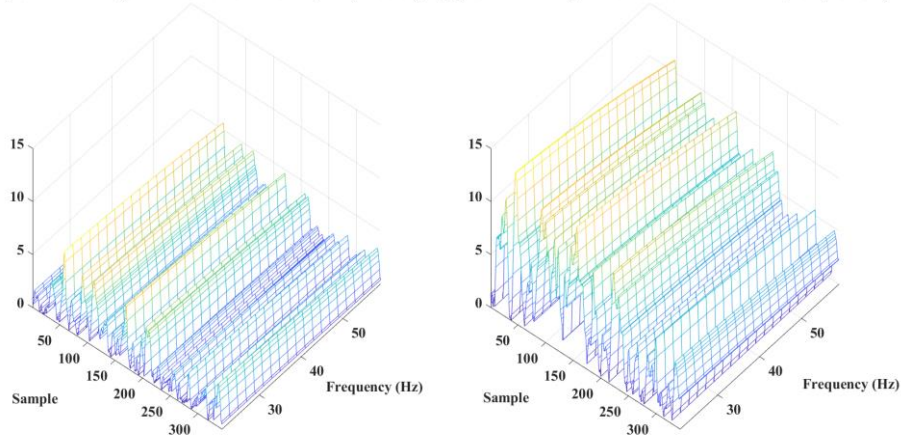
Figure 2. (a) STFT spectrum of seizure free data, (b) STFT spectrum of seizure active data. The seizure active data is collected from case *'Chb01_03'* from 3009s to 3011s, and the seizure free data is collected in the same case from 2800s to 2802s.

3.3 Classification through deep learning method

According to the size of the input data through STFT analysis, a 29-layer Google-Net CNN is constructed and shown in Figure.3.
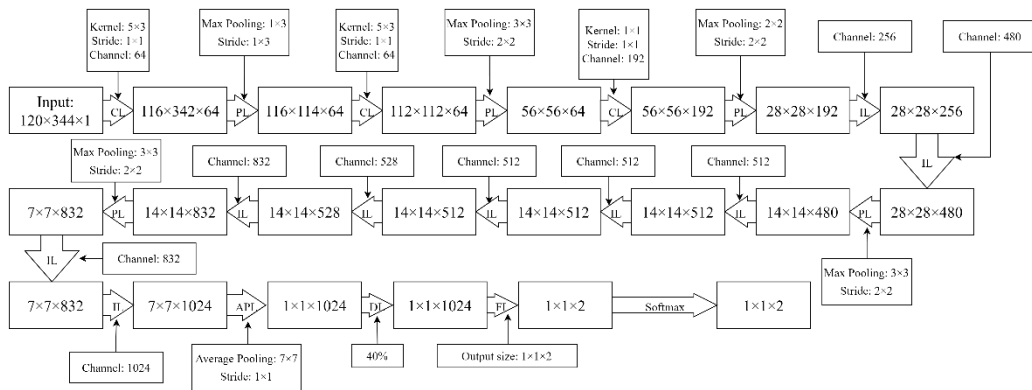
Figure. 3. The 29-layer Google-net CNN architecture, 'CL' is convolution layer, 'PL' is max pooling layer, 'IL' is inception layer, 'APL' is average pooling layer, 'DL' is dropout layer and 'FL' is fully connected layer.

3.3.1 Leaving one out training method

In the study, the leave-one-out training method is employed to evaluate the performance of the proposed method. This approach involves using one set of data as the test set while using the remaining data for training. In this experiment, a total of 16 models are trained, with each model being trained on a different combination of training and test data. For training purposes, the EEG raw data from 10 minutes before seizure onset and 5 minutes after seizure onset are used for each subject data.

3.3.2 Google-Net convolutional neural network

In the proposed Google-net CNN model, the graph data with dimensions of 120×344 matrices are used as input. The model is trained using a learning rate of 0.01 and 30 epochs. The Google-Net CNN model consists of three individual convolution layers and a total of fifty-four convolutions using nine inceptions. All convolutions in the model utilize rectified linear activation function ReLU along with batch normalization. The three individual convolution layers in the model have sixty-four filters each, with convolution kernels of size 5×3, 5×3, and 1×1, respectively. The nine inceptions in the model are designed similarly, and the detailed architecture of an inception is depicted in Figure 4.
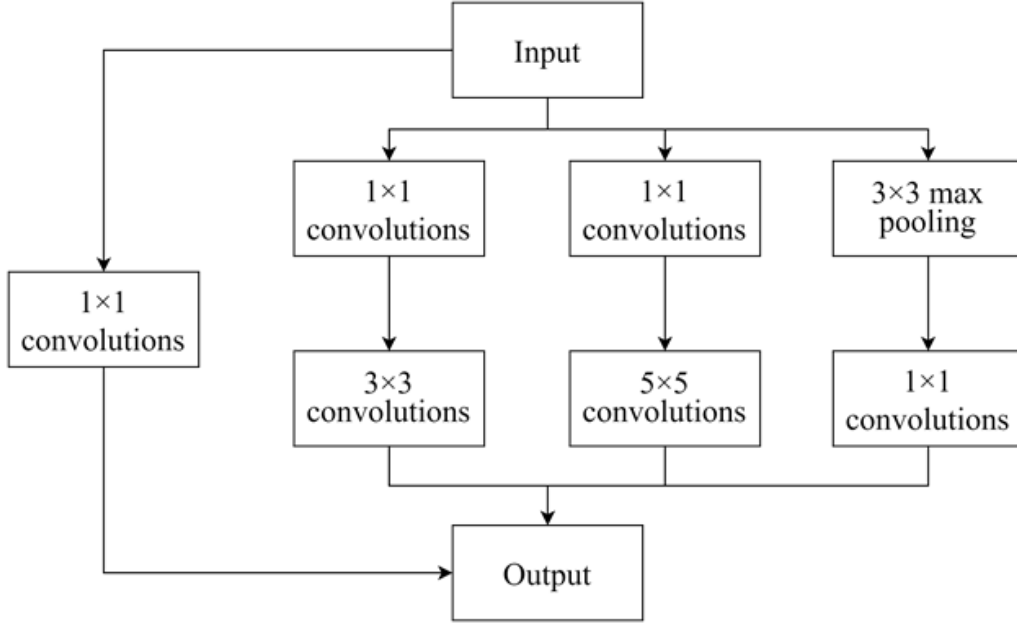
Figure 4. Architecture of an inception in Google-Net CNN model.

In addition, the Google-Net CNN architecture described in the study includes a total of six pooling layers. These pooling layers consist of five max pooling layers and one average pooling layer. Six pooling layers of this architecture are selected as 1×3, 3×3, 3×3, 3×3, 3×3, 7×7 size and 1×3, 2×2, 2×2, 2×2, 2×2, 1×1 stride, respectively. To alleviate the occurrence of overfitting in the CNN model, a 40% dropout layer is designed in the architecture. Finally, the last two layers of the CNN model consist of a fully connected layer and a Softmax classifier layer, respectively. Table 2 in the paper provides a summary of the Google-net architecture, including the hyperparameter settings for each layer.

TABLE 2
THE GOOGLE-NET CNN ARCHITECTURE USED IN EEG SEIZURE DETECTION

Level	Layer	Input data size	Output data size	Hyperparameter settings
-	Image-data input	120×344×1		
1	Convolution layer	120×344×1	116×342×64	Kernel size: 5×3 Stride: 1×1 Channel: 64
2	Max Pooling layer	116×342×64	116×114×64	Pooling size: 1×3 Stride: 1×3
3	Convolution layer	116×114×64	112×112×64	Kernel size: 5×3 Stride: 1×1 Channel: 64
4	Max Pooling layer	112×112×64	56×56×64	Pooling size: 3×3 Stride: 2×2
5	Convolution layer	56×56×64	56×56×192	Kernel size: 1×1 Stride: 1×1 Channel: 192
6	Max Pooling layer	56×56×192	28×28×192	Pooling size: 2×2 Stride: 2×2

7

7	Inception layer	28×28×192	28×28×256	Channel: 256
9	Inception layer	28×28×256	28×28×480	Channel: 480
11	Max Pooling layer	28×28×480	14×14×480	Pooling size: 3×3 Stride: 2×2
12	Inception layer	14×14×480	14×14×512	Channel: 512
14	Inception layer	14×14×512	14×14×512	Channel: 512
16	Inception layer	14×14×512	14×14×512	Channel: 512
18	Inception layer	14×14×512	14×14×528	Channel: 528
20	Inception layer	14×14×528	14×14×832	Channel: 832
22	Max Pooling layer	14×14×832	7×7×832	Pooling size: 3×3 Stride: 2×2
23	Inception layer	7×7×832	7×7×832	Channel: 832
25	Inception layer	7×7×832	7×7×1024	Channel: 1024
27	Average Pooling layer	7×7×1024	1×1×1024	Pooling size: 7×7 Stride: 1×1
28	Dropout layer	1×1×1024	1×1×1024	40%
29	Fully Connected layer	1×1×1024	1×1×2	
-	Softmax	1×1×2	1×1×2	

199 In this training progress, a hold-out validation method is employed to validate the deep learning
200 model during the training process. The training data is randomly divided into a training set and
201 a validation set, with the validation set comprising 20% of the training data. During training,
202 the performance of each model is evaluated periodically using the validation set. The validation
203 accuracy is calculated and recorded at regular intervals, with a validation frequency of 50
204 iterations. Table 3 presents the validation accuracy results obtained during the training process,
205 showcasing the performance of each model on the validation set at different stages of training.

206 TABLE 3
207 THE VALIDATION ACCURACY OF STFT SPECTRUM WITH GOOGLE-NET TRAINING MODELS.

Case	Validation Accuracy of STFT (%)
Patient 1	96.75
Patient 2	96.90
Patient 3	96.48
Patient 4	96.90
Patient 5	96.89
Patient 7	96.96
Patient 8	97.06

8

Patient 9	97.22
Patient 10	96.69
Patient 17	96.92
Patient 18	97.00
Patient 19	97.00
Patient 20	97.02
Patient 22	96.84
Patient 23	96.82
Patient 24	96.33
Mean ± SD	96.86 ± 0.22

208 In Figure 5, the progress of training the Google-net CNN model using STFT analysis for the
209 *'Patient 1'* case is depicted. The figure shows the changes in loss and accuracy during the
210 training process for both the training data and validation data. The training loss and accuracy
211 curves indicate how well the model is fitting the training data over iterations. The validation
212 accuracy curve shows the performance of the model on the validation set during training.
213 According to the figure, the proposed Google-net CNN model successfully distinguished the
214 imbalanced features of seizure-free and seizure-active states in this case. The model achieved
215 a validation accuracy of 96.75% for this particular case, indicating its ability to accurately
216 classify EEG signals related to seizures.
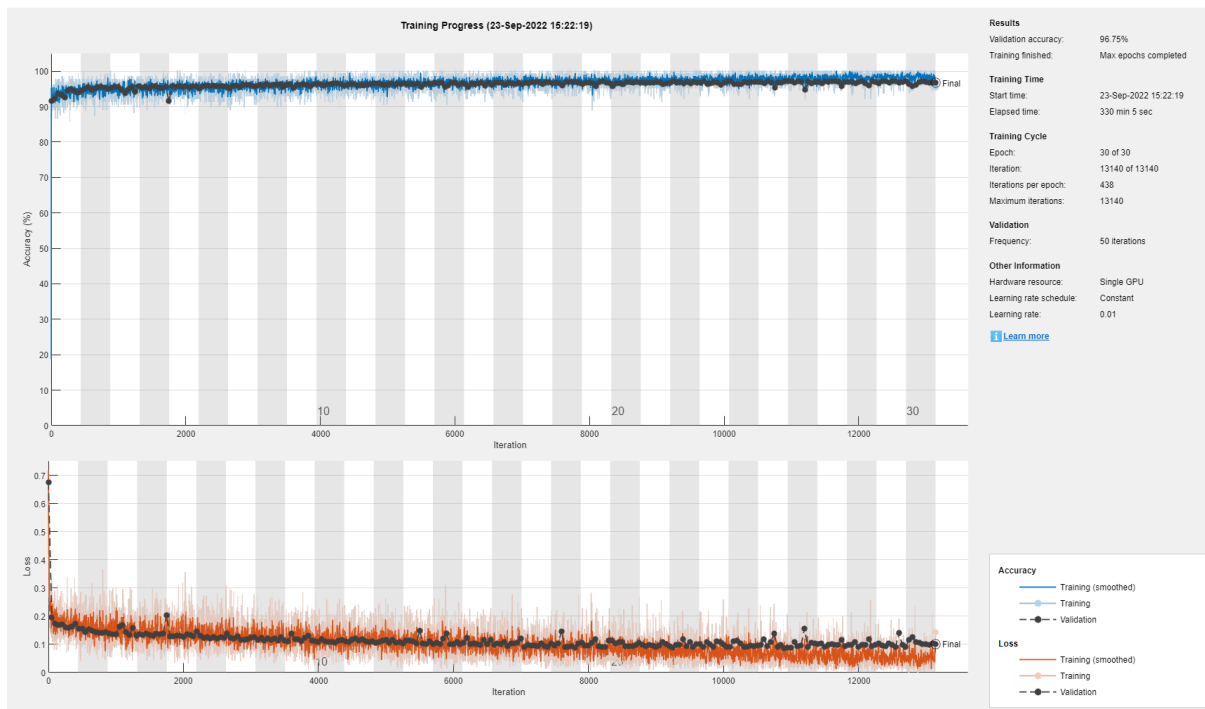
218 Figure 5. The training progress for *'Patient 1'* case via STFT analysis and Google-net CNN
219 based on MATLAB 2021b software.

4. Results and Comparison

221 By evaluating a real-time seizure onset detection method, four main parameters are applied in
222 this study which include the accuracy, sensitivity, FP rate and the delay of the seizure onsets.

223 Accuracy measures how well the proposed method correctly identifies seizure onset events and
224 non-seizure events, and the formula is described in the equation (3)

9

$$Acc = \frac{TP + TN}{TP + TN + FP + FN} \tag{3}$$

where '*TP*', '*TN*', '*FP*', '*FN*' correspond to the true positive, true negative, false positive and false negative.

Sensitivity, also known as recall or true positive rate, measures the ability of the algorithm to correctly identify seizure events or seizure onset. In active seizure detection, the goal is to accurately detect the occurrence of seizure activity in real-time EEG signals. Sensitivity quantifies the proportion of actual seizure events that are correctly detected by the algorithm. The algorithm of sensitivity is defined in equation (4)

$$Sen = \frac{TP}{Number\ of\ seizures} \tag{4}$$

Delay of the seizure onset measures the time delay between the actual occurrence of a seizure onset and the detection of that onset by the method. It reflects the temporal accuracy of the detection algorithm. The delay is typically calculated as the time elapsed from the onset of the seizure to the detection of the seizure onset.

4.1 Results of the proposed method

In the real-time application based on Database CHB-MIT, 41280 eigenvalues from 120×344 matrix graph data are selected. Google-net CNN model is utilized to evaluate the model using leaving one training method. As a result, Table 4 reported 97.74% in accuracy, 98.90% in sensitivity, 1.94% in false positive rate, 9.85 seconds delay in this study.

TABLE 4
REAL TIME DETECTION USING STFT AND GOOGLE-NET METHOD

Case	Number of seizures	True positive	FP rate (%)	Sensitivity (%)	Delay (s)	Accuracy (%)
Patient 1	7	7	2.34	100.00	2.45	97.46
Patient 2	3	3	2.30	100.00	6.35	97.64
Patient 3	7	7	0.37	100.00	3.73	99.26
Patient 4	4	4	0.72	100.00	22.02	99.06
Patient 5	5	5	2.22	100.00	8.82	97.63
Patient 7	3	3	3.10	100.00	3.02	96.85
Patient 8	5	5	2.12	100.00	6.62	96.83
Patient 9	4	4	7.69	100.00	1.52	92.30
Patient 10	7	7	5.82	100.00	1.45	94.07
Patient 17	3	3	0.14	100.00	31.02	99.48
Patient 18	6	5	0.30	83.33	17.02	99.25
Patient 19	3	3	0.26	100.00	5.35	99.58
Patient 20	8	8	0.25	100.00	17.90	99.28
Patient 22	3	3	0.69	100.00	9.02	99.20
Patient 23	7	7	0.75	100.00	13.31	98.47
Patient 24	16	16	1.93	100.00	8.02	97.55
Total	91	90				
Mean			1.94		9.85	97.74
Sensitivity		98.90				

4.2 Comparison with different frequency bands

By analysing the properties of the EEG signals within different frequency bands, the study aimed to determine which specific frequency range or band yielded the most promising results for real-time epilepsy seizure detection. This approach helps to reduce computing costs by focusing on the most relevant frequency components of the EEG signals. Six frequency bands are considered in this experiment which include δ band (1-4 Hz), θ band (4-8 Hz), α band (8-12 Hz), β band (12-30 Hz), γ band (30-60 Hz) and selected frequency band (20-60 Hz), the comparison is described in Table 5.

TABLE 5

THE COMPARISON BETWEEN DIFFERENT FREQUENCY BAND

Frequency band	Accuracy (%)	Sensitivity (%)	FP rate (%)
δ band (1-4 Hz)	90.23	91.20	10.84
θ band (4-8 Hz)	92.45	93.41	8.93
α band (8-12 Hz)	93.38	93.41	7.61
β band (12-30 Hz)	94.56	96.70	5.94
γ band (30-60 Hz)	96.93	98.90	3.12
Selected band (20-60 Hz)	**97.74**	**98.90**	**1.94**

According to Table 6, the selected frequency band brain has been verified as the best frequency band to detect the EEG epilepsy seizure signal.

4.3 Comparison with different deep learning models

Another two CNN methods are compared with the proposed Google-net CNN model in testing data which contains VGG-net CNN and Squeeze-net CNN. In these comparison work, the same input data with the same validation method are applied to conduct the EEG epilepsy signal detection and compared with the results of the proposed method. The input data for the Google-Net CNN model was a 120×344 matrix of imaged-like data, while for VGG-net CNN and Squeeze-net CNN models, the first three layers of the Google-Net CNN model were used to represent a 224×224×3 input. The results of these three deep learning methods are summarized in Table 6.

TABLE 6

RESULTS OF 2 DEEP LEARNING METHODS AND PROPOSED METHODS

Deep learning methods	Accuracy (%)	Sensitivity (%)	FP rate (%)	Delay (s)
VGG-net CNN	95.89	84.62	3.70	8.33
Squeeze-net CNN	97.23	91.20	2.37	12.41
Google-net CNN	97.74	98.90	1.94	9.85

Table 7 indicates that the Google-Net CNN model outperformed the VGG-net CNN and Squeeze-net CNN models in real-time EEG epilepsy seizure onset detection. The Google-Net CNN model, with its complex architecture and multiple layers, seems to have demonstrated better capabilities in capturing and understanding the relevant patterns and features in the EEG data for seizure detection.

5. Discussion

5.1 Time-frequency domain analysis

Continuous wavelet transform (CWT) is another commonly used time-frequency analysis techniques that provide insights into the frequency content of a signal over time. The CWT

11

provides variable time and frequency resolution. It uses a wavelet function that can be adjusted in scale to analyse the signal at different frequencies with varying time resolution. Additionally, CWT can capture both high and low frequencies with good temporal localization. It can provide detailed information about transient events or signals with varying frequency content over time. Moreover, CWT is more flexible in terms of the choice of wavelet function and the ability to adapt the analysis to different frequency bands or signal characteristics. This allows for better customization and optimization based on the specific requirements of the application. In this study, the CWT spectrum also tests in the EEG seizure onset detection work, and the frequency resolution are selected into 2 Hz as well. The details are shown in the Figure 6 and the results are described in the Table 7.

(a) CWT analysis of seizure-free input (P3-O1)   (b) CWT analysis of seizure-active input (P3-O1)
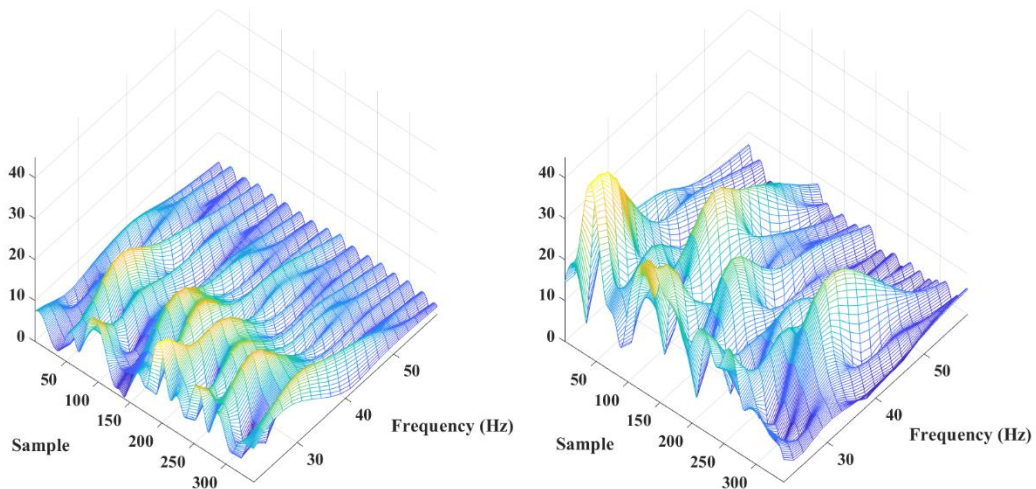
Figure 6. (a) CWT spectrum of seizure free data, (b) CWT spectrum of seizure active data. The seizure active data is collected from case *'Chb01_03'* from 3009s to 3011s, and the seizure free data is collected in the same case from 2800s to 2802s.

TABLE 7
REAL TIME DETECTION USING CWT AND GOOGLE-NET METHOD

Case	Number of seizures	True positive	FP rate (%)	Sensitivity (%)	Delay (s)	Accuracy (%)
Patient 1	7	7	3.02	100.00	16.88	96.59
Patient 2	3	3	2.67	100.00	5.69	97.28
Patient 3	7	7	1.63	100.00	15.16	97.89
Patient 4	4	4	1.60	100.00	26.52	98.12
Patient 5	5	5	3.68	100.00	3.42	96.29
Patient 7	3	3	1.56	100.00	3.02	98.33
Patient 8	5	5	1.85	100.00	5.22	96.93
Patient 9	**4**	**4**	**53.08**	**100.00**	**-8.98**	**46.91**
Patient 10	7	7	6.09	100.00	3.16	93.70
Patient 17	3	3	2.01	100.00	15.02	97.63
Patient 18	6	5	0.72	83.33	25.62	98.79
Patient 19	3	3	0.84	100.00	2.35	98.91
Patient 20	8	8	3.38	100.00	14.52	96.18
Patient 22	3	3	3.33	100.00	6.35	96.42

12

Patient 23	7	7	8.31	100.00	6.59	90.94
Patient 24	16	16	9.16	100.00	5.15	90.28
Total	91	90				
Mean			6.43		9.11	93.20
Sensitivity		98.90				

293 It is evident that, from Table 7, the CWT spectrum with Google-net CNN model is hard to
294 detect case *'Patient 09',* which just achieved 46.91% accuracy and 53.08% FP rate. The STFT
295 can provide a better performance in this research area.

5.2 Real-time application

297 In real-time applications, it is essential to process the data within a limited time frame to
298 provide timely and actionable results. If the calculation time exceeds the overlapping time
299 between consecutive windows, it can result in a delay that renders the detection impractical for
300 real-time use. Therefore, selecting an appropriate window size is crucial to ensure that the
301 computational requirements of the method align with the desired real-time performance.
302 Moreover, the parameter of delay is an important consideration when detecting EEG seizure
303 onset. A large sliding window input, due to a larger window size, can result in a significant
304 delay parameter. This delay refers to the time it takes for the detection algorithm to identify the
305 onset of a seizure after it occurs. A large delay can reduce the clinical relevance of the detection
306 method, as timely intervention or response may be compromised. In this study, selecting a 2-
307 second sliding window is a reasonable choice to balance performance detection and avoid
308 significant delays in real-time applications while ensuring good performance detection.

309 In our previous work [13, 14], the eigenvalue calculation step added to the overall calculation
310 time. The decision to utilize the STFT spectrum directly as input for the Google-Net CNN
311 model has proven to be an effective strategy for minimizing processing time and enabling real-
312 time applications in EEG seizure detection in this research. The processing time of the proposed
313 method is just 0.02 second.

5.3 Previous works comparison

315 Comparisons with the related works in EEG epilepsy seizure onset detection are listed in Table
316 8. In this study, the proposed method receives 97.74% in accuracy, 98.90% in sensitivity,
317 1.94% in false positive rate, and 9.85-second results in the testing data. Compared with the
318 previous related work, the proposed method can achieve satisfactory detection results using the
319 CHB-MIT database. Moreover, the study highlights the efficiency of the proposed method in
320 terms of processing time. It reports a processing time of just 0.02 seconds for every 2-second
321 EEG episode. This indicates that the method is computationally efficient and capable of
322 performing real-time seizure detection with minimal delay.

TABLE 8

COMPARISON OF THE RELATED WORKS IN EEG EPILEPSY SEIZURE DETECTION

Reference	Sensitivity (%)	FP rate (%)	Delay (s)
Zarei, A., et al. (2021) [5]	96.81	2.74	-
Abdelhameed, A., et al. (2021) [25]	98.72	1.14	-
Alharthi, M.K., et al. (2022) [4]	96.85	3.02	-
Amiri, M., et al. (2022) [12]	98.44	0.81	-
Shayeste, H., et al. (2022) [11]	99.52	0.38	-
L. Jiang., et al. (2022) [26]	97.72	4.38	-

13

Our previous work (2022) [13]	96.15	3.24	10.42
Our previous work (2023) [14]	98.90	2.13	10.46
Proposed method	98.90	1.94	9.85

325 However, there are limitations in this study. The experiment conducted in the study had a
326 frequency resolution of 2 Hz instead of 1 Hz. This reduction in frequency resolution was due
327 to limitations in the CPU memory capacity of the workstation used for the study. A higher
328 frequency resolution could potentially provide more detailed information and improve the
329 accuracy of the seizure detection. The selection of CNN models was limited in the study due
330 to GPU memory constraints. As a result, the study could not include CNN models such as
331 Efficient-Net CNN and ResNet-50 CNN. These models are known for their effectiveness in
332 various computer vision tasks and may have provided additional insights and potentially
333 improved the performance of the proposed method if they could have been utilized.

Conclusion

335 This study proposes an EEG-based real-time epilepsy seizure detection approach that combines
336 signal processing techniques with deep learning methods, specifically utilizing time-frequency
337 spectrum and Google-Net CNN models. This approach starts by applying the STFT method to
338 extract signal features and remove redundant information. This step helps to improve the
339 robustness of epilepsy detection using EEG signals. The study then employs the Google-Net
340 CNN model, designed specifically for image-like data, and compares its performance with the
341 Squeeze-net and VGG-net CNN models. The evaluation results demonstrate that the Google-
342 Net CNN model achieves better performance in classifying the image-like data. Additionally,
343 the STFT method is found to be superior to the CWT in terms of reducing the false positive
344 rate. The proposed real-time seizure detection method achieved impressive results on the CHB-
345 MIT Database, with 97.74% accuracy, 98.90% sensitivity, 1.94% false positive rate, and 9.85-
346 second delay when utilizing the STFT spectrum. Based on these findings, the study concludes
347 that the proposed method is suitable for real-time seizure detection and holds great potential
348 for impactful clinical applications. The future plan includes testing the seizure prediction aspect
349 of the method in clinical applications using portable EEG devices and brainwave monitors.

350 Conflicts of Interest: None.

351 Funding: None.

352 Ethical Approval: Not required.

Reference

354 [1] Panayiotopoulos, C.P., A clinical guide to epileptic syndromes and their treatment. 2010.
355 [2] Organization, W.H., Epilepsy: a public health imperative. 2019: World Health
356 Organization.
357 [3] Zandi, A.S., et al., Automated real-time epileptic seizure detection in scalp EEG recordings
358 using an algorithm based on wavelet packet transform. IEEE Transactions on Biomedical
359 Engineering, 2010. 57(7): p. 1639-1651.
360 [4] Alharthi, M.K., et al., Epileptic Disorder Detection of Seizures Using EEG Signals. Sensors,
361 2022. 22(17): p. 6592.
362 [5] Zarei, A. and B.M. Asl, Automatic seizure detection using orthogonal matching pursuit,
363 discrete wavelet transform, and entropy based features of EEG signals. Computers in Biology
364 and Medicine, 2021. 131: p. 104250.

14

[6] Bhattacharyya, A., et al., *Tunable-Q wavelet transform based multiscale entropy measure for automated classification of epileptic EEG signals.* Applied Sciences, 2017. **7**(4): p. 385.

[7] Li, C., et al., Seizure Onset Detection Using Empirical Mode Decomposition and Common Spatial Pattern. IEEE Transactions on Neural Systems and Rehabilitation Engineering, 2021. 29: p. 458-467.

[8] Oweis, R.J. and E.W. Abdulhay, Seizure classification in EEG signals utilizing Hilbert-Huang transform. Biomedical engineering online, 2011. 10(1): p. 1-15.

[9] Hu, W., et al., Mean amplitude spectrum based epileptic state classification for seizure prediction using convolutional neural networks. Journal of Ambient Intelligence and Humanized Computing, 2019: p. 1-11.

[10] Bomela, W., et al., Real-time inference and Detection of Disruptive eeG networks for epileptic Seizures. Scientific Reports, 2020. 10(1): p. 1-10.

[11] Shayeste, H. and B.M. Asl, Automatic seizure detection based on Gray Level Co-occurrence Matrix of STFT imaged-EEG. Biomedical Signal Processing and Control, 2023. 79: p. 104109.

[12] Amiri, M., H. Aghaeinia, and H.R. Amindavar, Automatic epileptic seizure detection in EEG signals using sparse common spatial pattern and adaptive short-time Fourier transform-based synchrosqueezing transform. Biomedical Signal Processing and Control, 2023. 79: p. 104022.

[13] Shen, M., et al., An EEG based real-time epilepsy seizure detection approach using discrete wavelet transform and machine learning methods. Biomedical Signal Processing and Control, 2022. 77: p. 103820.

[14] Shen, M., et al., *Real-time epilepsy seizure detection based on EEG using tunable-Q wavelet transform and convolutional neural network.* Biomedical Signal Processing and Control, 2023. **82**: p. 104566.

[15] Omidvar, M., A. Zahedi, and H. Bakhshi, EEG signal processing for epilepsy seizure detection using 5-level Db4 discrete wavelet transform, GA-based feature selection and ANN/SVM classifiers. Journal of Ambient Intelligence and Humanized Computing, 2021: p. 1-9.

[16] Donos, C., M. Dümpelmann, and A. Schulze-Bonhage, Early seizure detection algorithm based on intracranial EEG and random forest classification. International journal of neural systems, 2015. 25(05): p. 1550023.

[17] Gao, Y., et al., Deep convolutional neural network-based epileptic electroencephalogram (EEG) signal classification. Frontiers in neurology, 2020. 11: p. 375.

[18] Cao, X., et al., Automatic seizure classification based on domain-invariant deep representation of EEG. Frontiers in Neuroscience, 2021: p. 1313.

[19] Wang, X., et al., One dimensional convolutional neural networks for seizure onset detection using long-term scalp and intracranial EEG. Neurocomputing, 2021. 459: p. 212-222.

[20] Chen, H., Y. Song, and X. Li, A deep learning framework for identifying children with ADHD using an EEG-based brain network. Neurocomputing, 2019. 356: p. 83-96.

[21] Ozcan, A.R. and S. Erturk, Seizure prediction in scalp EEG using 3D convolutional neural networks with an image-based approach. IEEE Transactions on Neural Systems and Rehabilitation Engineering, 2019. 27(11): p. 2284-2293.

[22] Shen, M., et al., Detection of alcoholic EEG signals based on whole brain connectivity and convolution neural networks. Biomedical Signal Processing and Control, 2023. 79: p. 104242.

[23] Shen, M., et al., *Automatic identification of schizophrenia based on EEG signals using dynamic functional connectivity analysis and 3D convolutional neural network.* Computers in Biology and Medicine, 2023: p. 107022.

[24] Goldberger, A.L., et al., PhysioBank, PhysioToolkit, and PhysioNet: components of a new research resource for complex physiologic signals. circulation, 2000. 101(23): p. e215-e220.

[25] Abdelhameed, A. and M. Bayoumi, A deep learning approach for automatic seizure detection in children with epilepsy. Frontiers in Computational Neuroscience, 2021. 15: p. 29.

[26] Jiang, L., et al., Seizure detection algorithm based on improved functional brain network structure feature extraction. Biomedical Signal Processing and Control, 2023. 79: p. 104053.

16

Declaration of interests

☒The authors declare that they have no known competing financial interests or personal relationships that could have appeared to influence the work reported in this paper.

☐The authors declare the following financial interests/personal relationships which may be considered as potential competing interests:

CHAPTER 6: PAPER 4 – Detection of alcoholic EEG signals based on whole brain connectivity and convolution neural networks

6.1 Overview of Paper 4

The details of the Paper 4 are given below:

- Paper title: "Detection of alcoholic EEG signals based on whole brain connectivity and convolution neural networks."
- Paper length: 8 pages
- Journal: Biomedical signal processing and control
    - Rank: Q1 (Biomedical Engineering)
    - Impact factor: 5.1 (2022-2023)
    - Cite Score: 8.2 (2022)
    - SJR: 1.071 (2022)
    - SNIP: 1.552 (2022)
- DOI: https://doi.org/10.1016/j.bspc.2022.104242
- First author: Mingkan Shen
- Corresponding author: Mingkan Shen

HDR thesis author's declaration

☒ The authors declare that they have no known competing financial   interests or personal relationships that could have appeared to influence the work reported in this paper.

☐ The authors declare the following financial interests/personal relationships which may be considered as potential competing interests:

Table 6.1: Authorship contributions of Paper 4

Conception and design of study	Mingkan Shen, Peng Wen, Bo Song, Yan Li
Analysis and interpretation of data	Mingkan Shen
Drafting the manuscript	Mingkan Shen
Revising the manuscript critically for important intellectual content	Mingkan Shen, Peng Wen, Bo Song, Yan Li

| Approval of the version of the manuscript to be published | Mingkan Shen, Peng Wen, Bo Song, Yan Li |

6.2   Summary of Paper 4

The intricate and dynamic connections within the brain offer profound insights into its functional states. In neuroscience, one significant challenge lies in detecting abnormalities or deviations from standard patterns, particularly in conditions such as alcoholism that subtly and deeply influence brain function. This paper delves into the paradigm of detecting EEG signals indicative of alcoholism by leveraging whole brain connectivity analysis in tandem with CNN.

Beyond its socio-cultural impacts, alcoholism creates a distinct mark on the electrical activity of the brain. To understand these marks, a thorough analysis of brain connectivity stands essential. With advanced analytical techniques, this study explores the inter-relations and synchronizations across different regions of the brain, as reflected in EEG signals. To enhance the detection process, this research processes these connectivity patterns through convolutional neural networks, a sophisticated machine learning method renowned for its strength in pattern recognition and image analysis.

In this research, which includes EEG datasets from 20 individuals (10 individuals with alcoholism and 10 without), the proposed methodology highlights not only the efficacy of melding whole brain connectivity analysis with CNN but also the subtle shifts that alcohol triggers in brainwave patterns. The implications of this study go beyond simple detection. By illuminating the neural signatures associated with alcoholism, the study sets the stage for timely interventions, improved therapeutic strategies, and a more profound grasp of the neurobiological bases of addictive behaviours.

6.3   Paper file

Detection of alcoholic EEG signals based on whole brain connectivity and convolution neural networks

Mingkan Shen [a,*], Peng Wen [a], Bo Song [a], Yan Li [b]

[a] School of Mechanical and Electrical Engineering, University of Southern Queensland, Toowoomba, QLD 4350, Australia
[b] School of Science, University of Southern Queensland, Toowoomba, QLD 4350, Australia

ABSTRACT

Alcoholism is a common complex brain disorder caused by excessive drinking of alcohol and severely affected the basic function of the brain. This paper investigates classification of the alcoholic electroencephalogram (EEG) signals through whole brain connectivity analysis and deep learning methods. The whole brain connectivity analysis is proposed and implemented using mutual information algorithm. Continuous Wavelet transform was applied to extract time–frequency domain information in each selected frequency bands from EEG signal. The 2D and 3D convolutional neural networks (CNN) were used to classify the alcoholic subjects and health control subjects. UCI Alcoholic EEG dataset is employed to evaluate the proposed method, a 96.25 ± 3.11 % accuracy, 0.9806 ± 0.0163 F1-score result in 3D-CNN model was obtained via leaving-one out training method of all the testing subjects.

1. Introduction

Alcoholism is a physical disease that is addicted to drinking, similarly to obsessive–compulsive disorder [1]. The most common negative effects of alcoholism patients are digestive system diseases which include Ulcers, esophageal bleeding, stomach cancer, acute and chronic pancreatic inflammation and nervous system disorders such as mentally handicapped, Alzheimer, stroke [2]. In addition, the excessive alcohol consumption can cause high blood pressure and gout. According to the report of World Health Organization (WHO), alcoholism is regarded as the third highest risk factor for causing diseases, and it summarized that about 3.3 million deaths every year result from the excessive alcohol consumption [3]. Long-term consumption of alcohol impairs the development of the brain that severely damage the brain's grey and white matter [4]. Similarly, in short-term, alcohol may cause issues in cognition problems and memory loss [5].

Early diagnosis of alcoholism will help individual subjects understand their condition and prevent permanent damage. Traditional alcoholism identification methods are based on questionnaires, breath test and blood tests. Pham, T.T.L., S. Callinan, and M. Livingston used questionnaires method to assess the prevalence of risky drinking among people with a range of chronic diseases [6]. However, the data used in their work is self-reported data which may exist inaccurate responses in

their study. Bertholet, N., et al. stated that the breath test and blood test for identifying alcoholism are questionable as the biomarkers can only provide 66 % sensitivity in carbohydrate-deficient transferrin blood test and missed 70–80 % of cases in breath test [7]. Electroencephalogram (EEG), which records brain activities electronically from the scalp and is the most popular technique in detecting complex brain disorder, can support more accurate classification of the alcoholism brain and health control brain [8,9]. Compared with traditional methods of alcoholism identification, EEG is low-cost, non-invasive, high accuracy of detection and less reliant on trained professionals in practical applications [10]. EEG as the recorded brain activity signals has different features in time domain, frequency domain and time–frequency domain. However, traditional research methods such as Fast Fourier Transform etc are not suitable for analysing the resting-state EEG because EEG signals are considered to be non-stationary time series in this condition, and it can also be computationally expensive for high-density EEGs.

To overcome this limitation, the brain network analysis was proposed as another analogous solution. Many researchers focus on connectivity analysis of brain networks in detecting complex brain disorders such as epilepsy, Alzheimer diseases, schizophrenia etc, and alcoholism can also use connectivity analysis to extract features from EEG raw signal to do the detection work. The connectivity analysis of brain network is derived from the data of EEG and depicts the functional

---

* Corresponding author.
E-mail addresses: Mingkan.Shen@usq.edu.au (M. Shen), Paul.Wen@usq.edu.au (P. Wen), Bo.Song@usq.edu.au (B. Song), Yan.Li@usq.edu.au (Y. Li).

connections between different brain regions where the brain regions are regarded as nodes and the connections as edges. In EEG alcoholism detection, the nodes and edges of the graph represent the EEG channels and the connections between channels. Mumtaz et al. proposed the power coherence functional connectivity of frequency domain to detect the resting-state EEG alcoholic signal and achieved a result of 89.3 % accuracy and 88.5 % sensitivity [11]. Goksen et al. highlighted the functional connectivity measured by mutual information of time domain correlation to classify alcoholism subject and got a result of 82.33 % accuracy and 85.33 % sensitivity [12].

Machine learning methods is widely used in classification work. Comparing with the traditional statistical classification methods, the machine learning methods can provide more accuracy classification results. Nonnegative least squares (NNLS) classifier proposed by Bajaj et al. combined with time–frequency images features of short time Fourier transform (STFT) in alcoholism signal detection and achieved a result of 95.83 % accuracy [13]. Goksen et al. proposed KNN based on relative entropy features got a result of 80.33 % accuracy and 82.67 % sensitivity result [12]. Fayyaz et al. used support vector machine and long short-term memory (LSTM) with peak visualization method achieved a result of 90.97 % in accuracy [14]. Farsi also reported the LSTM algorithm of deep learning methods could directly classify the EEG alcoholism signal and achieved a result of 93 % accuracy [15]. Patidar, S., et al. used Tunable-Q wavelet transform and extracted features as centered correntropy from the decomposition level. Patidar, S., et al. proposed least squares-support vector with 10-fold cross validation method to detect EEG alcoholic signal and achieved an accuracy of 97.02 % [16]. Agarwal, S. and M. Zubair highlighted a method which combined sliding singular spectrum analysis (S-SSA), independent component analysis (ICA) and XGBoost classifier to detect alcoholic subjects and obtained an accuracy of 98.97 % [17].

Traditional machine learning methods require manual feature extraction and model matching, while deep learning methods greatly simplifies the preprocessing process, which can automatically extract features and complete decoding at the same time. In addition, deep learning can directly deal with common events such as eye movements, artifacts, or background EEG, optimizing traditional methods, and giving full play to the end-to-end decoding characteristics of deep learning. The convolution neural network (CNN) is one of the mainstream deep learning algorithms. Most CNN models are used in the image classification work, such as the AlexNet and GoogleNet architectures. In EEG analysis, the CNN models are also used widely, in particular in the image-liked EEG data. Chen et al. combined the mutual information function connectivity and convolution neural networks (CNN) models to detect the attention-deficit/hyperactivity disorder (ADHD) based on EEG signal and obtained a 94.67 % accuracy [18]. Khan et al. applied this method to detect alcoholism EEG data, they used the partial directed coherence with a 3D-CNN model, and achieved an 87.85 % accuracy and 100 % correct classification of all testing subjects [19]. CNN also proposed by Mukhtar, H., S.M. Qaisar, and A. Zaguia to detect alcoholism in a normalized 8-second length EEG data segment directly and achieve 98 % accuracy [20].

In this paper, we proposed the brain connectivity analysis with CNN model to detect EEG alcoholic signal. MI functional connectivity can reveal the abnormal connectivity and nodes (channels) of alcoholic diseases. It can also be used to achieve a satisfying detection result. CNN is used widely in graph classification work because its perfect performance, and it can also achieve good results dealing with the image-like data. Thus, we applied the CNN models and designed a framework suitable for our experiment.

The main contributions of this study are: (1) Firstly, a deep learning enabled whole brain connectivity analysis method was applied to detect alcoholic EEG signal; (2) Design a framework of a 3D-CNN, and apply the image classification method to detect EEG signal and get an accuracy of 96.25 $\pm$ 3.11 % using leaving-one out training method for all the testing subjects; (3) Brain rhythms factor was taken into consideration in

detecting the alcoholic EEG, and the gamma band (30–40 Hz) was found to be the most significant rhythm. (4) After the evaluation of all cross mutual information (CMI) connectivity values, the adjacent connectivities between the left parietal part, the left frontal part, the right temporal part, the right frontal part and the right parietal part were found to be the fuzzy locations in determining alcoholism. All the experiments in this study were carried out in a Dell workstation with dual Intel Xeon E5-2697 V3 CPUs using MATLAB 2021b.

The first section of the paper provided a brief introduction of the work. Section 2 described the details of the dataset. The pre-processing, functional connectivity analysis and classification were also introduced in this section. Section 3 reported our experimental work using the proposed method and the results obtained. The threshold selection of CMI, brain rhythms selection, statistical analysis of CMI values and machine learning method comparison were evaluated in Section 4. We also listed the previous work results to compare the proposed method in this section. Section 5 concluded the work.

2. Methodology

In this EEG based alcoholism detection study, there are four major steps. The Butterworth algorithm was applied to denoise the EEG raw data and the time–frequency domain features were extracted using continuous wavelet transform (CWT) as a pre-processing measure. After that, the extracted features were converted into image-like connectivity matrix through the CMI algorithm. The image-like data is, then, fed to the CNN model as input, and then the training data with leaving-one out training method is used to train the input and test and evaluate the results. The framework of the proposed method is described in Fig. 1:

2.1. Datasets

The data used in this study is collected from the University of California, Irvine Knowledge Discovery in Databases Archive UCI KDD [21]. Dataset SMNI_CMI_TRAIN and Dataset SMNI_CMI_TEST contain data for 10 alcoholic and 10 control subjects, with 10 runs per subject per paradigm. In these two datasets, each dataset has 600 recorded files with 256 Hz sample rate and 64 channels including the EOG signals and the reference channel ND.

2.2. Pre-processing

The sliding window technique is used in this study. A 5-second sliding window was developed and data within the moving window was considered as the input data, and the sliding window overlap was selected as 1 s. A Butterworth zero-phase filter/algorithm is used to denoise the EEG raw data. The CWT algorithm is used to extract time – frequency domain features in different frequency bands with delta band (1–4 Hz), theta band (4–8 Hz), alpha band (8–12 Hz), beta band (12–30 Hz), gamma band (30–40 Hz) and whole band (1–40 Hz). The formula of CWT with 1 Hz frequency resolution is shown as follow:

$$W_{x_i}(t,f) = \int x_i(\lambda) \cdot \overline{\phi_{t,f}(t-\lambda)} d\lambda \qquad (1)$$

where $W_{x_i}(t,f)$ is the energy density in frequency f of the ith channel at time instant t, $\overline{\phi_{t,f}(t-\lambda)}$ is the complex conjugates of $\phi_{t,f}(t-\lambda)$.

The Morlet wavelet method is selected as the mother wavelet, and the algorithm was described as follow:

$$\phi_{t,f}(\lambda) = A \cdot e^{i2\pi f(\lambda-t)} \cdot e^{\frac{-(\lambda-t)^2}{2\sigma^2}} \qquad (2)$$

where $\sigma = \frac{8}{2\pi f}$ is the time spread of the wavelet.

After the denoising and CWT, the data is converted into 256*4 (delta band), 256*5 (theta band), 256*5 (alpha band), 256*19 (beta band), 256*11 (gamma band) and 256*40 (whole band) matrix respectively.
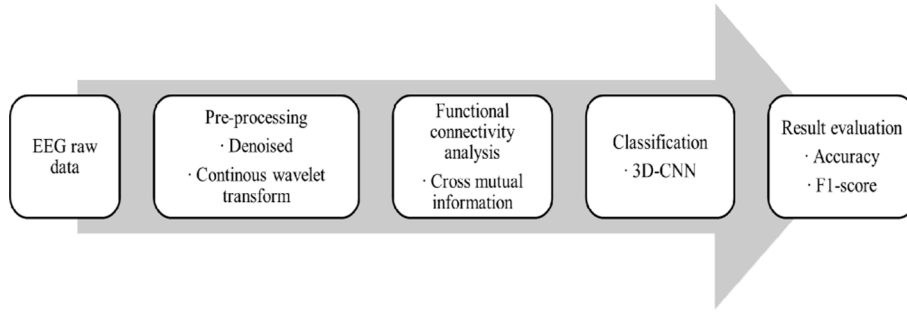
Fig. 1. The framework of CWT, CMI functional connectivity and 3D-CNN methods for seizure detection.

2.3. The cross mutual information functional brain connectivity

The cross mutual information (CMI) based on the CWT algorithm is applied to construct the functional brain matrix in time–frequency domain. The algorithm of CMI between two different channels is shown as follow:

$$MI(F_i, F_j) = H(F_i) + H(F_j) - H(F_i, F_j) \tag{3}$$

where, the $H(F_i)$ is the entropy of Channel i, which describe as:

$$H(F_i) = -\sum_{b=1}^{40} p(F_{i,b}) \log_2 p(F_{i,b}) \tag{4}$$

where F_i is the averaged power signals at the ith channel. The $p(F_{i,b})$ is the probability density function of each frequency bin. The bin is selected as 40.

$H(F_i, F_j)$ is the joint entropy of two channel's averaged power signals, given by:

$$H(F_i, F_j) = -\sum_{b=1}^{40} p(F_{i,b}, F_{j,b}) \log_2 p(F_{i,b}, F_{j,b}) \tag{5}$$

Similarly, the bin is selected as 40 and $p(F_{i,b}, F_{j,b})$ is the probability density function of averaged power signals for channel i and j.

After the calculation, the cross mutual information between channel i and j is obtained:

$$MI(F_i, F_j) = \sum_{b=1}^{40} p(F_{i,b}, F_{j,b}) \log_2 \frac{p(F_{i,b}, F_{j,b})}{p(F_{i,b}) p(F_{j,b})} \tag{6}$$

Thus, the data of six frequency bands (delta band, theta band, alpha band, beta band, gamma band and whole band) are all converted into 64*64 matrix through cross mutual information algorithm. As an example, the image-like CMI matrix of an alcoholic subject co2a0000364 in gamma band is shown in Fig. 2.
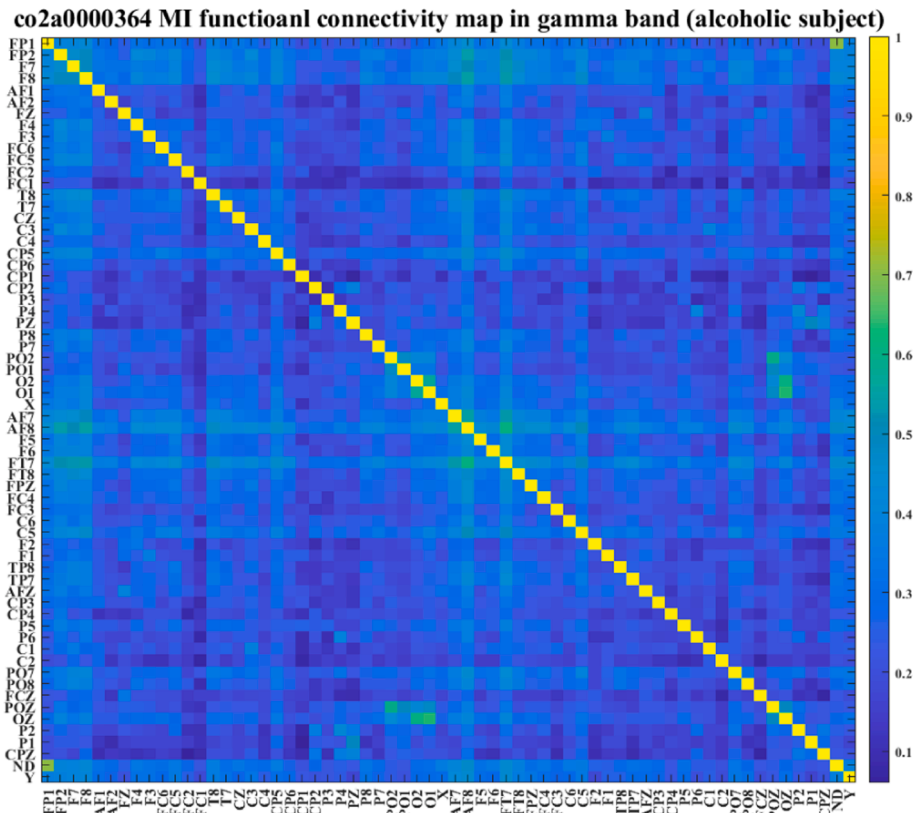
Fig. 2. Cross mutual information functional connectivity matrix of alcoholic subject co2a0000364 in gamma band.

2.4. Classification via convolutional neural networks

The functional connectivity matrix shown above is image-like data which represents the brain connection network. 20 subjects' data (10 HC subjects and 10 alcoholic subjects) from UCI alcoholic EEG dataset was used in this study. In leaving-one out training method, one subject data is used for testing and the other 19 subjects were used for training. As a result, 20 models have been trained. In addition, 20 % random training data is selected as the validation data via hold-out validation method. The input data is the 64*64 size imaged-like data constructed using the CMI algorithm. The training progress selects the learning rate as 0.01, and epochs as 400. Table 1 summarizes the architectural details of the 2D-CNN model as shown below:

The 2D-CNN model includes 6 convolution layers with batch normalization, 3 max pooling layer, 5 ReLU layers and 1 fully connected layer. The 6 convolution layers all use 64 filters with convolution kernels of 3*3, 3*3, 3*3, 3*3, 3*3, and 2*2, respectively. Batch normalization of each convolution layer is to reduce the internal covariance shift which can improve training speed and reduce the over-fitting phenomenon. The 3 Max pooling layers of this architectural is to reduce the cost of training calculation with 2*2 size and 2*2 stride. The activation function ReLU is defined as f(x) = max(0,x) which is used to activate or deactivate a node based on mapped value. The last part is the fully connected layer followed by a Softmax classifier for the identification using the concatenated outputs of the last layers.

Based on the 2D-CNN model with functional connectivity analysis, the gamma band has a better performance than other frequency bands. 3D-CNN in gamma band was designed to further improve the accuracy of the results. The CWT and CMI algorithms are used to compute the functional matrix in each Hz frequency such as (30–31 Hz, 31–32 Hz, …, 39–40 Hz). Thus, the input data size of each segment has changed into 3D imaged-like data size 64*64*10. The 3D functional matrix of the same subject in Fig. 2 is shown in Fig. 3:

In the 3D-CNN model, the learning rate is still selected as 0.01 and

the epochs selected as 400 for comparison with the 2D-CNN results. In addition, the 3D-CNN architectural is designed to classify the input data shown in Fig. 3. Table 2 summarizes the architectural details of the 3D-CNN model with the hyperparameter settings in each layer.

Similar as the architectural of 2D-CNN, this model contains 6 convolution layers with batch normalization, 3 max pooling layers, The 5 ReLU layers and 1 fully connected layer as well. The difference is the hyperparameter settings of each layer. In this model, the 6 convolution layers all use 64 filters with dimensions of 3*3*3, 3*3*3, 3*3*1, 3*3*1, 3*3*1, and 2*2*1 respectively. The size of kernel in 3 max pooling layers are set as 2*2*2, 2*2*2, and 2*2*1 with stride 2*2*2, 2*2*2, and 2*2*1. Other hyperparameter setting is the same as the 2D-CNN such as the ReLU algorithm, fully connected layer and softmax classifier. The optimizer based Deep Network Designer of MATLAB 2021b of HC subject co2c0000345 is shown in Fig. 4.

3. Experiments and results

Accuracy is a direct parameter in method evaluation which is define as follow:

$$Acc = \frac{TP + TN}{TP + TN + FP + FN} \tag{7}$$

where '*TP*' is the true positive, '*TN*' is the true negative, '*FP*' is the false positive and '*FN*' is the false negative.

In statistical analysis of binary classification, the F1-score is an accuracy measure of a test. It is calculated from the precision and recall of the test, where the precision is the number of true positive results divided by the number of all positive results, including those not identified correctly, and the recall is the number of true positive results divided by the number of all samples that should have been identified as positive. In this study, we use the leaving-one out training method that makes the true negative and false positive being zero. The formula of F1-score were shown in equation (10).

$$PRECISION = \frac{TP}{TP + FP} = \frac{TP}{TP} = 1 \tag{8}$$

$$RECALL = \frac{TP}{TP + FN} = Acc \tag{9}$$

$$F1 - score = 2 * \frac{PRECISION * RECALL}{PRECISION + RECALL} = \frac{2 * Acc}{1 + Acc} \tag{10}$$

where '*TP*' is the true positive, '*FP*' is the false positive, '*FN*' is the false negative and '*Acc*' is accuracy.

3.1. Results for 2D and 3D convolutional neural networks

Based on the performance in alcoholic subjects' detection on gamma band which detailly discussed in Discussion part section B, 2D and 3D CNN methods are applied to detect EEG alcoholic signal in this study. We achieved 86.25 ± 6.48 % accuracy, 0.9249 ± 0.0378 F1-score and 96.25 ± 3.11 % accuracy, 0.9806 ± 0.0163 F1-score respectively. The details are summarized in Table 3 and Table 4.

4. Discussion

4.1. Time-frequency domain functional connectivity analysis

The Mutual information measures the degree of interdependence between two variables which widely used in studies of analysing synchronicity. Joint entropy, as one of the significant parameters of mutual information, describes the distribution of the signal. The bin selection of the joint entropy changes the distribution of the data. The challenge in calculating the CMI from experimental data is to estimate $p(F_{i,b}, F_{j,b})$ from histograms. For a given number of data points, using larger sam-

Table 1

The architecture of 2D-CNN for training and test of the alcoholic detection.

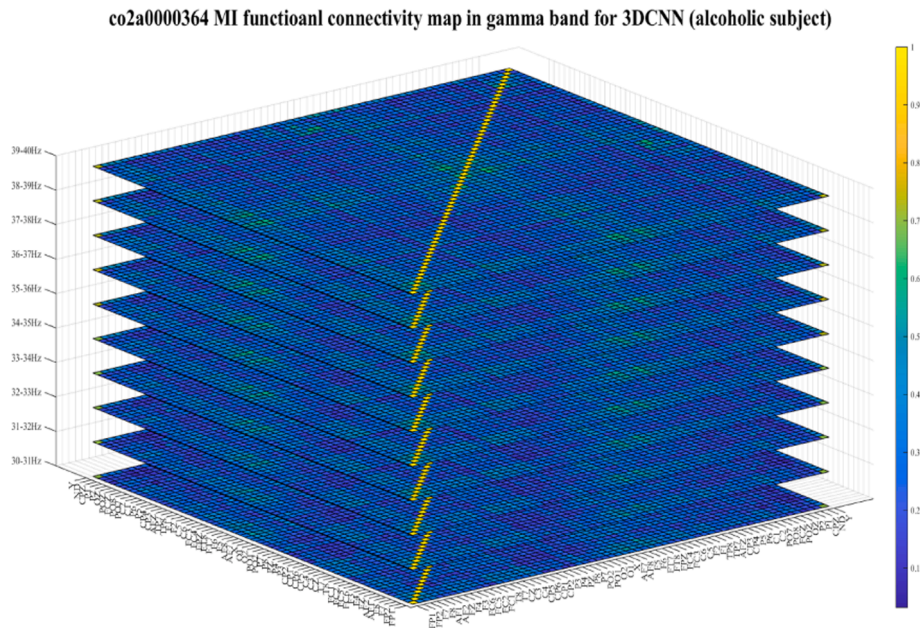| Layer	Input Size	Output Size	Trainable parameters
2D imaged-data input	64*64*1		
Convolution layer	64*64*1	62*62*64	Kernel size: 3*3 Stride: 1*1 Channel: 64
ReLU	62*62*64	62*62*64	
Max Pooling layer	62*62*64	31*31*64	Pooling Size: 2*2 Stride: 2*2
Convolution layer	31*31*64	29*29*64	Kernel size: 3*3 Stride: 1*1 Channel: 64
ReLU	29*29*64	29*29*64	
Max Pooling layer	29*29*64	14*14*64	Pooling Size: 2*2 Stride: 2*2
Convolution layer	14*14*64	12*12*64	Kernel size: 3*3 Stride: 1*1 Channel: 64
ReLU	12*12*64	12*12*64	
Max Pooling layer	12*12*64	6*6*64	Pooling Size: 2*2 Stride: 2*2
Convolution layer	6*6*64	4*4*64	Kernel size: 3*3 Stride: 1*1 Channel: 64
ReLU	4*4*64	4*4*64	
Convolution layer	4*4*64	2*2*64	Kernel size: 3*3 Stride: 1*1 Channel: 64
ReLU	2*2*64	2*2*64	
Convolution layer	2*2*64	1*1*64	Kernel size: 2*2 Stride: 1*1 Channel: 64
Fully Connected layer	1*1*64	1*1*2	
Softmax	1*1*2		

Fig. 3. 10 layers cross mutual information functional connectivity matrix of alcoholic subject in gamma band.

Table 2
The architecture of 3D-CNN for training and test of the alcoholic detection.

Layer	Input Size	Output Size	Trainable parameters
3D imaged-data input	64*64*10*1		
Convolution layer	64*64*10*1	62*62*8*64	Kernel size: 3*3*3 Stride: 1*1*1 Channel: 64
ReLU	62*62*8*64	62*62*8*64	
Max Pooling layer	62*62*8*64	31*31*4*64	Pooling Size: 2*2*2 Stride: 2*2*2
Convolution layer	31*31*4*64	29*29*2*64	Kernel size: 3*3*3 Stride: 1*1*1 Channel: 64
ReLU	29*29*2*64	29*29*2*64	
Max Pooling layer	29*29*2*64	14*14*1*64	Pooling Size: 2*2*2 Stride: 2*2*2
Convolution layer	14*14*1*64	12*12*1*64	Kernel size: 3*3*1 Stride: 1*1*1 Channel: 64
ReLU	12*12*1*64	12*12*1*64	
Max Pooling layer	12*12*1*64	6*6*1*64	Pooling Size: 2*2*1 Stride: 2*2*1
Convolution layer	6*6*1*64	4*4*1*64	Kernel size: 3*3*1 Stride: 1*1*1 Channel: 64
ReLU	4*4*1*64	4*4*1*64	
Convolution layer	4*4*1*64	2*2*1*64	Kernel size: 3*3*1 Stride: 1*1*1 Channel: 64
ReLU	2*2*1*64	2*2*1*64	
Convolution layer	2*2*1*64	1*1*1*64	Kernel size: 2*2*1 Stride: 1*1*1 Channel: 64
Fully Connected layer	1*1*1*64	1*1*1*2	
Softmax	1*1*1*2		

pling bins to construct the histograms produces more accurate estimates of the average probability, but then the estimate of $p(F_{i,b}, F_{j,b})$ will be over detrended, and underestimate the $MI(F_i, F_j)$. Using smaller bins is better in indicating changes in $p(F_{i,b}, F_{j,b})$ over short distances, but it produces fluctuations because of the smaller sample size, which will overestimate $MI(F_i, F_j)$. Empirically, the bin of joint entropy was selected as 40, as shown in Fig. 5:

To extract the features from both time domain and frequency domain, CWT method is applied to obtain the power spectrum of time–frequency domain. In alcoholic EEG detection, the data of gamma band (30–40 Hz) provides the best performance in detection than other frequency bands. The CWT method and CMI algorithm of brain connectivity analysis can consider both time domain and frequency domain features, which improves the performance of classification results.

4.2. Brain rhythms selection

In this study, the functional connectivity is constructed in different frequency bands, delta band (1–4 Hz), theta band (4–8 Hz), alpha band (8–12 Hz), beta band (12–30 Hz), gamma band (30–40 Hz) and whole band (1–40 Hz), to find the best brain rhythms in EEG alcoholic subject detection. Table 5 summarized the results of the accuracy and sensitivity of the classification between alcoholic subjects and health control subjects in each frequency bands.

To reduce the computational cost, the gamma band data is selection to fed into the deep learning methods.

4.3. Different classification method comparison

In this experiment of alcoholic detection via CWT, CMI and 3D-CNN models, we get a 96.25 ± 3.11 % accuracy using the gamma band. The SVM, KNN and decision tree methods with random 20 % hold-out validation of leaving-one out training method were applied to conduct the alcoholic signal detection and compared with the results of the 3D-CNN models. In 3D-CNN model, we used the 64*64*10 (40960) imaged-like data as input. But the value of CMI matrix is symmetrical, in addition, the values between the same nodes, such as (Fz to Fz), are all equal to 1. To reduce the computing costs, we used (64*64–64)/2*10 = 20160 eigenvalues as the input. The results of these three machine learning methods are summarized in Table 6.

It is evident that, from Table 6, the 3D-CNN model provides a better performance in alcoholic signal detection than the aforementioned three machine learning methods.

4.4. Statistical significance of CMI connectivity in whole brain connectivity

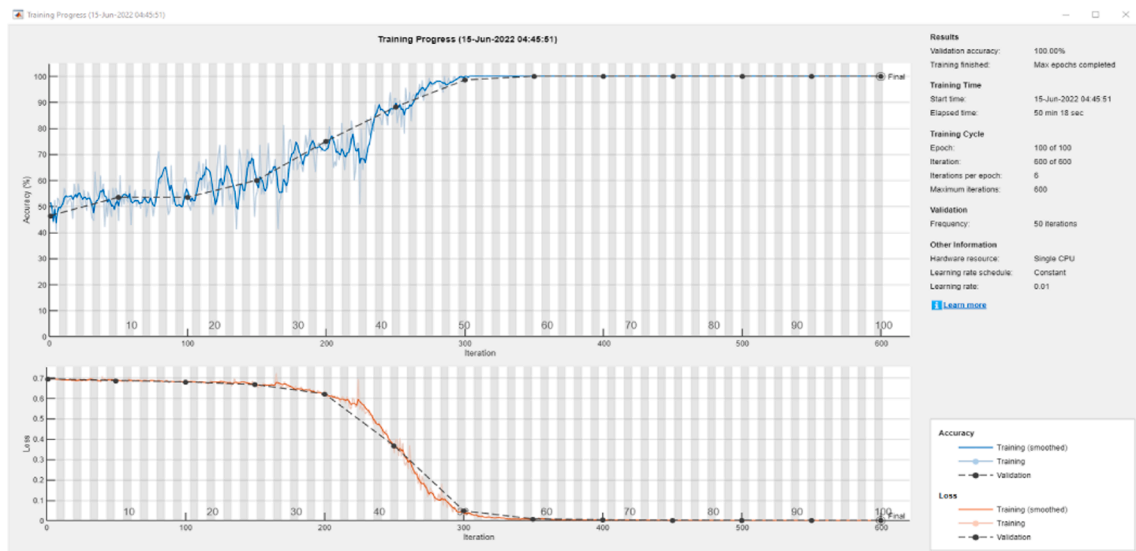Finding the connectivity location can aid in detecting the location of

Fig. 4. The optimizer for 3D-CNN model of HC subject co2C0000345.

Table 3
Classification performance of 2D-CNN test.

Subject No.	CMI matrices	Samples identified as		Acc (%)
		ALC	HC	
Co2a0000364	56	48	8	85.71
Co2a0000365	56	50	6	89.29
Co2a0000368	56	49	7	87.50
Co2a0000369	56	44	12	78.57
Co2a0000370	56	47	9	83.93
Co2a0000371	56	48	8	85.71
Co2a0000372	56	49	7	87.50
Co2a0000375	56	52	4	92.86
Co2a0000377	56	56	0	100.00
Co2a0000378	56	40	16	71.43
Co2c0000337	56	5	51	91.07
Co2c0000338	56	12	44	78.57
Co2c0000339	56	11	45	80.36
Co2c0000340	56	8	48	85.71
Co2c0000341	56	6	50	89.29
Co2c0000342	56	7	49	87.50
Co2c0000344	56	7	49	87.50
Co2c0000345	56	3	53	94.64
Co2c0000346	56	12	44	78.57
Co2c0000347	56	6	50	89.29
Mean ± Std				86.25 ± 6.48

'*ALC*' is the alcoholic subject, '*HC*' is the healthy control subject, and '*Acc*' is accuracy.

Table 4
Classification performance of 3D-CNN test.

Subject No.	CMI matrices	Samples identified as		Acc (%)
		ALC	HC	
Co2a0000364	56	55	1	98.21
Co2a0000365	56	51	5	91.07
Co2a0000368	56	55	1	98.21
Co2a0000369	56	55	1	98.21
Co2a0000370	56	56	0	100.00
Co2a0000371	56	55	1	98.21
Co2a0000372	56	55	1	98.21
Co2a0000375	56	56	0	100.00
Co2a0000377	56	56	0	100.00
Co2a0000378	56	51	5	91.07
Co2c0000337	56	5	51	91.07
Co2c0000338	56	0	56	100.0
Co2c0000339	56	3	53	94.64
Co2c0000340	56	4	52	92.86
Co2c0000341	56	3	53	94.64
Co2c0000342	56	3	53	94.64
Co2c0000344	56	3	53	94.64
Co2c0000345	56	2	54	96.43
Co2c0000346	56	3	53	94.64
Co2c0000347	56	1	55	98.21
Mean ± Std				96.25 ± 3.11

'*ALC*' is the alcoholic subject, '*HC*' is the healthy control subject, and '*Acc*' is accuracy.

symptoms in alcoholism patients. We calculated all CMI connectivity values and listed the top 7 channels ($\geq$0.05) with the major difference in CMI mean values between HC subjects and alcoholic subjects in Table 7:

We found that the major difference happened to the connectivity between the left parietal part, the left frontal part, the right temporal part, the right frontal part and the right parietal part. In addition, the most difference connectivities are between adjacent channels. The HC subjects' CMI values in this location are obviously more remarkable than the alcoholic subjects.

4.5. Performance comparison with previous work

Table 8 summarizes the performance of the proposed method and other peer works in alcoholic signal detection. The proposed method achieved a result of 96.25 ± 3.11 % in accuracy through function connectivity analysis and 3D-CNN deep learning model.

The proposed method achieved a satisfying result of 96.25 ± 3.11 %

in accuracy. In addition, this method can also determine fuzzy locations of the abnormal connectivity area caused by alcoholic diseases. Furthermore, the sliding window technique applied can capture the dynamics of alcoholism [11,25–27]. However, this study still has several limitations. Firstly, there is more work to be done to implement real-time detection, as the proposed method cannot calculate a sliding window size smaller than 10 s. Secondly, the alcoholic diseases' location is fuzzy, this method cannot detect the alcoholic diseases in specific regions of interest in the brain at the moment.

5. Conclusion

In this paper, the whole brain connectivity analysis is applied and implemented using mutual information algorithm. The functional connectivity maps between the whole brain regions are estimated using CWT and CMI algorithms. The 2D and 3D convolutional neural networks are applied to classify the alcoholic subjects and health control subjects.
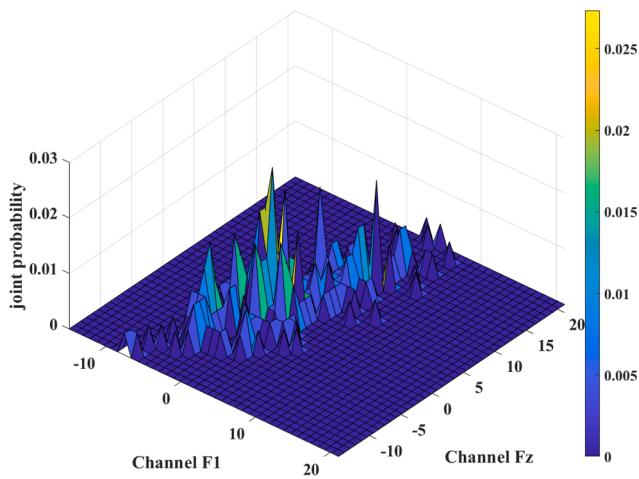
Fig. 5. Joint entropy of channel F1 and channel Fz.

Table 5

Results of 2D-CNN in different brain rhythms.

Frequency bands	Acc (%)
Delta band (1–4 Hz)	52.02 ± 7.98
Theta band (4–8 Hz)	55.66 ± 6.73
Alpha band (8–12 Hz)	62.50 ± 6.34
Beta band (12–30 Hz)	75.84 ± 7.65
Gamma band (30–40 Hz)	86.25 ± 6.48
Whole band (1–40 Hz)	72.54 ± 7.56

'*Acc*' is accuracy.

Table 6

Results of 3 machine learning methods.

Machine learning methods	Validation Acc (%)	Acc (%)
Decision tree	94.93 ± 0.88	88.93 ± 6.15
SVM	99.72 ± 0.32	95.18 ± 5.41
KNN	99.82 ± 0.36	91.67 ± 6.03
Proposed Method 3D-CNN	99.77 ± 0.29	96.25 ± 3.11

'*Acc*' is accuracy.

Table 7

The mean value of CMI values.

CMI location (Channel to Channel)	CMI values in HC subjects	CMI values in alcoholic subjects
FP2-AF2	0.2534 ± 0.0337	0.1850 ± 0.0313
P4-P8	0.2314 ± 0.0332	0.1811 ± 0.0357
P8-PO2	0.2213 ± 0.0318	0.1682 ± 0.0296
F7-F5	0.2392 ± 0.0449	0.1848 ± 0.0236
T7-C5	0.2080 ± 0.0256	0.1555 ± 0.0279
P5-P7	0.2983 ± 0.0310	0.2309 ± 0.0390
P6-P8	0.2845 ± 0.0295	0.2286 ± 0.0274

'ALC' is the alcoholic subject, 'HC' is the healthy control subject.

In particular, the 2D-CNN model achieved results of 86.25 ± 6.48 % in accuracy and 0.9249 ± 0.0378 F1-score of gamma band data which have better performance than other frequency bands. Based on the 2D-CNN results, a 3D-CNN was proposed to improve the detection results further and 96.25 ± 3.11 % accuracy and 0.9806 ± 0.0163 F1-score of all the testing subjects. Furthermore, we analysed the CMI values in the whole connectivity and found the most significant channels that can detect the fuzzy brain connectivities location of symptoms in alcoholism patients.

Table 8

Comparison of the proposed method and previous works in EEG alcoholism detection.

References	Channels	Features	Classifier	Acc (%)
Mumtaz et al. (2017) [11]	19	Coherence functional connectivity	Logistic regression	89.3
Goksen et al. (2017) [12]	19	Mutual information functional connectivity	KNN	82.33
Patidar, S., et al. (2017) [16]	64	Tunable-Q wavelet transform, centered correntropy	LS-SVM	97.02
Malar et al. (2020) [22]	64	Wavelet decomposition	Extreme learning machine	87.6
Farsi et al. (2020) [15]	64	EEG signal	LSTM	93
Agarwal, S. and M. Zubair (2021) [17]	64	S-SSA, ICA	XGBoost classifier	98.97
Mukhtar, H., S.M. Qaisar, and A. Zaguia (2021) [20]	64	Normalized EEG signal	CNN	98
Khan et al. (2021) [19]	6	Effective connectivity (DMN)	3D-CNN	87.85 ± 4.64
Kumari, N et al. (2022) [23]	19	Raw EEG signal	CNN	92.7
Li, H. and Wu, Lei (2022) [24]	64	Discrete Wavelet Transformation	CNN, Bi-LSTM	99.32
Proposed method	64	Cross mutual information functional connectivity	3D-CNN	96.25 ± 3.11

Declaration of Competing Interest

The authors declare that they have no known competing financial interests or personal relationships that could have appeared to influence the work reported in this paper.

Data availability

No data was used for the research described in the article.

References

[1] M. Oscar-Berman, K. Marinković, Alcohol: effects on neurobehavioral functions and the brain, Neuropsychol. Rev. 17 (3) (2007) 239–257.

[2] D. Das, S. Zhou, J.D. Lee, Differentiating alcohol-induced driving behavior using steering wheel signals, IEEE Trans. Intell. Transp. Syst. 13 (3) (2012) 1355–1368.

[3] Organization, W.H., Technical package for cardiovascular disease management in primary health care: healthy-lifestyle counselling, World Health Organization, 2018.

[4] S.F. Tapert, et al., fMRI measurement of brain dysfunction in alcohol-dependent young women, Alcohol. Clin. Exp. Res. 25 (2) (2001) 236–245.

[5] A. Priya, et al., Efficient method for classification of alcoholic and normal EEG signals using EMD, J. Eng. 2018 (3) (2018) 166–172.

[6] T.T.L. Pham, S. Callinan, M. Livingston, Patterns of alcohol consumption among people with major chronic diseases, Aust. J. Primary Health 25 (2) (2019).

[7] N. Bertholet, et al., How accurate are blood (or breath) tests for identifying self-reported heavy drinking among people with alcohol dependence? Alcohol Alcohol. 49 (4) (2014) 423–429.

[8] E.A. de Bruin, et al., Abnormal EEG synchronisation in heavily drinking students, Clin. Neurophysiol. 115 (9) (2004) 2048–2055.

[9] E.A. De Bruin, et al., Moderate-to-heavy alcohol intake is associated with differences in synchronization of brain activity during rest and mental rehearsal, Int. J. Psychophysiol. 60 (3) (2006) 304–314.

[10] A. Craik, Y. He, J.L. Contreras-Vidal, Deep learning for electroencephalogram (EEG) classification tasks: a review, J. Neural Eng. 16 (3) (2019), 031001.

[11] W. Mumtaz, et al., An EEG-based machine learning method to screen alcohol use disorder, Cogn. Neurodyn. 11 (2) (2017) 161–171.

[12] N. Gökşen, S. Arıca, A simple approach to detect alcoholics using electroencephalographic signals, in: EMBEC & NBC 2017, Springer, 2017, pp. 1101–1104.

[13] V. Bajaj, et al., A hybrid method based on time–frequency images for classification of alcohol and control EEG signals, Neural Comput. Appl. 28 (12) (2017) 3717–3723.

[14] A. Fayyaz, M. Maqbool, M. Saeed, Classifying alcoholics and control patients using deep learning and peak visualization method, in: Proceedings of the 3rd International Conference on Vision, Image and Signal Processing, 2019.

[15] L. Farsi, et al., Classification of alcoholic EEG signals using a deep learning method, IEEE Sens. J. 21 (3) (2020) 3552–3560.

[16] S. Patidar, et al., An integrated alcoholic index using tunable-Q wavelet transform based features extracted from EEG signals for diagnosis of alcoholism, Appl. Soft Comput. 50 (2017) 71–78.

[17] S. Agarwal, M. Zubair, Classification of Alcoholic and Non-Alcoholic EEG Signals Based on Sliding-SSA and Independent Component Analysis, IEEE Sens. J. 21 (23) (2021) 26198–26206.

[18] H. Chen, Y. Song, X. Li, A deep learning framework for identifying children with ADHD using an EEG-based brain network, Neurocomputing 356 (2019) 83–96.

[19] D.M. Khan, et al., Effective Connectivity in Default Mode Network for Alcoholism Diagnosis, IEEE Trans. Neural Syst. Rehabil. Eng. 29 (2021) 796–808.

[20] H. Mukhtar, S.M. Qaisar, A. Zaguia, Deep convolutional neural network regularization for alcoholism detection using EEG signals, Sensors 21 (16) (2021) 5456.

[21] K. Bache, M. Lichman, UCI Machine Learning Repository. University of California, School of Information and Computer Science, Irvine, CA, 2013, 2017.

[22] E. Malar, M. Gauthaam, Wavelet analysis of EEG for the identification of alcoholics using probabilistic classifiers and neural networks, Int. J. Intell. Sustain. Comput. 1 (1) (2020) 3–18.

[23] N. Kumari, S. Anwar, V. Bhattacharjee, A Deep Learning-Based Approach for Accurate Diagnosis of Alcohol Usage Severity Using EEG Signals, IETE J. Res. (2022) 1–15.

[24] H. Li, L. Wu, EEG Classification of Normal and Alcoholic by Deep Learning, Brain Sci. 12 (6) (2022) 778.

[25] T.P. Teo, et al., Feasibility of predicting tumor motion using online data acquired during treatment and a generalized neural network optimized with offline patient tumor trajectories, Med. Phys. 45 (2) (2018) 830–845.

[26] A.-S. Wessam, Y. Li, P. Wen, K-complexes detection in EEG signals using fractal and frequency features coupled with an ensemble classification model, Neuroscience 422 (2019) 119–133.

[27] M. Shen, et al., An EEG based real-time epilepsy seizure detection approach using discrete wavelet transform and machine learning methods, Biomed. Signal Process. Control 77 (2022), 103820.

CHAPTER 7: PAPER 5 – Automatic identification of schizophrenia based on EEG signals using dynamic functional connectivity analysis and 3D convolutional neural network

7.1 Overview of Paper 5

The details of the Paper 5 are given below:

- Paper title: "Automatic identification of schizophrenia based on EEG signals using dynamic functional connectivity analysis and 3D convolutional neural network."

- Paper length: 8 pages

- Journal: Computers in Biology and Medicine
    - Rank: Q1 (Computer Science Applications)
    - Impact factor: 7.7 (2022-2023)
    - Cite Score: 9.2 (2022)
    - SJR: 1.222 (2022)
    - SNIP: 1.798 (2022)

- DOI: https://doi.org/10.1016/j.compbiomed.2023.107022

- First author: Mingkan Shen

- Corresponding author: Mingkan Shen

HDR thesis author's declaration

☒ The authors declare that they have no known competing financial interests or personal relationships that could have appeared to influence the work reported in this paper.

☐ The authors declare the following financial interests/personal relationships which may be considered as potential competing interests:

Figure 7.1: Authorship contributions of Paper 5

Conception and design of study	Mingkan Shen, Peng Wen, Bo Song, Yan Li
Analysis and interpretation of data	Mingkan Shen

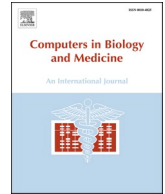| Drafting the manuscript	Mingkan Shen
Revising the manuscript critically for important intellectual content	Mingkan Shen, Peng Wen, Bo Song, Yan Li

7.2   Summary of Paper 5

The intricate landscape of the human brain, with its myriad connections and pathways, continually adapts and evolves over time, especially in response to various disorders. ScZ, a severe mental disorder, is one such condition that brings about marked changes in the brain's functional dynamics. The paper embarks on a cutting-edge approach to automatically identify ScZ by analysing EEG signals through dynamic functional connectivity analysis and leveraging the computational might of 3D-CNN.

ScZ does not only manifest as a collection of symptoms on the surface but also imprints unique changes on the underlying neural activity. By observing and understanding these changes, there's potential for early diagnosis and intervention. This research employs dynamic functional connectivity analysis to chronicle the time-varying associations between distinct regions of the brain as represented by EEG signals. To take the detection process to the next level, these dynamic patterns are then subjected to 3D-CNN models, which are adept at recognizing intricate spatial-temporal patterns in data volumes.

Spanning EEG datasets from 84 individuals, 45 subjects diagnosed with ScZ and 39 subjects as controls, this research accentuates the power of combining dynamic brain connectivity techniques with the robustness of 3D-CNNs. This novel approach not only optimizes the automatic detection of ScZ but also shines a light on the deeper, often overlooked, neural alterations associated with the disorder. By demystifying these neural signatures, the study holds promise for more targeted therapeutic interventions and a holistic understanding of the enigmatic world of ScZ.

7.3   Paper file

Contents lists available at ScienceDirect

Computers in Biology and Medicine

journal homepage: www.elsevier.com/locate/compbiomed

Automatic identification of schizophrenia based on EEG signals using dynamic functional connectivity analysis and 3D convolutional neural network

Mingkan Shen [a,*], Peng Wen [a], Bo Song [a], Yan Li [b]

[a] School of Engineering, University of Southern Queensland, Toowoomba, Australia
[b] School of Mathematics, Physics and Computing, University of Southern Queensland, Toowoomba, Australia

ABSTRACT

Schizophrenia (ScZ) is a devastating mental disorder of the human brain that causes a serious impact of emotional inclinations, quality of personal and social life and healthcare systems. In recent years, deep learning methods with connectivity analysis only very recently focused into fMRI data. To explore this kind of research into electroencephalogram (EEG) signal, this paper investigates the identification of ScZ EEG signals using dynamic functional connectivity analysis and deep learning methods. A time-frequency domain functional connectivity analysis through cross mutual information algorithm is proposed to extract the features in alpha band (8–12 Hz) of each subject. A 3D convolutional neural network technique was applied to classify the ScZ subjects and health control (HC) subjects. The LMSU public ScZ EEG dataset is employed to evaluate the proposed method, and a 97.74 ± 1.15% accuracy, 96.91 ± 2.76% sensitivity and 98.53 ± 1.97% specificity results were achieved in this study. In addition, we also found not only the default mode network region but also the connectivity between temporal lobe and posterior temporal lobe in both right and left side have significant difference between the ScZ and HC subjects.

1. Introduction

Schizophrenia (ScZ) is a major neuropsychiatric disorder which causes psychosis and is associated with considerable disability [1,2]. Mainly ScZ patients have persistent delusions, persistent hallucinations, disorganized thinking and highly disorganized behavior [3–5]. World Health Organization (WHO) reported that ScZ disease affects approximately 24 million people throughout the world in 2022 [6]. Electroencephalogram (EEG) as an auxiliary mean of identification, which can provide perfect performance in identification with high accuracy results between ScZ subjects and health control (HC) subjects through the scalp brain electronically signal [7]. In addition, EEG supports several benefits rather than the other medical machine application such as functional magnetic resonance imaging (fMRI) and Magnetoencephalography (MEG), which includes low-cost prize in medical machine and less reliance on trained professionals for practical application [8,9].

Complex brain networks analysis is used widely to explore brain diseases such as Alzheimer diseases, Parkinso's diseases, alcoholism, epilepsy diseases and ScZ diseases etc, [10–12]. Chen et al. proposed

function connectivity calculated through the mutual information (MI) algorithm and improved Google-net CNN models to identify the attention-deficit/hyperactivity disorder (ADHD) subjects based on EEG signal and reported a result of 94.67% accuracy [13]. They also compared the connectivity features in the support vector machine (SVM) and multilayer perceptron and received 90.16% and 92.08% accuracy, respectively. Khan et al. applied the PDC connectivity method with a 3D-CNN model to detect alcoholism EEG data, and received a result of 87.85% accuracy [12]. In our previous work, we proposed the functional connectivity through the cross mutual information (CMI) algorithm as signal processing work with a 3D-CNN method to classify the alcoholic EEG data, and received a result of 96.25 ± 3.11% accuracy [14]. Inspired by the good classification results of the method which combined the EEG brain connectivity and graph deep learning models in research, combining brain connectivity analysis and graph classification in EEG ScZ identification is proposed in this paper.

The default mode network (DMN) is a popular location for resting state brain activity analysis through the fMRI and EEG data. There are three main well-recognized area of the DMN which contains the mesial

---

* Corresponding author.
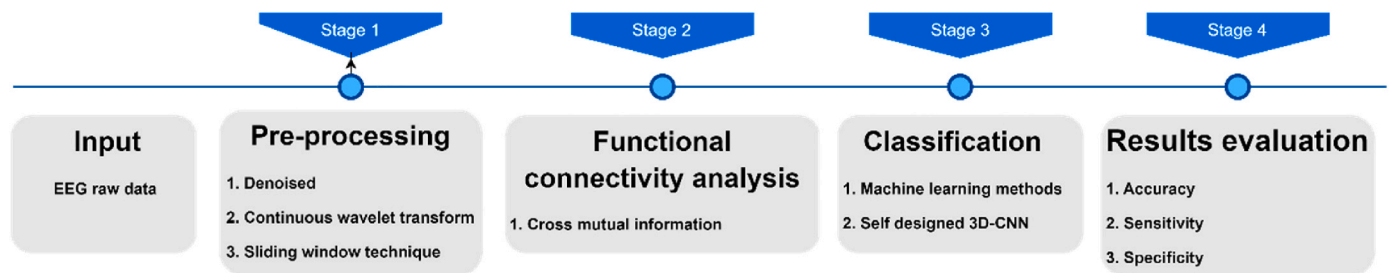 *E-mail address:* Mingkan.Shen@usq.edu.au (M. Shen).

Fig. 1. The framework of automatic identification of ScZ though dynamic functional connectivity analysis and deep learning method.

prefrontal cortex (MPC), the lateral posterior cortex (LPC) and posterior cingulate cortex/precuneus (PCC) [15]. Many ScZ identification work based on fMRI data used the DMN region as the nodes through the independent component analysis [16,17]. However, Phang et al. regarded local brain network connectivity cannot fully reflect abnormal brain region communication observed in ScZ [18]. In our study, the whole brain connectivity is used to identify the ScZ and verify the effect of the DMN region through the statistical significance of connectivity.

1.1. State of art section

Many researchers have attempted to identify ScZ from EEG data through traditional signal processing method with the machine learning and deep learning models. Shoeibi et al. proposed a deep learning model which combined 1D-CNN and long short-term memories (LSTMs) to detect the ScZ EEG signal and received an accuracy percentage of 99.25% result [19]. Siuly et al. applied a Google-net based deep features with an SVM model to classify the ScZ subjects and reported a result of 98.84% accuracy, 99.02% sensitivity and 98.58% specificity [20]. They also highlighted another method through a deep residual network and SVM classifier in the same dataset and achieved 99.23% accuracy [21]. Discrete wavelet transform (DWT) and relaxed local neighbor difference pattern (RLNDip) technique with artificial neural network (ANN) is proposed by N.J. Sairamya et al. to identify the EEG ScZ signal, and they reported a maximum accuracy of 100% in their study [22]. Principal component analysis (PCA) and k-nearest neighbours (k-NN) models stated via de Miras et al. to perform ScZ patients from healthy subjects, and achieved a result of 0.87 accuracy, 0.82 sensitivity and 0.90 specificity [23].

Comparing with the traditional signal processing method used in EEG signal detection, the brain network analysis not only can achieve a satisfied detection result, but also can find the abnormal connectivity area caused by ScZ diseases. In connectivity analysis, there are mainly two methods to identification patients and HC subjects. One is using graph theory measures of complex brain network analysis to summarize the details of the brain graph and using machine learning methods to classifier the data. Kim, J.-Y et al. proposed the global and local clustering coefficient as the brain network features and received their best accuracy of 80.66% through linear discriminant analysis classifier in ScZ detection [24]. Another method is directly using the machine learning and deep learning methods to classifier the brain connectivity matrix. Panischev et al. proposed cross correlation function algorithm to construct frequency domain functional connectivity for detecting ScZ and reported results of 80% in accuracy, 76% in sensitivity and 85% specificity [25]. Zhao, Z. et al. used partial directed coherence (PDC) and phase lag index (PLI) to calculate the effective and functional connectivity matrix, and they applied the SVM model to classifier the ScZ subject and achieved 95.16% accuracy 96.15% sensitivity and 94.44% specificity results [26]. Naira, T. and C. Alberto proposed the Pearson correlation connectivity with CNN to classifier the EEG ScZ signal and reported the results 90% in accuracy, 90% in sensitivity and 90% in specificity, respectively [27]. Phang et al. developed a directed functional connectivity through PDC with vector autoregressive model, then

classified the ScZ EEG signal via a multi-domain connectome CNN model and reported a result of 91.69 ± 4.67% in accuracy, 91.11 ± 8.31% in sensitivity and 92.50 ± 10.00% in specificity [18]. Chang, Q. et al. highlighted the graph neural network (GNN) to classify ScZ connectivity features calculated by PLI and partial correlation (PC) algorithms, and reported a result of 93.33% accuracy [28].

1.2. Objectives of this study

In this study, dynamic CMI connectivity method with 3D-CNN model is proposed to identify the EEG ScZ signal. The CMI connectivity can extract the time-frequency domain features and find abnormal connectivity area caused by the ScZ diseases. In addition, the 3D-CNN models were applied and designed as a framework to classify the graph data of brain connectivity matrix. Furthermore, extension to the dynamic connectivity analysis for improving the accuracy, moving sliding window is applied in this experiment. To reduce the computational cost, the graph theory measures of complex brain network analysis is used to select the corresponding brain rhythm of ScZ identification as well. All the experiments were simulated in MATLAB 2021b software on a Dell computer with an NVIDIA 2080TI GPU.

In this paper, Section I introduced the background and brief lecture review of the study area. Section II described the EEG ScZ Dataset. The pre-processing, time-frequency brain connectivity algorithm, machine learning and deep learning classification models were summarized as well. Section III reported the results and compared the different machine learning and deep learning models of this study. In Section IV, the selection of frequency bands, statistical analysis of whole brain connectivity values and dynamic analysis were evaluated. The limitation and comparison between the proposed method with previous work were proposed in this section as well. Section V is a brief conclusion of this paper.

2. Method

There are four main steps in EEG ScZ identification, the details are described in Fig. 1. In pre-processing progress, the band-pass filter is applied to denoise the EEG raw data, and continuous wavelet transform (CWT) is stated to extract selected frequency bands data. To extend into dynamic functional connectivity, the sliding window size is selected as 30 s with 1 s overlap in this study. Then, using MI algorithm to convert the data into the functional connectivity matrix. Finally, feeding the graph matrix into the machine learning and deep learning models for the classification work.

2.1. Dataset

The publicly ScZ EEG dataset collected from Lomonosov Moscow State University (LMSU) is used to evaluate the performance through the proposed method in this study [29,30]. The dataset LMUS contains 84 subjects which includes 45 ScZ subjects and 39 HC subjects. Each subjects' data is 60-s resting eye-closed state from 16 channels (F7, F3, F4, F8, T3, C3, Cz, C4, T4, T5, P3, Pz, P4, T6, O1 and O2) with 128 Hz
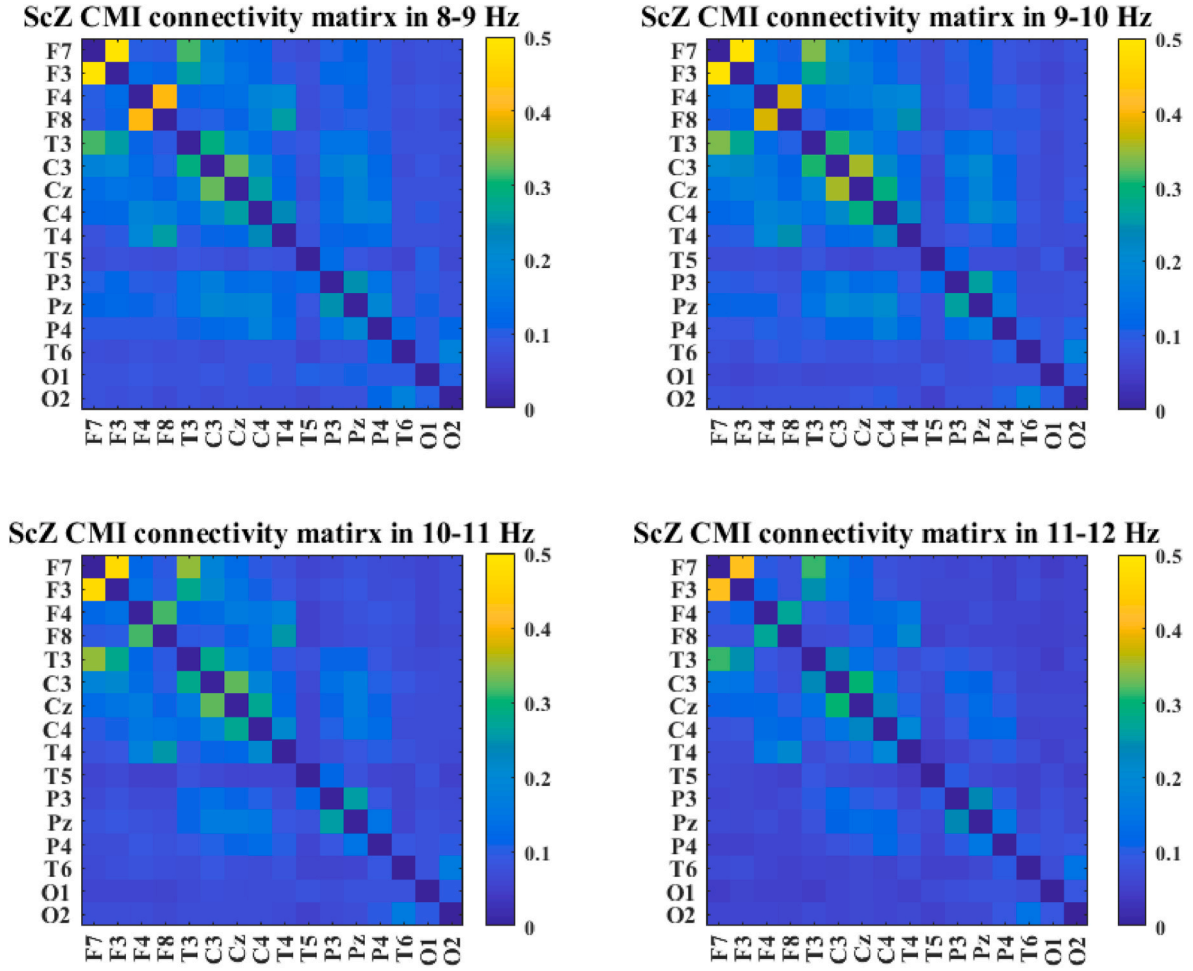
Fig. 2. CMI matrix of ScZ subject *'022w1'* in alpha band.

sample rate. All patients with ScZ were diagnosed at the Mental Health Research Center (MHRC) according to ScZ diagnostic criteria F20, F21, F25 of the ICD-10 classification of mental and behavioral disorders developed by the International Statistical Classification of Diseases and Related Health Problems. During the MHRC examination, the patient did not receive any chemotherapy.

2.2. Pre-processing

Sliding window technique is used in this study, to explore the dynamic changes of the functional connectivity. The sliding size was selected as 30 s within 1 s overlap. Band pass filter between 1 and 50 Hz denoised the EEG raw data through a six order Butterworth zero-phase filter algorithm.

CWT is proposed in the signal processing progress in this experiment, which converted the raw data into the time-frequency domain power spectrum in α band (8–12 Hz). The algorithm of CWT is shown in equation (1):

$$W_{x_i}(t,f) = \int x_i(\lambda) \times \overline{\varphi_{t,f}(t-\lambda)} d\lambda \qquad (1)$$

where 'W_{x_i}' is the power density, the 'f' is the selected frequency bands, 't' is the time instant, and 'i' means the number of the channel.

The mother wavelet calculated by the Morlet wavelet formula is described as follow in equation (2).

$$\varphi_{t,f}(\lambda) = A \times e^{i2\pi f(\lambda-t) \times e^{\frac{-(\lambda-t)^2}{2\sigma^2}}} \qquad (2)$$

where 'σ' is the time spread which equals to $\frac{8}{2\pi f}$.

The output of the pro-cessing progress is changed into 4×3840 size of each channel data.

2.3. Cross mutual information algorithm

Based on the CWT power spectrum density, MI is used to construct the CMI functional connectivity on the time-frequency data which measures the interdependence communication between two EEG channels. The MI formula is shown in equation (3).

$$MI(F_i, F_j) = H(F_i) + H(F_j) - H(F_i, F_j) \qquad (3)$$

where 'i' is the number of the channel, the $H(F_i)$ is the entropy and the details described in equation (4).

$$H(F_i) = -\sum_{b=1}^{40} p(F_{i,b}) \log_2 p(F_{i,b}) \qquad (4)$$

where F_i is the mean value of the band power. The $p(F_{i,b})$ is the probability power density.

The $H(F_i, F_j)$ is the joint entropy which describes the signal distribution, given by:

$$H(F_i, F_j) = -\sum_{b=1}^{40} p(F_{i,b}, F_{j,b}) \log_2 p(F_{i,b}, F_{j,b}) \qquad (5)$$

Similarly, $p(F_{i,b}, F_{j,b})$ is the probability power density of the mean value of the band power between the channel 'i' and 'j'. To avoid the over detrended phenomenon of $p(F_{i,b}, F_{j,b})$, the value of the bin is selected as

Table 1
The details of five group dataset.

	ScZ dataset	HC dataset
Group 1	022w1, 32w1, 33w1, 088w1, 103w, 113w1, 155w1, 156w1, 192w	S10W1, s12w1, S18W1, s20w1, S26W1, s27w1, S31W, S42W1
Group 2	219w1, 221w, 249w1, 276w1, 307w1, 312w1, 314w1, 342mw1, 382w1	s43w1, S47W1, S50W, s53w1, S55W1, S59W1, S60W, S72W1
Group 3	387-02w1, 387-03w1, 401w1, 423w, 429w1, 454-1W, 485w1, 508w1, 509w1	S78W, S85W1, s94w1, s152w1, S153W1, S154W1, S155W1, s157w1
Group 4	510-1W, 515w1, 517w1, 540w1, 548w, 573w1, 575w1, 585w1, 586w1	s158w1, S163W1, S164W1, S165W1, S167W1, S169W, s170w1, s173w1
Group 5	642w1, 683w1, 719w1, r229w1, r416w1, s083w1, S084–1W, s351w, s425w1	S174W1, s176w1, S177W1, s178w1, S179W1, S182W1, S196W1

40 in this study. In addition, the CMI formula is obtained in equation (6)

$$MI\left(F_i, F_j\right) = \sum_{b=1}^{40} p\left(F_{i,b}, F_{j,b}\right) \log_2 \frac{p\left(F_{i,b}, F_{j,b}\right)}{p\left(F_{i,b}\right)p\left(F_{j,b}\right)} \tag{6}$$

To obtain more information from the CMI connectivity matrix, functional connectivity matrix of each Hz frequency (8–9 Hz, 9–10 Hz, 10–11 Hz, 11–12 Hz) is computed. Thus, the data of alpha band (8–12 Hz) are all converted into $16 \times 16 \times 4$ matrix through CMI algorithm. As an example, the 4-level CMI matrix of a ScZ subject *'022w1'* of alpha band is shown in Fig. 2.

2.4. Classification via machine learning and deep learning methods

84 subjects' data (45 ScZ subjects and 39 HC subjects) from LMSU ScZ EEG dataset was applied to evaluate the proposed method in this research. The dataset was divided into 5 groups, each group has 9 ScZ subjects and 8 HC subjects, last group have 7 HC subjects and the details are listed in Table 1. To make sure the proposed method can overcome the robustness problem, 4 groups' data is used to training the model and another group data is used as the test data which have no overlapping of subject affiliations in the training and testing sets. In addition, the 20% random hold-out validation method is used in the training progress.

2.4.1. Three machine learning methods

Three basic machine learning methods were applied to test the ScZ EEG signal identification work which include the SVM, k-NN and decision tree (DT) methods. Because of the value of functional connectivity is symmetrical, just half data needs to feed into the machine learning models. For example, the value of F3–F4 and value of F4–F3 is same. Moreover, the CMI value of same node do not need to consider which all equals to 0. Thus, just 480 eigenvalues of 4-layer CMI connectivity matrix is used as the input.

2.4.2. Self-designed 3D-CNN model

In complex brain network analysis, researchers regarded the brain connectivity which includes structural connectivity, functional connectivity and effective connectivity (directed functional connectivity) as a graph. In this study, brain connectivity is considered as a whole graph. As the CNN has achieved good performance in photograph classification
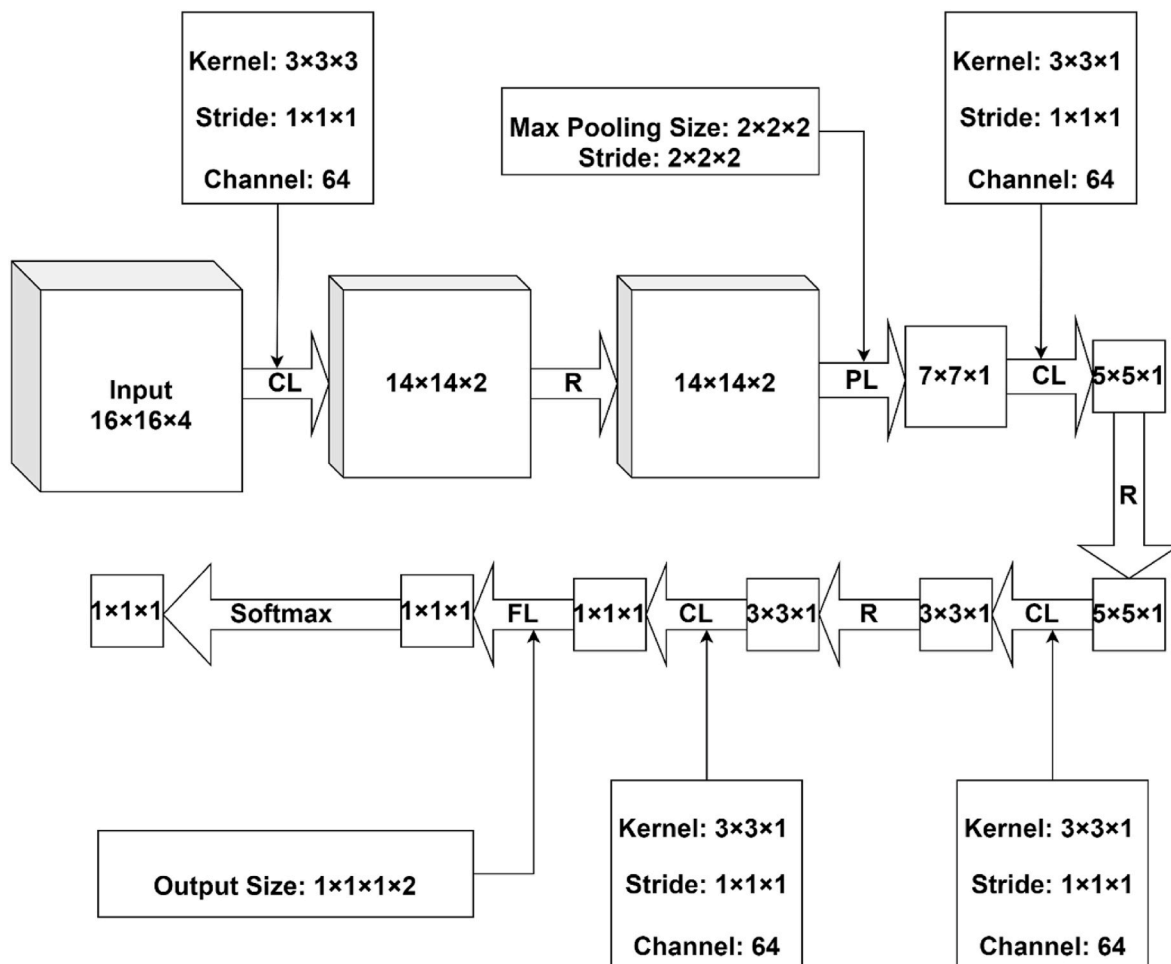
Fig. 3. Architecture of 11-layer 3D-CNN, *'CL'* is convolution layer, *'R'* is ReLU, *'PL'* is max pooling layer and *'FL'* is fully connected layer.

Table 2
The details of 3D-CNN architecture.

Layer	Input Size	Output Size	hyperparameters
3D imaged-data input	$16 \times 16 \times 4 \times 1$		
Convolution layer	$16 \times 16 \times 4 \times 1$	$14 \times 14 \times 2 \times 64$	Kernel size: $3 \times 3 \times 3$ Stride: $1 \times 1 \times 1$ Channel: 64
ReLU	$14 \times 14 \times 2 \times 64$	$14 \times 14 \times 2 \times 64$	
Max Pooling layer	$14 \times 14 \times 2 \times 64$	$7 \times 7 \times 1 \times 64$	Pooling Size: $2 \times 2 \times 2$ Stride: $2 \times 2 \times 2$
Convolution layer	$7 \times 7 \times 1 \times 64$	$5 \times 5 \times 1 \times 64$	Kernel size: $3 \times 3 \times 1$ Stride: $1 \times 1 \times 1$ Channel: 64
ReLU	$5 \times 5 \times 1 \times 64$	$5 \times 5 \times 1 \times 64$	
Convolution layer	$5 \times 5 \times 1 \times 64$	$3 \times 3 \times 1 \times 64$	Kernel size: $3 \times 3 \times 1$ Stride: $1 \times 1 \times 1$ Channel: 64
ReLU	$3 \times 3 \times 1 \times 64$	$3 \times 3 \times 1 \times 64$	
Convolution layer	$3 \times 3 \times 1 \times 64$	$1 \times 1 \times 1 \times 64$	Kernel size: $3 \times 3 \times 1$ Stride: $1 \times 1 \times 1$ Channel: 64
Fully Connected layer	$1 \times 1 \times 1 \times 64$	$1 \times 1 \times 1 \times 2$	
Softmax	$1 \times 1 \times 1 \times 2$		

work, we used 3D-CNN model to classifier the ScZ brain connectivity graph and a 10-layer 3D-CNN shown in Fig. 3 was constructed. In addition, Table 2 shows the details of the architecture.

There are four convolution layers, three ReLU layers, one max pooling layer and one fully connected layer designed in the 3D-CNN architecture. To reduce the over-fitting phenomenon, batch normalization work is added in each convolution layers. The hyperparameters of the convolution layers are selected as 64 filters, and the kernels size selected as $3 \times 3 \times 3$, $3 \times 3 \times 1$, $3 \times 3 \times 1$, and $3 \times 3 \times 1$, respectively. To improve the training speed, the max pooling layers is designed to reduce the cost of training calculation in this architectural. The hyperparameters of this max pooling layer is selected as $2 \times 2 \times 2$ size and $2 \times$

2×2 stride. ReLU is calculated follow the $f(x) = max(0,x)$ formula. The fully connected layer which selected as the two classes classification work. Finally, a Softmax classifier for the identification using the concatenated outputs of the last layers. The training progress based on the MATLAB 2021b for testing Group 1 is shown in Fig. 4.

The 20% random hold-out validation method with 50 iterations validation frequency is used in whole comparison models include three machine learning methods and the self-designed 3D-CNN model in this study. The validation accuracy is summarized in Table 3 for the training models.

3. Results

Three parameters were calculated to evaluate the proposed method in LMSU ScZ EEG dataset include the accuracy, sensitivity, and specificity are defined as below. Accuracy is a direct parameter in method evaluation, and is defined in equation (7):

$$Acc = \frac{TP + TN}{TP + TN + FP + FN} \tag{7}$$

where '*TP*', '*TN*', '*FP*', '*FN*' correspond to the true positive, true negative, false positive and false negative.

Sensitivity is the parameter to measure the ability to recognize the patient cases correctly.

Table 3
The Validation accuracy for three machine learning methods and 3D-CNN model.

	Test group	SVM	KNN	DT	3D-CNN
Validation accuracy (%)	Group 1	100.00	100.00	96.91	98.82
	Group 2	99.76	100.00	99.29	100.00
	Group 3	100.00	100.00	99.06	100.00
	Group 4	98.27	100.00	97.39	99.76
	Group 5	99.52	100.00	98.34	100.00
	Mean ± Std	99.51 ± 0.72	100.00 ± 0.00	98.20 ± 1.03	99.72 ± 0.51
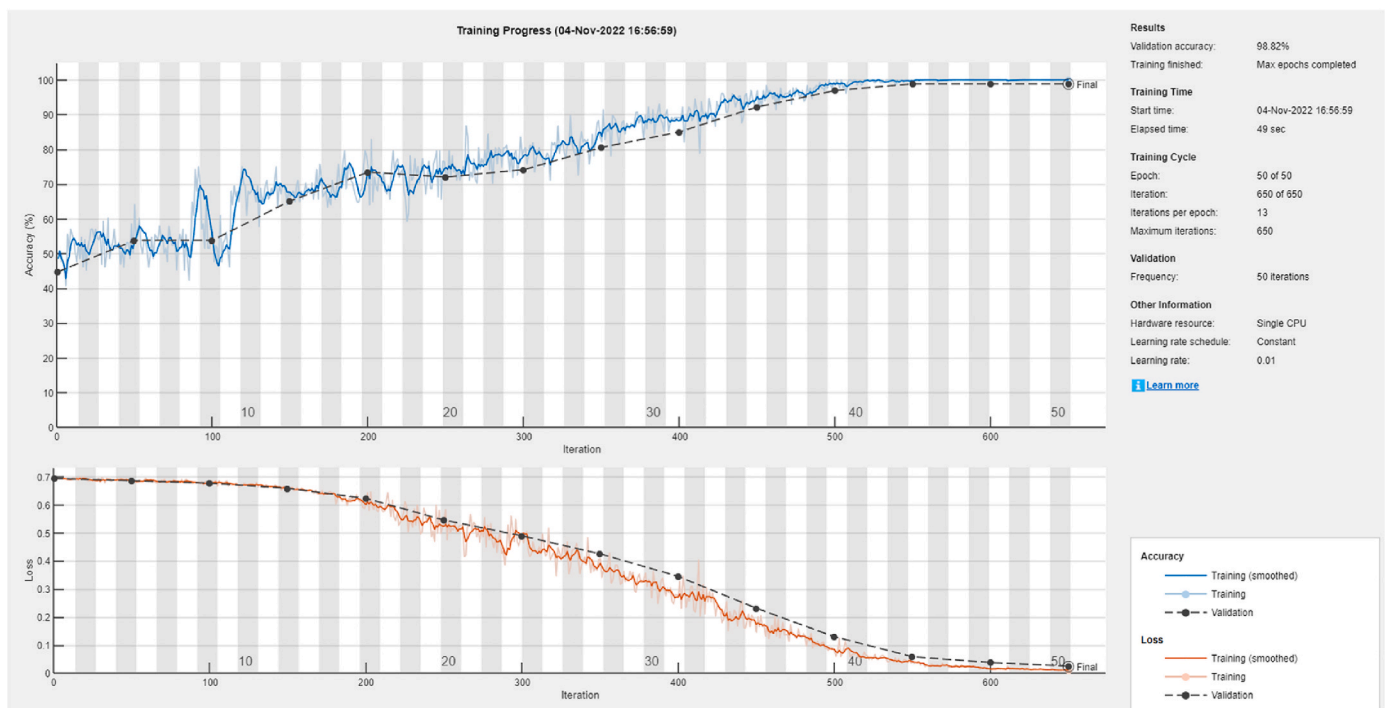
Fig. 4. The training progress for self-designed 3D-CNN model for testing Group 1.

Table 4
The test results for three machine learning methods and 3D-CNN model.

Results	Test group	SVM	k-NN	DT	3D-CNN
Accuracy (%)	Group 1	85.69	57.66	68.55	97.98
	Group 2	82.86	67.94	63.91	97.38
	Group 3	85.28	53.54	72.98	97.18
	Group 4	90.12	70.16	82.26	99.60
	Group 5	87.50	67.34	83.06	96.57
	Mean ± Std	86.29 ± 2.71	63.33 ± 7.28	74.15 ± 8.41	**97.74 ± 1.15**
Sensitivity (%)	Group 1	88.94	55.30	55.76	95.59
	Group 2	100.00	51.15	71.43	100.00
	Group 3	82.95	36.41	41.47	96.77
	Group 4	100.00	77.88	88.94	99.09
	Group 5	99.54	71.43	73.73	93.10
	Mean ± Std	94.29 ± 7.91	58.43 ± 16.55	66.27 ± 18.18	**96.91 ± 2.76**
Specificity (%)	Group 1	83.15	59.50	78.49	100.00
	Group 2	69.53	81.00	58.06	95.55
	Group 3	87.10	67.03	97.49	97.49
	Group 4	82.44	64.16	77.06	100.00
	Group 5	78.14	64.16	90.32	99.62
	Mean ± Std	80.07 ± 6.70	67.17 ± 8.19	80.28 ± 15.04	**98.53 ± 1.97**

$$Sen = \frac{TP}{TP + FN} \tag{8}$$

Specificity refers to the probability of a negative test, conditioned on truly being negative.

$$Spe = \frac{TN}{TN + FP} \tag{9}$$

3.1. Results for machine learning methods and 3D-CNN

SVM, k-NN, DT and 3D-CNN method are applied to detect EEG ScZ signal in this study. Comparing the results of each model, self-designed 3D-CNN model achieved the best performance which received results of 97.74 ± 1.15% accuracy, 96.91 ± 2.76% sensitivity and 98.53 ± 1.97% specificity of test data. The details are summarized in Table 4.

According to Table 4, it is obvious that the self-designed deep learning model can provide a better performance in ScZ signal identification than the SVM, k-NN and DT methods. Although these three machine learning methods can also achieve high rate in validation accuracy, they failed to provide a better classification result in the testing data. Comparing with these three machine learning methods, our self-designed 3D-CNN can overcome the robustness problem which shows the excellent identification result in the testing data of each subject. The standard deviation of our self-designed method is significant smaller than three machine learnings, it indicates that the proposed method can detect each subject in LMSU publicly ScZ dataset.

Table 6
The mean value of CMI values.

CMI location (Channel to Channel)	CMI values in ScZ subjects	CMI values in HC subjects
T4 - T6	0.117 ± 0.054	0.190 ± 0.090
T3 - T5	0.130 ± 0.097	0.191 ± 0.099
Cz - C4	0.193 ± 0.063	0.240 ± 0.082
Cz - Pz	0.132 ± 0.035	0.171 ± 0.100
Pz - P4	0.169 ± 0.048	0.203 ± 0.070
F3 – F4	0.149 ± 0.052	0.182 ± 0.055

4. Discussion

4.1. Brain rhythms selection through complex brain network analysis

To reduce the computational cost, selecting corresponding frequency bands is necessary. The brain network is constructed via multi-channel EEG data. Complex brain network analysis has its origins in the mathematical study of networks and is known as the graph theory [31]. The complex brain network analysis describes large-scale organization of brain networks into neurobiologically meaningful and easily computable measures [32]. Four graph theory parameters are chosen to select the brain rhythms which provide significant differences between ScZ subjects and HC subjects which include modularity, efficiency, diffusion efficiency and clustering coefficient. The statistical analysis results of the graph theory parameters in different frequency bands are listed in Table 5.

According to the statistical analysis results in four graph theory parameters, we found the alpha band (8–12 Hz) data have the most difference between the ScZ subjects and HC subjects. Thus, the alpha band is selected to analysis ScZ identification work in this study.

4.2. Statistical analysis in CMI connectivity matrix

DMN is regarded as the highly active network as compared to others which makes DMN as the key contributor in maintaining brain's functional organization which related to the sensory, motor executive control, visual components, frontal, parietal, auditory, temporal and parietal [33]. In ScZ diseases analysis, DMN brain connectivity of fMRI data is used widely [16,17]. The DMN is identifiable in three regions which includes PCC, LPC and MPC [15]. In this experiment, the Brodmann areas (BA) is used to correspond to the DMN region [34]. Channel Pz is the precuneus location in BA07, channel Cz, F3 and F4 are the MPC part in BA08/09, BA08/09 left hemisphere and BA08/09 right hemisphere respectively [35]. The LPC region corresponds to the channel P3 and P4 which in the BA39/40 left hemisphere and BA39/40 right hemisphere area [35]. In this study, the top 6 functional connectivity with the major difference of CMI values (≥0.03) between ScZ subjects and HC subjects was shown in Table 6:

Based on statistical significance of CMI connectivity of whole brain, we found not only the DMN region but also the T4-T6 and T3-T5 connectivity have obviously difference between ScZ and HC subjects which corresponding to the area between temporal lobe and posterior temporal

Table 5
Statistical analysis of graph theory measures in different brain rhythms.

	Measures	Brain rhythms				
		δ band (1–4 Hz)	θ band (4–8 Hz)	α band (8–12 Hz)	β band (12–30 Hz)	γ band (30–60 Hz)
ScZ subjects	Modularity	5.084 ± 1.073	4.956 ± 1.015	4.632 ± 1.082	5.386 ± 1.117	6.052 ± 1.392
	Efficiency	0.205 ± 0.025	0.132 ± 0.020	0.112 ± 0.021	0.074 ± 0.017	0.064 ± 0.019
	Diffusion Efficiency	0.050 ± 0.002	0.044 ± 0.002	0.041 ± 0.003	0.033 ± 0.004	0.031 ± 0.005
	Clustering Coefficient	0.245 ± 0.027	0.162 ± 0.021	0.137 ± 0.023	0.093 ± 0.020	0.083 ± 0.022
HC subjects	Modularity	5.101 ± 0.893	4.825 ± 0.955	4.392 ± 0.766	5.428 ± 1.036	5.871 ± 1.015
	Efficiency	0.205 ± 0.020	0.131 ± 0.018	0.116 ± 0.022	0.076 ± 0.017	0.065 ± 0.017
	Diffusion Efficiency	0.050 ± 0.001	0.044 ± 0.002	0.043 ± 0.003	0.034 ± 0.004	0.031 ± 0.004
	Clustering Coefficient	0.246 ± 0.021	0.161 ± 0.020	0.139 ± 0.025	0.094 ± 0.019	0.083 ± 0.019

Table 7
The comparison between five sliding window size.

Sliding window size	Accuracy (%)	Sensitivity (%)	Specificity (%)
2-s	80.13 ± 1.80	73.52 ± 4.99	88.14 ± 3.98
5-s	86.21 ± 3.17	79.38 ± 4.98	93.89 ± 3.44
10-s	90.27 ± 2.89	87.28 ± 6.46	93.63 ± 4.52
30-s	97.74 ± 1.15	96.91 ± 2.76	98.53 ± 1.97

Table 8
Comparison of the proposed method and previous works in EEG ScZ identification.

References	Dataset	Technique	Accuracy (%)	Sensitivity (%)	Specificity
Aslan and Akin (2020) [37]	45 ScZ subjects and 39 HC subjects	STFT + VGG-16 CNN	95	95.37	94.68
Phang et al. (2020) [18]	45 ScZ subjects and 39 HC subjects	Partial directed coherence + multi-domain connectome CNN	91.69 ± 4.67	91.11 ± 8.31	89.64 ± 9.48
Shoeibi et al. (2021) [19]	14 ScZ subjects and 14 HC subjects	1D-CNN, LSTMs	99.25	–	–
Siuly et al. (2022) [20]	49 ScZ subjects and 32 HC subjects	Google-net features + SVM	98.84	99.02	98.58
Sairamya et al. (2022) [22]	45 ScZ subjects and 39 HC subjects	DWT + relaxed local neighbor difference pattern	100	–	–
de Miras et al. (2023) [23]	11 ScZ subjects and 31 HC subjects	PCA + k-NN	87	82	90
Siuly et al. (2023) [21]	49 ScZ subjects and 32 HC subjects	Deep ResNet + SVM	99.23	99.36	99.02
Proposed method	45 ScZ subjects and 39 HC subjects	CMI + 3D-CNN	97.74 ± 1.15	96.91 ± 2.76	98.53 ± 1.97

lobe in both right and left side. It is the evidence that using the whole brain connectivity analysis is essential.

4.3. Dynamic analysis with the sliding window size selection

Y. Sun et al. reported the ScZ-related aberrations in the dynamic properties of resting-state function connectivity in fMRI [36]. Considering the same issue, we use sliding window technique to extend the functional connectivity into time-varying functional connectivity. However, if the sliding window is too big, it is hard to cluster the dynamic changes in detection, and if the sliding window is too small, it will decrease the classifier accuracy. We compared the 2-s, 5-s, 10-s and 30-s sliding window sizes, and the results shows the 30-s sliding window size can achieve better performance in this study and the details summarized in Table 7.

4.4. Performance comparison with previous work and future work

Table 8 summarizes the performance of the proposed method and other peer works in EEG ScZ signal identification. The proposed method achieved a result of 97.74 ± 1.15% in accuracy, 96.91 ± 2.76% sensitivity and 98.53 ± 1.97% specificity through function connectivity analysis and 3D-CNN deep learning model. Comparing with the previous works, our proposed method can supply an excellent performance in LMSU publicly ScZ dataset (45 ScZ subjects and 39 HC subjects). Furthermore, our proposed method is capable of fuzzy localization of the ScZ disease locations as well. Through the statistical analysis in CMI connectivity matrix of whole brain network, we found the temporal lobe and posterior temporal lobe in both right and left side and the DMN region have significant differences in brain network analysis.

Comparing with SVM, k-NN and DT models, our self-designed 3D-CNN can overcome the robustness problem in classifying the CMI connectivity matrix between ScZ and HC subjects. In addition, the sliding window technique applied can capture the dynamics of ScZ signal and improve the performance of the results. However, the dynamic model depends on the sliding window technique to cluster the dynamic state more clearly. Furthermore, the source model reconstruction technique can be applied to achieve more precise localization of ScZ disease.

5. Conclusion

In this paper, the whole brain connectivity analysis is applied and implemented using mutual information algorithm. The time-frequency domain functional connectivity calculated by CWT and CMI is firstly used in ScZ identification and the frequency resolution is selected in 1 Hz in this experiment. Sliding window technique is proposed to extend the functional connectivity to time-varying functional connectivity for exploring dynamic properties of resting-state function connectivity in EEG. To reduce the computational cost, graph theory measures of complex brain network analysis is used to select brain rhythms and find alpha band (8–12 Hz) is the significance frequency band for ScZ identification work. The 3D-CNN models are applied to classify the ScZ subjects and health control subjects and achieved a result of 97.74 ± 1.15% in accuracy, 96.91 ± 2.76% sensitivity and 98.53 ± 1.97% specificity. Comparing with the machine learning methods, regarding the brain connectivity matrix as a whole graph with 3D-CNN can overcome the robustness problem. Furthermore, we analysed the CMI values in the whole connectivity and found not only the DMN region but also the connectivity between temporal lobe and posterior temporal lobe in both right and left side has significant difference between the ScZ and HC subjects.

Declaration of competing interest

The authors declare that they have no known competing financial interests or personal relationships that could have appeared to influence the work reported in this paper.

References

[1] M.E. Shenton, et al., A review of MRI findings in schizophrenia, Schizophrenia Res. 49 (1–2) (2001) 1–52.
[2] P. Krukow, et al., Abnormalities in hubs location and nodes centrality predict cognitive slowing and increased performance variability in first-episode schizophrenia patients, Sci. Rep. 9 (1) (2019) 1–13.
[3] S.L. Rossell, R.A. Batty, Elucidating semantic disorganisation from a word comprehension task: do patients with schizophrenia and bipolar disorder show differential processing of nouns, verbs and adjectives? Schizophrenia Res. 102 (1–3) (2008) 63–68.
[4] C. Simonsen, et al., Neurocognitive dysfunction in bipolar and schizophrenia spectrum disorders depends on history of psychosis rather than diagnostic group, Schizophr. Bull. 37 (1) (2011) 73–83.
[5] J. Gomez-Pilar, et al., Altered predictive capability of the brain network EEG model in schizophrenia during cognition, Schizophrenia Res. 201 (2018) 120–129.
[6] Pacific, W. and S.A.W. Hasan, Magnitude and Impact.

[7] A. Craik, Y. He, J.L. Contreras-Vidal, Deep learning for electroencephalogram (EEG) classification tasks: a review, J. Neural. Eng. 16 (3) (2019), 031001.

[8] G.G. Brown, W.K. Thompson, Functional Brain Imaging in Schizophrenia: Selected Results and Methods, Behavioral neurobiology of schizophrenia and its treatment, 2010, pp. 181–214.

[9] M.-h.R. Ho, et al., Time–frequency discriminant analysis of MEG signals, Neuroimage 40 (1) (2008) 174–186.

[10] P. Van Mierlo, et al., Network perspectives on epilepsy using EEG/MEG source connectivity, Front. Neurol. 10 (2019) 721.

[11] H. Yu, et al., Functional brain connectivity in Alzheimer's disease: an EEG study based on permutation disalignment index, Phys. Stat. Mech. Appl. 506 (2018) 1093–1103.

[12] D.M. Khan, et al., Effective connectivity in default mode network for alcoholism diagnosis, IEEE Trans. Neural Syst. Rehabil. Eng. 29 (2021) 796–808.

[13] H. Chen, Y. Song, X. Li, A deep learning framework for identifying children with ADHD using an EEG-based brain network, Neurocomputing 356 (2019) 83–96.

[14] M. Shen, et al., Detection of alcoholic EEG signals based on whole brain connectivity and convolution neural networks, Biomed. Signal Process Control 79 (2023), 104242.

[15] M.E. Raichle, et al., A default mode of brain function, Proc. Natl. Acad. Sci. USA 98 (2) (2001) 676–682.

[16] S. Zhang, et al., Abnormal default-mode network homogeneity and its correlations with neurocognitive deficits in drug-naive first-episode adolescent-onset schizophrenia, Schizophrenia Res. 215 (2020) 140–147.

[17] J. Fan, et al., Resting-state default mode network related functional connectivity is associated with sustained attention deficits in schizophrenia and obsessive-compulsive disorder, Front. Behav. Neurosci. 12 (2018) 319.

[18] C.-R. Phang, et al., A multi-domain connectome convolutional neural network for identifying schizophrenia from EEG connectivity patterns, IEEE J. Biomed. Health Inf. 24 (5) (2019) 1333–1343.

[19] A. Shoeibi, et al., Automatic diagnosis of schizophrenia in EEG signals using CNN-LSTM models, Front. Neuroinf. (2021) 58.

[20] S. Siuly, et al., SchizoGoogLeNet: the googlenet-based deep feature extraction design for automatic detection of schizophrenia, Comput. Intell. Neurosci. 2022 (2022) 1–13.

[21] S. Siuly, et al., Exploring deep residual network based features for automatic schizophrenia detection from EEG, Phys. Eng. Sci. Med. (2023) 1–14.

[22] N. Sairamya, M. Subathra, S.T. George, Automatic identification of schizophrenia using EEG signals based on discrete wavelet transform and RLNDiP technique with ANN, Expert Syst. Appl. 192 (2022), 116230.

[23] J.R. de Miras, et al., Schizophrenia classification using machine learning on resting state EEG signal, Biomed. Signal Process Control 79 (2023), 104233.

[24] J.-Y. Kim, H.S. Lee, S.-H. Lee, EEG source network for the diagnosis of schizophrenia and the identification of subtypes based on symptom severity—a machine learning approach, J. Clin. Med. 9 (12) (2020) 3934.

[25] O.Y. Panischev, et al., Use of cross-correlation analysis of EEG signals for detecting risk level for development of schizophrenia, Biomed. Eng. 47 (3) (2013) 153–156.

[26] Z. Zhao, et al., Classification of schizophrenia by combination of brain effective and functional connectivity, Front. Neurosci. 15 (2021), 651439.

[27] T. Naira, C. Alberto, Classification of People Who Suffer Schizophrenia and Healthy People by EEG Signals Using Deep Learning, 2020.

[28] Q. Chang, et al., Classification of first-episode schizophrenia, chronic schizophrenia and healthy control based on brain network of mismatch negativity by graph neural network, IEEE Trans. Neural Syst. Rehabil. Eng. 29 (2021) 1784–1794.

[29] N. Gorbachevskaya, S. Borisov, EEG Data of Healthy Adolescents and Adolescents with Symptoms of Schizophrenia, 2002.

[30] S. Borisov, et al., Analysis of EEG structural synchrony in adolescents with schizophrenic disorders, Hum. Physiol. 31 (3) (2005) 255–261.

[31] M. Rubinov, O. Sporns, Complex network measures of brain connectivity: uses and interpretations, Neuroimage 52 (3) (2010) 1059–1069.

[32] M. Kaushal, et al., Large-scale network analysis of whole-brain resting-state functional connectivity in spinal cord injury: a comparative study, Brain Connect. 7 (7) (2017) 413–423.

[33] B.A. Seitzman, et al., The state of resting state networks, Top. Magn. Reson. Imag.: TMRI 28 (4) (2019) 189.

[34] D.A. Kaiser, Cortical cartography, Biofeedback 38 (1) (2010) 9–12.

[35] L. Koessler, et al., Automated cortical projection of EEG sensors: anatomical correlation via the international 10–10 system, Neuroimage 46 (1) (2009) 64–72.

[36] Y. Sun, et al., Dynamic reorganization of functional connectivity reveals abnormal temporal efficiency in schizophrenia, Schizophr. Bull. 45 (3) (2019) 659–669.

[37] Z. Aslan, M. Akın, Automatic Detection of Schizophrenia by Applying Deep Learning over Spectrogram Images of EEG Signals, 2020.

CHAPTER 8: PAPER 6 – 3D convolutional neural network for schizophrenia detection using as EEG-based functional brain network

8.1 Overview of Paper 6

The details of the Paper 6 are given below:

- Paper title: "3D convolutional neural network for schizophrenia detection using as EEG-based functional brain network."
- Paper length: 16 pages
- Journal: Biomedical signal processing and control
    - Rank: Q1 (Biomedical Engineering)
    - Impact factor: 5.1 (2022-2023)
    - Cite Score: 8.2 (2022)
    - SJR: 1.071 (2022)
    - SNIP: 1.552 (2022)
- First author: Mingkan Shen
- Corresponding author: Mingkan Shen

HDR thesis author's declaration

☒ The authors declare that they have no known competing financial   interests or personal relationships that could have appeared to influence the work reported in this paper.

☐ The authors declare the following financial interests/personal relationships which may be considered as potential competing interests:

Figure 8.1: Authorship contributions of Paper 6

Conception and design of study	Mingkan Shen, Peng Wen, Bo Song, Yan Li
Analysis and interpretation of data	Mingkan Shen
Drafting the manuscript	Mingkan Shen
Revising the manuscript critically for important intellectual content	Mingkan Shen, Peng Wen, Bo Song, Yan Li

8.2   Summary of Paper 6

This paper delves into the potential of employing a functional brain network analysis for detecting ScZ using EEG signals. While traditional research primarily relies on f-MRI data for ScZ detection, this study offers a fresh approach that capitalizes on the high-frequency accuracy, non-invasiveness, and cost-effectiveness of EEG.

To differentiate between ScZ patients and healthy controls, the study implements a MVAR and magnitude squared coherence algorithm. These techniques focus on the dynamic nature of resting-state brain connectivity, particularly in the alpha band frequency range (8-12 Hz), which has been identified as crucial for ScZ detection. The proposed 3D-CNN model classifies these functional brain network features, demonstrating impressive accuracy, sensitivity, and specificity results, outperforming traditional models like SVM, k-NN, and DT.

Furthermore, the research pinpoints abnormal brain connectivity regions in ScZ patients, notably in the DMN region, and the temporal and posterior temporal lobes in both brain hemispheres. These findings offer valuable insights and potential biomarkers for understanding and identifying the neural abnormalities associated with ScZ.

In essence, this paper provides a comprehensive methodology for ScZ detection using EEG signals, paving the way for more accurate and efficient diagnostic tools in the future.

8.3   Paper file

Manuscript Number:	BSPC-D-23-02303
Article Type:	Research Paper
Keywords:	ScZ; EEG; multivariate autoregressive model; coherence; 3D-CNN; brain network analysis
Corresponding Author:	Mingkan Shen University of Southern Queensland AUSTRALIA
First Author:	Mingkan Shen
Order of Authors:	Mingkan Shen
	Peng Wen
	Bo Song
	Yan Li
Abstract:	Schizophrenia (ScZ) is a chronic mental disorder affecting the function of the brain, which causes emotional, social, and cognitive problems. This paper explored the functional brain network and deep learning methods to detect ScZ using electroencephalogram (EEG) signals. Functional brain network analysis was proposed and implemented using a multivariate autoregressive model and coherence connectivity algorithm. The three machine learning techniques and 3D-convolutional neural network (CNN) models were applied to classify the ScZ patients and health control subjects, and then the public LMSU database was utilized to assess the performance. The proposed 3D-CNN method achieved the performance of a 98.47 ± 1.47% in accuracy, 99.26 ± 1.07% in sensitivity, and 97.23 ± 3.76% in specificity. Moreover, in addition to the default mode network region, the temporal and posterior temporal lobes of both right and left hemispheres were found as the significant difference areas in ScZ brain network analysis.
Suggested Reviewers:	Chee-Ming Ting cmting@utm.my
	Jicong Zhang jicongzhang@buaa.edu.cn
	Siuly Siuly siuly_1976@yahoo.com

3D convolutional neural network for schizophrenia detection using as EEG-based functional brain network

Mingkan Shen[1], Peng Wen[1], Bo Song[1] and Yan Li[2]

[1] *School of Engineering, University of Southern Queensland, Toowoomba, Australia*

[2] *School of Mathematics, Physics and Computing, University of Southern Queensland, Toowoomba, Australia*

Corresponding Author: Mingkan Shen, Mingkan.Shen@usq.edu.au

1   **Abstract**

2   Schizophrenia (ScZ) is a chronic mental disorder affecting the function of the brain, which
3   causes emotional, social, and cognitive problems. This paper explored the functional brain
4   network and deep learning methods to detect ScZ using electroencephalogram (EEG) signals.
5   Functional brain network analysis was proposed and implemented using a multivariate
6   autoregressive model and coherence connectivity algorithm. The three machine learning
7   techniques and 3D-convolutional neural network (CNN) models were applied to classify the
8   ScZ patients and health control subjects, and then the public LMSU database was utilized to
9   assess the performance. The proposed 3D-CNN method achieved the performance of a 98.47
10   $\pm$ 1.47% in accuracy, 99.26 $\pm$ 1.07% in sensitivity, and 97.23 $\pm$ 3.76% in specificity. Moreover,
11   in addition to the default mode network region, the temporal and posterior temporal lobes of
12   both right and left hemispheres were found as the significant difference areas in ScZ brain
13   network analysis.

14   Key words: ScZ, EEG, multivariate autoregressive model, coherence, 3D-CNN, brain network
15   analysis.

1. Introduction

17   Schizophrenia (ScZ) is a mental neuropsychiatric disorder of the brain, which affects emotional
18   behaviours, persistent delusions, and cognitive deficit symptoms [1-3]. Regarding to the report
19   of World Health Organization in 2022, approximately 24 million people suffered from ScZ
20   disease [4]. In clinical detection, electroencephalogram (EEG) is an auxiliary approach to
21   detect brain's electronic signal, which can provide high accuracy detection without any
22   physical intrusion [5]. Compared with the other two popular brain detection techniques, the
23   functional magnetic resonance imaging (f-MRI) and Magnetoencephalography (MEG), EEG
24   can provide two apparent advantages, including less reliance on the trained and lower cost
25   medical equipment [6,7].

26   Majority of researchers, in recent years, detected the ScZ diseases through functional brain
27   network analysis using f-MRI data because the f-MRI technique can directly solve the space
28   resolution problem [8-10]. Long, Q, et al. utilized independent vector analysis to extract
29   common subspace components from fMRI data in individuals with ScZ and health control (HC)

30   participants [8]. They found significant differences in functional brain networks between the
31   two groups. The results of their study contribute to our understanding of the neural mechanisms
32   underlying ScZ and provide insights into the potential biomarkers or targets for diagnosis and
33   treatment. Fu, Z et al. applied a brain activity-connectivity algorithm to fMRI data from
34   individuals diagnosed with ScZ [9]. This algorithm involved estimating brain activity
35   fluctuations and assessing connectivity patterns between different brain regions. By covarying
36   the brain activity with connectivity measures, the researchers investigated how changes in brain
37   activity related to fluctuations in network efficiency. Zhang, G et al. applied the Joint directed
38   acyclic graph estimation model to detect abnormal fMRI connectivity in ScZ [10]. Their
39   findings revealed decreased functional integration, disrupted hub structures, and characteristic
40   edges in ScZ subjects. These results contribute to the understanding of the neural underpinnings
41   of ScZ and provide insights into the specific connectivity abnormalities associated with the
42   disorder. Inspired by the deep understanding of ScZ diseases through functional brain network
43   analysis in f-MRI data, the functional brain network analysis is explored into EEG signal in
44   this study.

45   The default mode network (DMN) has been found to exhibit significant differences in resting-
46   state brain activity between individuals with ScZ and HC subjects [11]. The DMN is a network
47   of brain regions that are consistently active during rest and are involved in self-referential
48   thinking, introspection, and mind-wandering. The DMN consists of several key areas,
49   including the mesial prefrontal cortex (MPC), the lateral posterior cortex (LPC), and the
50   posterior cingulate cortex/precuneus (PCC) [11]. Zhang, S et al. applied the DMN region as a
51   node of f-MRI data to detect abnormal ScZ connectivity [12]. F-MRI DMN functional
52   connectivity analysis was also utilized via Fan. J et al to detect ScZ and obsessive-compulsive
53   disorder [13]. However, the study conducted by Phang et al. focused on the functional brain
54   network analysis of ScZ [14]. They employed whole brain connectivity analysis, which
55   involves investigating the connections and interactions among all brain regions, rather than
56   focusing solely on local brain networks. Based on the information provided, the study
57   highlights the importance of considering the entire brain's functional connectivity, including
58   regions within the DMN, to gain a more complete understanding of the abnormal brain activity
59   in ScZ.

60   In EEG analysis, traditional signal processing and machine learning, as well as deep learning
61   models, have been widely employed in classifying EEG ScZ signals. Baygin, M et al. proposed
62   collatz pattern technique and K-nearest neighbour (k-NN) classifier to detect EEG ScZ patients
63   and achieved 99.47% and 93.58% in accuracy using two public ScZ databases [15]. Akbari et
64   al. calculated ScZ features through phase space dynamic features and employed the k-NN
65   model for classification [16]. Their research reported an accuracy of 94.80%, sensitivity of
66   94.30%, and specificity of 95.20%. Lillo et al. utilized a convolutional neural network (CNN)
67   to identify ScZ diseases and achieved a success rate of 93% in accuracy [17]. They also
68   highlighted the ability of their study to achieve computer-assisted diagnosis in just 3 minutes.
69   Supakar et al. proposed a deep learning model that combines recurrent neural network (RNN)
70   and long short-term memory (LSTM) network to detect ScZ using the Lomonosov Moscow
71   State University (LMSU) dataset [18]. They achieved an accuracy of 98% in their experiment.
72   Sairamya et al. employed the discrete wavelet transform (DWT) and relaxed local neighbour
73   difference pattern (RLNDiP) technique to detect ScZ in the LMSU database [19]. Their
74   approach yielded a maximum accuracy of 100% in their experiment. Hassan et al. applied CNN

75 to extract ScZ signal features and classified the features using the logistic regression method
76 [20]. They obtained accuracies of 90% and 98% on subject-based and non-subject-based
77 testing, respectively. Gosala et al. utilized the wavelet scattering transform (WST) as a signal
78 processing method to detect ScZ EEG signals [21]. They reported accuracy rates of 97.98%,
79 sensitivity of 98.2%, specificity of 97.72%, and a Kappa score of 95.94% in SVM
80 classification.

81 The functional brain network is also applied to provide biomarkers of the ScZ diseases. Wang,
82 J et al. investigated the left frontal-parietal/temporal networks and found biomarkers of
83 auditory verbal hallucinations (AVH) in ScZ diseases through phase locking value (PLV)
84 connectivity algorithm. They also achieved a classification result of 80.95% accuracy in AVH
85 patients and non-AVH patients [22]. Prieto-Alcantara et al. explored neurophysiological
86 differences in different cognitive states between ScZ patients and HC subjects using the EEG
87 coherence connectivity method [23]. Their study provided evidence of these differences and
88 highlighted the potential of functional connectivity analysis in understanding ScZ. In our
89 previous work, dynamic functional connectivity analysis using the cross mutual information
90 (CMI) algorithm with a 3D CNN was applied to identify ScZ EEG signals [24]. The results
91 showed an accuracy of $97.74 \pm 1.15\%$, sensitivity of $96.91 \pm 2.76\%$, and specificity of $98.53 \pm$
92 1.97%. Furthermore, the fuzzy localization of ScZ diseases was investigated in this study as
93 well.

94 The multivariate auto-regressive model (MVAR) coherence functional brain network method
95 with 3D-CNN model is applied to detect the EEG ScZ signal in this Study. The MVAR
96 coherence method was utilized to estimate the connectivity between different brain regions
97 based on EEG data. This method allows for the extraction of frequency domain features,
98 enabling the identification of abnormal connectivity areas associated with ScZ. After that, the
99 3D-CNN model was designed to classify functional brain network features between ScZ
100 patients and HC subjects. This model leverages the extracted features from the MVAR
101 coherence brain network to differentiate between the two groups. The sliding window
102 technique was employed to capture the dynamic changes in ScZ by considering the time-
103 varying nature of the functional brain network. This technique allows for the analysis of EEG
104 signals in small overlapping windows, considering temporal variations and improving the
105 accuracy of the experiment. Moreover, the study analysed different brain rhythms to reduce
106 computational costs. It found that the alpha band (8-12 Hz) demonstrated the best performance
107 in testing data. This suggests that focusing on the alpha band frequency range yields meaningful
108 results in the context of ScZ analysis. Furthermore, the study performed statistical analysis on
109 the whole brain connectivity to verify abnormal connectivity areas. Specifically, abnormal
110 connectivity areas were identified in the DMN region, as well as the temporal lobe and posterior
111 temporal lobe of both hemispheres. All the experiments are simulated in MATLAB 2021b
112 software on a Dell workstation with an NVIDIA 3080TI GPU.

113 In this paper, Section 1 introduces the research background and the related works in recent
114 years. The objectives this study is also included in this section. Section 2 describes the proposed
115 methodology, which includes the data pre-processing, signal processing method, functional
116 brain network analysis and classification models. The dataset details are also report in this
117 section. The results and comparison of the experiment are listed in Section 3. In Section 4,
118 statistical analysis of whole brain connectivity, dynamic analysis and the comparison with
119 previous work are discussed while the conclusion is made in Section V.

2. Methodology

Five main procedures in ScZ detection based on the EEG signal are briefly summarized in Figure 1. There are two pre-processing steps, including denoised the EEG raw data and the sliding window size selection, to remove the artifacts and extend dynamic research. MVAR model is introduced to transform data from the time domain into the frequency domain, which can provide more spectrum information in different brain rhythms. To extract the brain graph features, the coherence algorithm is applied to construct the functional brain network. Machine learning models and 3D-CNN are used to classify the ScZ subjects and HC subjects using their brain graph features. Finally, three parameters are proposed to evaluate the designed method in this study.
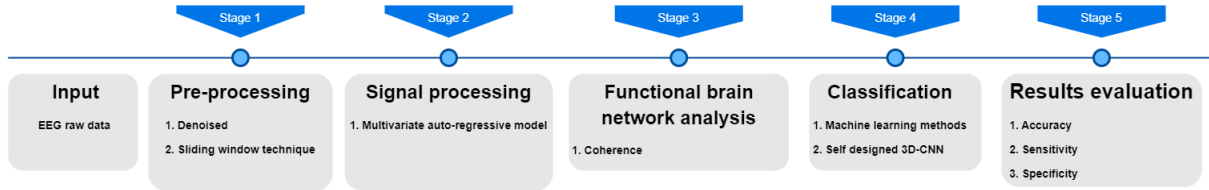
Figure. 1. The progress of ScZ automatic identification.

2.1 Datasets and pre-processing

In the evaluation of the proposed methodology for EEG ScZ detection, the researchers utilized a publicly available database called LMSU [25, 26]. This database consisted of EEG recordings from a total of 84 subjects, including 45 individuals diagnosed with ScZ and 39 HC subjects. The LMSU dataset provided EEG signals collected from 16 channels, namely F7, F3, F4, F8, T3, C3, Cz, C4, T4, T5, P3, Pz, P4, T6, O1, and O2. The sampling rate of the EEG signals in this dataset was 128 Hz.

By using a sliding window with a 30-second size and a 1-second overlap, the study considered short-term variations in the EEG signal, which can provide insights into the dynamic changes in brain activity associated with ScZ. The choice of these parameters indicates that the proposed methodology can potentially be applied in real-time applications, as it allows for continuous monitoring and analysis of the EEG signal. To prepare the EEG data for analysis, a 6th-order Butterworth zero-phase filter was applied to the raw data. This filter had a passband frequency range of 1-50 Hz. The purpose of this filtering step was to denoise the EEG signals and remove any artifacts that may have been present.

2.2 Multivariate auto-regressive model

The MVAR model is used to analyse multivariate time series data, such as EEG signals, by representing the relationships between variables, which is applied to convert the denoised EEG data into frequency domain features within the alpha band (8-12 Hz). The algorithm of MVAR model is illustrated in formula (1).

$$X(n) = \sum_{k=1}^{p} A(k) \times X(n-k) + W(n) \tag{1}$$

where $A(k)$ are M $\times$ M coefficient matrix which calculates the linear interaction in lag k from $x_j(n-k)$ to $x_i(n), (i, j = 1, ..., M)$ of MVAR model. The noise is also considered in this formula which $W(n)$ is a vector of Gaussian noise with a covariance matrix Σ. To calculate the coefficient matrix $A(k)$ and covariance matrix Σ, the Yule-Walker equation is used to describe

157 the relationship between two matrices [27]. p is the order of the MVAR model and calculate
158 via the Akaike Information Criterion (AIC) algorithm. The AIC can select the order number
159 fitting effect of the model and avoid the phenomenon of overfitting when the p is too large.
160 The formula of AIC is shown in equation (2).

161
$$AIC(p) = -\ln(\hat{l}) + 2k \tag{2}$$

162 In equation (2), k is the total parameters used for model fitting and $\ln(\hat{l})$ is the maximum
163 likelihood estimations of log likelihood. To convert the EEG data into frequency domain
164 spectrum, the Fourier transform is employed. The transfer matrix of MVAR model $H(f)$, and
165 cross-spectrum matrix $S(f)$ are estimated in equation (3) and (4).

166
$$H(f) = (\sum_{k=0}^{p} -A_k e^{-jk2\pi f})^{-1} \tag{3}$$

167
$$S(f) = H(f) \sum (H^H(f)) \tag{4}$$

168 where $H^H(f)$ is the conjugate transpose of $H(f)$, Σ is the noise covariance matrix. A_k is
169 the parameter of M × M coefficient matrix and the p is the model order.

2.3 Functional brain network analysis
171 The coherence connectivity based MVAR model is applied to construct the functional brain
172 network in the corresponding frequency domain. The algorithm of magnitude-squared
173 coherence between two different channels is shown in equation (5):

174
$$coh_{xy}(f) = \left| \frac{S_{xy}(f)}{\sqrt{S_{xx}(f)S_{yy}(f)}} \right|^2 \tag{5}$$

175 where, the $S_{xx}(f)$ is the power spectrum density of x, the $S_{yy}(f)$ is the power spectrum
176 density of y, and $S_{xy}(f)$ is the cross-spectral power spectrum density between x and y.
177 In the described experiment, to extract more information from the MVAR coherence
178 connectivity matrix, the functional brain network is computed for each frequency range within
179 the alpha band. Specifically, the frequency ranges of 8-9 Hz, 9-10 Hz, 10-11 Hz, and 11-12 Hz
180 are considered. Since the experiment involves EEG data from 16 channels, the resulting matrix
181 has dimensions of 16x16. For instance, the 4-level functional brain network of a subject
182 *'022w1'* in ScZ case is illustrated in Figure. 2.

183
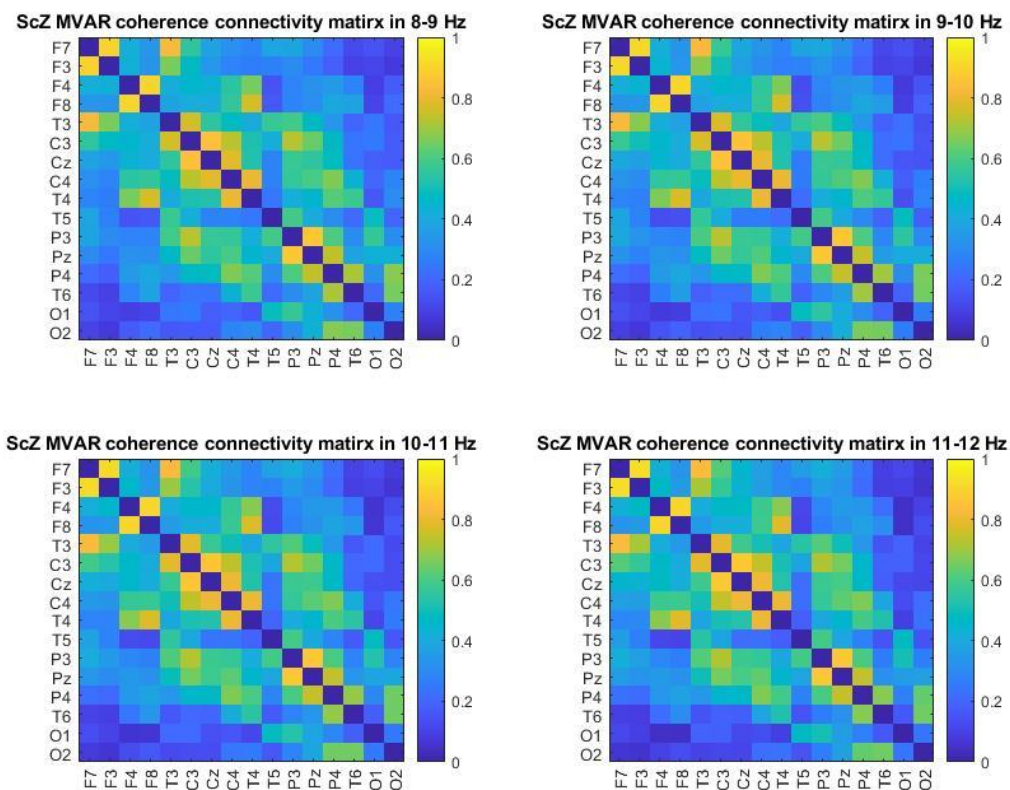
Figure. 2. Functional brain network of subject *'022w'* in ScZ case.

2.4 Classification

After the features of the functional brain network have been extracted from the EEG raw signal, the next task is to classify the features between ScZ patients and HC subjects through machine learning and deep learning methods. In this study, three machine learning methods include SVM, k-NN and decision tree (DT) models, and the proposed 3D-CNN were used to classify the testing data

2.4.1 Leaving one group out training method

By using the leaving one group out method, the experiment aims to assess the generalizability and performance of the model on unseen data. It helps to ensure that the model is not biased or overfitted to a specific group of subjects. Therefore, five models have been established in this study. The details of the 5-group dataset are summarized in Table I.

TABLE I
FIVE-GROUP DATA FOR CLASSIFICATION

	ScZ dataset	HC dataset
Group A	022w, 32w, 219w, 221w, 387-02w, 387-03w, 510-1w, 515w, 642w	s10w, s12w, s43w, s47w, s78w, s85w, s158w, s174w
Group B	33w, 088w, 249w, 276w, 401w, 423w, 517w, 683w, 719w	s18w, s20w, s50w, s94w, s163w, s164w, s176w, s177w
Group C	103w, 113w, 307w, 312w, 429w, 454-1w, 540w, 548w, r229w	s26w, s53w, s55w, s152w, s153w, s165w. s167w, s178w

6

Group D	155w, 156w, 314w, 485w, 508w, 573w, 575w, r416w, s083w	s27w, s31w, s59w, s60w, s154w, s169w, s170w, s179w
Group E	192w, s084-1w, 342w, 382w, 509w, s351w, 585w, 586w, s425w	s42w, s72w, s155w, s157w, s173w, s182w, s196w

198 *2.4.2 Machine learning methods*

199 The Classification Learner Toolbox in MATLAB 2021b is applied in this part. In training
200 progress, 80% of the data is used for training, and the remaining 20% is set aside for validation.
201 The training set is used to train the models, while the validation set is used to evaluate their
202 performance and tune any hyperparameters. The validation accuracy is listed in the Table II

203 TABLE II
204 THE VALIDATION ACCURACY OF SVM, K-NN AND DT

	Test group	SVM	KNN	DT
	Group A	99.52	100.00	98.21
	Group B	100.00	100.00	97.98
Validation	Group C	100.00	100.00	99.41
accuracy (%)	Group D	99.08	100.00	98.33
	Group E	99.73	100.00	99.03
	Mean ± Std	99.67 ± 0.38	100.00 ± 0.00	98.59 ± 0.60

205 In the functional brain network, the matrix is symmetrical and the coherence value between the
206 same node equals 0. To reduce the computational cost, about $(16 \times 16 - 16) / 2 \times 4 = 480$ values
207 of the 4-layer functional brain network matrix are selected as input.

208 *2.4.3 Deep learning method*

209 In functional brain network analysis, the brain is regarded as a large-scale network, which is
210 also known as the brain graph that consists of the nodes and edges. The nodes here are the EEG
211 channel, and the edges are the brain connectivity. CNN is an advanced deep learning method
212 that has been successfully applied in photograph classifications, such as Google-net CNN,
213 VGG-net CNN, and Alex-net CNN. Therefore, the 3D-CNN is designed and employed to
214 classify the brain graph data in this study. The architecture of the 10-layer 3D-CNN is shown
215 in the Figure. 3.

216

217
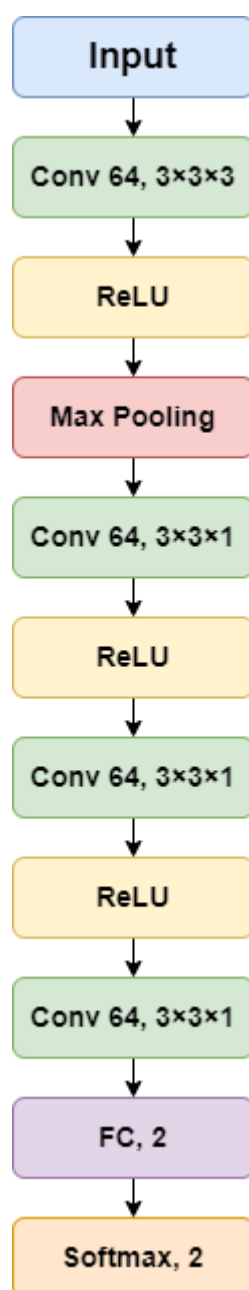
Figure. 3. 10-layer 3D-CNN architecture, '*Conv*' is the convolution layer and '*FC*' is the fully
connected layer.

The designed 3D-CNN model in the experiment consists of four convolution layers, three
ReLU layers, one max pooling layer, and one fully connected layer. The architecture aims to
classify subjects with ScZ and HC subjects. To address overfitting, batch normalization is
applied in the four convolution layers. Batch normalization helps stabilize and normalize the
activations within each mini batch during training, reducing the likelihood of overfitting. The
first convolution layer has a kernel size of 3×3×3 and 64 channels. After this layer, a max
pooling layer is employed to reduce the dimensions of the 3D-image input into 2D-image data.
The subsequent three convolution layers all have a kernel size of 3×3×1 and 64 channels. The
purpose of these layers is to capture relevant features from the input data. A max pooling layer
with a size of 2×2×2 and a stride of 2×2×2 is used to down sample the feature maps and reduce
the computational cost during training. ReLU layers follow each convolution layer. The ReLU

231   activation function introduces non-linearity to the model by setting negative values to zero,
232   allowing the network to learn complex patterns and improve its representational power. Since
233   the experiment focuses on classifying ScZ and HC subjects, the fully connected layer is
234   designed for two-class classification. This layer aggregates the learned features and performs
235   classification based on the extracted information. The last layer of the architecture is a Softmax
236   classifier, which provides the prediction results of the proposed method. The Softmax function
237   assigns probabilities to each class, indicating the model's confidence in its predictions. The
238   details of the input size and output size of each layer are summarized in Table III.

239   TABLE III
240   THE DETAILS OF DEEP LEARNING METHOD ARCHITECTURE

Layer Level	Input Size	Output Size	hyperparameters
-	$16\times16\times4\times1$		
Level 1 (Conv)	$16\times16\times4\times1$	$14\times14\times2\times64$	Kernel size: $3\times3\times3$ Stride: $1\times1\times1$ Channel: 64
Level 2 (ReLU)	$14\times14\times2\times64$	$14\times14\times2\times64$	
Level 3 (Max Pooling)	$14\times14\times2\times64$	$7\times7\times1\times64$	Pooling Size: $2\times2\times2$ Stride: $2\times2\times2$
Level 4 (Conv)	$7\times7\times1\times64$	$5\times5\times1\times64$	Kernel size: $3\times3\times1$ Stride: $1\times1\times1$ Channel: 64
Level 5 (ReLU)	$5\times5\times1\times64$	$5\times5\times1\times64$	
Level 6 (Conv)	$5\times5\times1\times64$	$3\times3\times1\times64$	Kernel size: $3\times3\times1$ Stride: $1\times1\times1$ Channel: 64
Level 7 (ReLU)	$3\times3\times1\times64$	$3\times3\times1\times64$	
Level 8 (Conv)	$3\times3\times1\times64$	$1\times1\times1\times64$	Kernel size: $3\times3\times1$ Stride: $1\times1\times1$ Channel: 64
Level 9 (FC)	$1\times1\times1\times64$	$1\times1\times1\times2$	
Level 10 (Softmax)	$1\times1\times1\times2$		

241   * '*Conv*' is the convolution layer and '*FC*' the fully connected layer.

242   The same validation method with 50 iterations validation frequency is used in the designed 3D-
243   CNN model and achieved 100% validation accuracy using the leaving one group out training
244   method. The optimizer of the proposed deep learning model in MATLAB 2021b is shown in
245   Figure. 4.
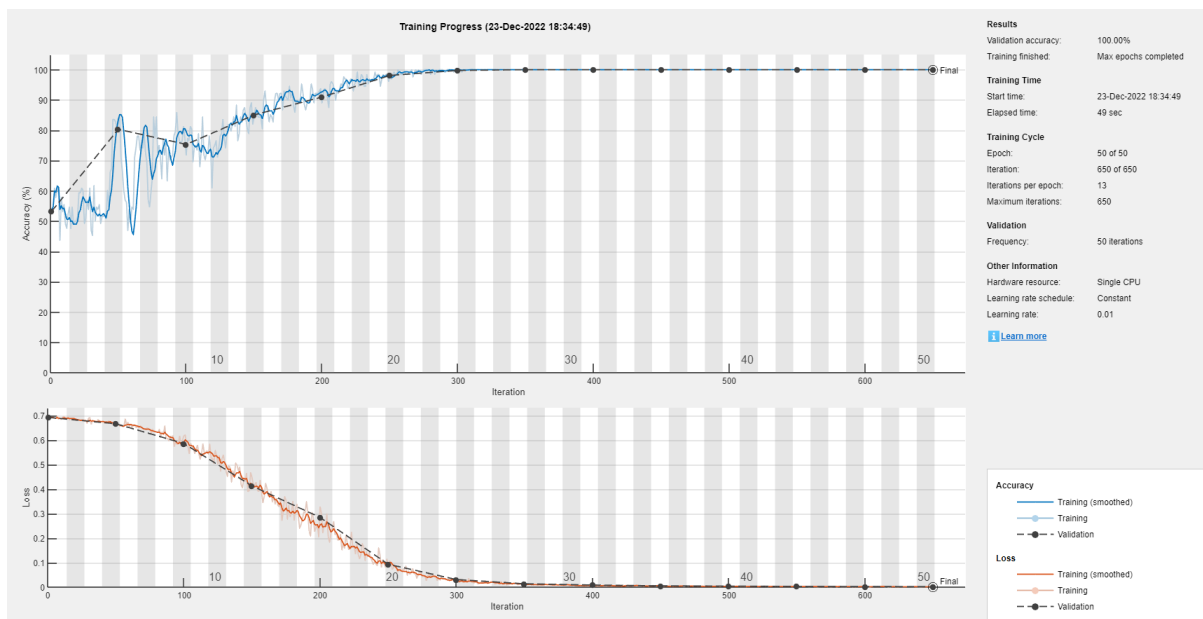
Figure. 4. The optimizer of self-designed 3D-CNN model of testing group A.

3. Results and Comparison

In the evaluation of the proposed method for EEG ScZ detection using the LMSU database, accuracy, sensitivity, and specificity are calculated as performance metrics. Accuracy represents the proportion of correctly classified samples (both true positives and true negatives) out of the total number of samples. Higher accuracy values indicate better performance in classifying ScZ and HC subjects. The formula of accuracy is described in equation (6).

$$Acc = \frac{TP + TN}{TP + TN + FP + FN} \tag{6}$$

where '*TP*', '*TN*', '*FP*', '*FN*' correspond to the true positive, true negative, false positive and false negative.

Sensitivity, also known as true positive rate or recall, measures the proportion of ScZ subjects that are correctly identified as positive by the classification model. It indicates the ability of the method to correctly detect ScZ cases. Higher sensitivity values indicate a lower rate of false negatives, suggesting a better ability to identify true positive ScZ subjects. The algorithm of sensitivity is shown in equation (7).

$$Sen = \frac{TP}{TP + FN} \tag{7}$$

Specificity measures the proportion of HC subjects that are correctly identified as negative by the classification model. It represents the ability of the method to correctly identify HC cases. Higher specificity values indicate a lower rate of false positives, indicating a better ability to correctly identify true negative HC subjects.

$$Spe = \frac{TN}{TN + FP} \tag{8}$$

268 **3.1 Results of the proposed method**
269 Three machine learning methods, SVM, k-NN and DT, and the proposed 3D-CNN are used to
270 detect EEG ScZ functional brain network. From Table IV, the proposed 3D-CNN has achieved
271 the best performance in this study, which reports the results of 98.47 ± 1.47% accuracy, 99.26
272 ± 1.07% sensitivity, and 97.23 ± 3.76% specificity of testing data.

273 TABLE IV
274 THE TEST RESULTS FOR SVM, K-NN, DT AND 3D-CNN MODEL

Results	Test group	SVM	k-NN	DT	3D-CNN
	Group A	89.92	77.22	74.19	98.59
	Group B	84.48	79.23	79.64	98.19
	Group C	79.81	74.80	79.44	96.17
Accuracy (%)	Group D	89.52	74.60	76.01	100.00
	Group E	84.48	80.44	77.22	99.40
	Mean ± Std	85.64 ± 4.18	77.26 ± 2.60	77.30 ± 2.31	**98.47 ± 1.47**
	Group A	86.46	73.21	90.83	97.67
	Group B	76.72	79.52	76.42	100.00
	Group C	76.86	70.54	83.63	100.00
Sensitivity (%)	Group D	86.34	71.16	84.03	100.00
	Group E	81.53	74.59	82.91	98.64
	Mean ± Std	81.58 ± 4.81	73.80 ± 3.58	83.56 ± 5.11	**99.26 ± 1.07**
	Group A	91.24	75.58	45.62	99.07
	Group B	92.63	73.57	78.83	95.85
	Group C	80.52	72.81	65.90	91.24
Specificity (%)	Group D	90.32	70.51	55.76	100.00
	Group E	83.41	83.87	60.37	100.00
	Mean ± Std	87.62 ± 5.33	75.27 ± 5.14	61.30 ± 12.31	**97.23 ± 3.76**

275 According to Table IV, these three machine learning models achieve very high validation
276 result, but they could not overcome the robustness problem. Furthermore, the standard
277 deviation of the proposed method is significantly smaller than the machine learning methods,
278 which implies that every subject can be detected stably through the 3D-CNN model. It also
279 indicates that the proposed 3D-CNN model can be used in the clinical applications.

280 **3.2 Comparison with different complex brain network methods**
281 Based on the MVAR model, five other connectivity algorithms are used to evaluate the
282 proposed method, which includes the directed coherence (DC), directed transform function
283 (DTF), PDC, generalized partial directed coherence (GPDC) and partial coherence (PCO). The
284 details of the comparison are show in Table V.

285 TABLE V
286 THE COMPARISON BETWEEN DIFFERENT CONNECTIVITY METHODS

Connectivity method	Accuracy (%)	Sensitivity (%)	Specificity (%)
DC	74.44 ± 6.78	77.24 ± 12.90	62.67 ± 18.17
DTF	72.06 ± 4.31	71.30 ± 6.87	61.11 ± 5.41
PDC	79.32 ± 6.12	85.37 ± 3.19	63.96 ± 17.44
GPDC	78.87 ± 5.40	90.29 ± 12.93	62.03 ± 23.35

PCO	81.29 ± 10.39	77.63 ± 11.86	80.55 ± 11.99
Proposed method	**98.47 ± 1.47**	**99.26 ± 1.07**	**97.23 ± 3.76**

287 The effective connectivity methods, including DC, DTF, PDC, GPDC algorithm, consider the
288 directionality of brain connectivity, which can determine the causality information between the
289 connectivity. However, it cannot obtain high accuracy detection results in this study as shown
290 in Table V.

291 **3.3 Comparison with different frequency bands**
292 In the experiment, a frequency band selection analysis is performed to optimize computing
293 costs while maintaining the effectiveness of EEG ScZ identification. The MVAR coherence is
294 constructed in different frequency bands, namely δ band (0-4 Hz), θ band (4-8 Hz), α band (8-
295 12 Hz), β-1 band (12-16 Hz), β-2 band (16-20 Hz), β-3 band (20-24 Hz), and β-4 band (24-28
296 Hz). The purpose of this analysis is to identify the brain rhythms within these frequency bands
297 that yield the best results in EEG ScZ identification. The results of this analysis are summarized
298 in Table VI, which provides information on the performance metrics (such as accuracy,
299 sensitivity, and specificity) achieved in each frequency band.

300 TABLE VI
301 THE COMPARISON BETWEEN DIFFERENT FREQUENCY BAND

Frequency band	Accuracy (%)	Sensitivity (%)	Specificity (%)
δ band (0-4 Hz)	85.04 ± 5.30	80.42 ± 6.59	87.37 ± 5.76
θ band (4-8 Hz)	90.20 ± 4.23	85.85 ± 2.60	92.81 ± 8.56
α band (8-12 Hz)	**98.47 ± 1.47**	**99.26 ± 1.07**	**97.23 ± 3.76**
β-1 band (12-16 Hz)	92.39 ± 4.49	91.78 ± 5.46	90.78 ± 5.21
β-2 band (16-20 Hz)	92.42 ± 5.60	92.20 ± 7.49	90.60 ± 5.98
β-3 band (20-24 Hz)	92.82 ± 5.34	92.58 ± 5.92	90.97 ± 8.71
β-4 band (24-28 Hz)	91.17 ± 7.05	87.36 ± 8.76	93.73 ± 7.41

302 According to Table VI, the alpha band brain has been verified as the best frequency band to
303 detect the ScZ EEG signal.

4. Discussion

4.1 Statistical analysis of MVAR coherence connectivity
306 In functional brain network analysis, different brain regions correspond to different functions.
307 Through the statistical analysis of brain connectivity value, the biomarker of abnormal
308 connectivity between the ScZ patients and HC subjects can be found. DMN region is the most
309 significant part of the brain, which is related to the function of sensory, motor executive control
310 and visual components [28]. There are three brain regions in DMN, including LPC, MPC and
311 PCC [11]. In EEG analysis, Brodmann areas (BA) are applied to correspond to the DMN region
312 with the EEG electrodes and the details shown in Table VII [29,30].

313 TABLE VII
314 EEG ELECTRODES IN THE BRODMANN AREAS OF DMN REGIONS [31]

DMN region	Brodmann area	EEG channel
LPC	BA39/40, Right	P4
LPC	BA39/40, Left	P3
MPC	BA08/09, Middle	Cz
MPC	BA08/09, Right	F4

| MPC | BA08/09, Left | F3 |
| PCC | BA07, Middle | Pz |

315 Based on the derived mean value and standard deviation of the whole brain connectivity of the
316 functional brain network, the abnormal connectivities with the major difference mean value ($\geq$
317 0.10) between ScZ subjects and HC subjects are listed in Table VIII.

318 TABLE VIII
319 THE MEAN VALUE OF CONNECTIVITY VALUES

Abnormal connectivity	Connectivity values of ScZ	Connectivity values of HC
T4 - T6	0.496 ± 0.188	0.732 ± 0.134
F3 - F4	0.287 ± 0.136	0.441 ± 0.156
T3 - T5	0.558 ± 0.180	0.710 ± 0.147
Cz - P4	0.421 ± 0.125	0.538 ± 0.169
P4 - Pz	0.502 ± 0.137	0.609 ± 0.164
Cz - Pz	0.548 ± 0.134	0.651 ± 0.167

320 From the statistical analysis results of Table VIII, not only the connectivity of DMN regions
321 but also the connectivity of T4 - T6 and T3 - T5 are the biomarkers of the ScZ disease, which
322 corresponds to the temporal lobe and posterior temporal lobe area in both right and left side. It
323 also indicates that the whole brain connectivity analysis of the functional brain network is
324 necessary.

325 **4.2 Dynamic analysis**
326 In this study, the sliding window technique was used to capture the dynamic changes of ScZ
327 diseases in the EEG data. However, selecting an appropriate window size is crucial as it affects
328 the ability to capture the dynamic properties of ScZ and the detection accuracy of the method.
329 If the window size is chosen to be too large, it may be difficult to capture the underlying
330 dynamic properties of ScZ. Larger window sizes tend to smooth out rapid changes and
331 variations in the data, potentially leading to a loss of important temporal information. This can
332 make it challenging to cluster and analyse the dynamic patterns associated with ScZ accurately.
333 On the other hand, selecting a window size that is too small can lead to decreased detection
334 accuracy. Smaller window sizes might not capture sufficient information about the temporal
335 dynamics of ScZ, and the analysis may be affected by noise or random fluctuations within
336 shorter time intervals. This can result in decreased sensitivity and specificity of the method. As
337 a result, the sliding window size of 3-second, 5-second. 10-second, 30-second and 40-second
338 are evaluated with the proposed method, and the results are shown in the Table IX.

339 TABLE IX
340 DYNAMIC ANALYSIS OF FUNCTIONAL BRAIN NETWORK

Sliding window size	Accuracy (%)	Sensitivity (%)	Specificity (%)
3-second	87.91 ± 7.05	83.56 ± 6.99	90.00 ± 9.53
5-second	89.11 ± 5.59	85.30 ± 5.13	90.66 ± 9.01
10-second	90.20 ± 5.55	86.40 ± 5.78	92.10 ± 7.91
30-second	**98.47 ± 1.47**	**99.26 ± 1.07**	**97.23 ± 3.76**
40-second	90.89 ± 7.12	86.25 ± 8.62	94.56 ± 7.47

341 **4.3 Previous works comparison**
342 Comparisons with the related works in EEG ScZ detection are listed in Table X. In this study,
343 the proposed method receives $98.47 \pm 1.47\%$ accuracy, $99.26 \pm 1.07\%$ sensitivity, and $97.23 \pm$
344 3.76% specificity results in the testing data. Compared with the previous related work, the

345 proposed method can achieve satisfactory detection results using the public LMSU dataset. In
346 addition, the biomarkers of abnormal connectivity in DMN regions, temporal lobe and
347 posterior temporal lobe area in both hemispheres are confirmed in this research.

348 TABLE X
349 COMPARISON OF THE RELATED WORKS IN EEG ScZ DETECTION

Related works	Method	Accuracy (%)	Sensitivity (%)	Specificity (%)
Baygin, M et al (2021) [15]	Collatz pattern technique + k-NN	99.47	99.20	99.80
Akbari, H et al. (2021) [16]	Phase space dynamic features + k-NN	94.80	94.30	95.20
Lillo, E et al. (2022) [17]	CNN	93.00	-	-
Supakar, R et al. (2022) [18]	RNN - LSTM	98.00	98.00	98.00
Sairamya, N.J et al, (2022) [19]	DWT + RLNDip	100	-	-
Hassan, F et al. (2023) [20]	CNN + logistic regression	98.05 ± 1.13	99.00 ± 1.00	97.00 ± 2.00
Gosala, B et al. (2023) [21]	WST + SVM	97.98	98.20	97.72
Our previous work [24]	CMI + 3D-CNN	97.74 ± 1.15	96.91 ± 2.76	98.53 ± 1.97
Proposed method	MVAR coherence + 3D-CNN	98.47 ± 1.47	99.26 ± 1.07	97.23 ± 3.76

350 This EEG based ScZ detection study still has some limitations. Sliding window technique is
351 not an advanced method to cluster the dynamic state of brain activity. In addition, it is difficult
352 to use the statistical analysis of whole brain connectivity to achieve high precision localization
353 of ScZ disease. To overcome these limitations, the dynamic modelling analysis and source
354 model reconstruction research will be the focus in our future research plan.

Conclusion

356 In this study, the researchers propose and implement a functional brain network analysis using
357 the magnitude squared coherence algorithm. The MVAR model is applied in the signal
358 processing stage, with a frequency resolution of 1 Hz. The goal is to explore the dynamic
359 properties of resting-state brain connectivity in ScZ disease. To capture the dynamic nature of
360 the brain connectivity, the sliding window technique is employed which transforms the EEG
361 signal into time-varying data. This allows for the analysis of changes in connectivity patterns
362 over time. In comparing different functional brain methods, the magnitude squared coherence
363 algorithm demonstrates the best performance in EEG ScZ detection. The proposed method
364 achieves impressive results with 98.47% accuracy, 99.26% sensitivity, and 97.23% specificity
365 in evaluation and testing. Additionally, the researchers highlight the effectiveness of the
366 proposed 3D-CNN model, which overcomes the robustness issues observed in other models
367 such as SVM, k-NN, and DT. This suggests that the 3D-CNN model is better suited for EEG
368 ScZ detection. To reduce computational costs, the study identifies the alpha band (8-12 Hz) as
369 the optimal frequency range for EEG ScZ detection. This frequency band is associated with
370 the best performance in accurately classifying ScZ and HC subjects. Furthermore, the research

371 findings highlight the presence of abnormal connectivity in the DMN region and the temporal
372 lobe, as well as the posterior temporal lobe, in both hemispheres of ScZ patients. These regions
373 serve as potential biomarkers for identifying and understanding the neural abnormalities
374 associated with ScZ.

Reference

376 1.   Samsom, J.N. and A.H. Wong, *Schizophrenia and depression co-morbidity: what we have*
377   *learned from animal models.* Frontiers in psychiatry, 2015. **6**: p. 13.
378 2.   Krishnan, P.T., et al., *Schizophrenia detection using MultivariateEmpirical Mode*
379   *Decomposition and entropy measures from multichannel EEG signal.* Biocybernetics and
380   Biomedical Engineering, 2020. **40**(3): p. 1124-1139.
381 3.   Krukow, P., et al., *Abnormalities in hubs location and nodes centrality predict cognitive*
382   *slowing and increased performance variability in first-episode schizophrenia patients.*
383   Scientific Reports, 2019. **9**(1): p. 9594.
384 4.   Pacific, W. and S.A.W. Hasan, *Magnitude and impact.*
385 5.   Craik, A., Y. He, and J.L. Contreras-Vidal, *Deep learning for electroencephalogram (EEG)*
386   *classification tasks: a review.* Journal of neural engineering, 2019. **16**(3): p. 031001.
387 6.   Brown, G.G. and W.K. Thompson, *Functional brain imaging in schizophrenia: selected*
388   *results and methods.* Behavioral neurobiology of schizophrenia and its treatment, 2010: p.
389   181-214.
390 7.   Ho, M.-h.R., et al., *Time–frequency discriminant analysis of MEG signals.* NeuroImage,
391   2008. **40**(1): p. 174-186.
392 8.   Long, Q., et al., *Independent vector analysis for common subspace analysis: Application to*
393   *multi-subject fMRI data yields meaningful subgroups of schizophrenia.* NeuroImage, 2020.
394   **216**: p. 116872.
395 9.   Fu, Z., et al., *Dynamic state with covarying brain activity-connectivity: On the*
396   *pathophysiology of schizophrenia.* Neuroimage, 2021. **224**: p. 117385.
397 10.   Zhang, G., et al., *Detecting abnormal connectivity in schizophrenia via a joint directed*
398   *acyclic graph estimation model.* Neuroimage, 2022. **260**: p. 119451.
399 11.   Raichle, M.E., et al., *A default mode of brain function.* Proceedings of the National Academy
400   of Sciences, 2001. **98**(2): p. 676-682.
401 12.   Zhang, S., et al., *Abnormal default-mode network homogeneity and its correlations with*
402   *neurocognitive deficits in drug-naive first-episode adolescent-onset schizophrenia.*
403   Schizophrenia Research, 2020. **215**: p. 140-147.
404 13.   Fan, J., et al., *Resting-state default mode network related functional connectivity is associated*
405   *with sustained attention deficits in schizophrenia and obsessive-compulsive disorder.*
406   Frontiers in behavioral neuroscience, 2018. **12**: p. 319.
407 14.   Phang, C.-R., et al., *A multi-domain connectome convolutional neural network for identifying*
408   *schizophrenia from EEG connectivity patterns.* IEEE journal of biomedical and health
409   informatics, 2019. **24**(5): p. 1333-1343.
410 15.   Baygin, M., et al., *Automated accurate schizophrenia detection system using Collatz pattern*
411   *technique with EEG signals.* Biomedical Signal Processing and Control, 2021. **70**: p. 102936.
412 16.   Akbari, H., et al., *Schizophrenia recognition based on the phase space dynamic of EEG*
413   *signals and graphical features.* Biomedical Signal Processing and Control, 2021. **69**: p.
414   102917.
415 17.   Lillo, E., M. Mora, and B. Lucero, *Automated diagnosis of schizophrenia using EEG*
416   *microstates and Deep Convolutional Neural Network.* Expert Systems with Applications,
417   2022. **209**: p. 118236.
418 18.   Supakar, R., P. Satvaya, and P. Chakrabarti, *A deep learning based model using RNN-LSTM*
419   *for the Detection of Schizophrenia from EEG data.* Computers in Biology and Medicine,
420   2022. **151**: p. 106225.

421 19. Sairamya, N., M. Subathra, and S.T. George, *Automatic identification of schizophrenia using*
422   *EEG signals based on discrete wavelet transform and RLNDiP technique with ANN.* Expert
423   Systems with Applications, 2022. **192**: p. 116230.
424 20. Hassan, F., S.F. Hussain, and S.M. Qaisar, *Fusion of multivariate EEG signals for*
425   *schizophrenia detection using CNN and machine learning techniques.* Information Fusion,
426   2023. **92**: p. 466-478.
427 21. Gosala, B., et al., *Wavelet transforms for feature engineering in EEG data processing: An*
428   *application on Schizophrenia.* Biomedical Signal Processing and Control, 2023. **85**: p.
429   104811.
430 22. Wang, J., et al., *Discrimination of auditory verbal hallucination in schizophrenia based on*
431   *EEG brain networks.* Psychiatry Research: Neuroimaging, 2023. **331**: p. 111632.
432 23. Prieto-Alcántara, M., et al., *Alpha and gamma EEG coherence during on-task and mind*
433   *wandering states in schizophrenia.* Clinical Neurophysiology, 2023. **146**: p. 21-29.
434 24. Shen, M., et al., *Automatic identification of schizophrenia based on EEG signals using*
435   *dynamic functional connectivity analysis and 3D convolutional neural network.* Computers in
436   Biology and Medicine, 2023: p. 107022.
437 25. Gorbachevskaya, N. and S. Borisov, *EEG data of healthy adolescents and adolescents with*
438   *symptoms of schizophrenia.* 2002.
439 26. Borisov, S., et al., *Analysis of EEG structural synchrony in adolescents with schizophrenic*
440   *disorders.* Human Physiology, 2005. **31**(3): p. 255-261.
441 27. Seppänen, J.M., et al. *Analysis of electromechanical modes using multichannel Yule-Walker*
442   *estimation of a multivariate autoregressive model.* in *IEEE PES ISGT Europe 2013.* 2013.
443   IEEE.
444 28. Seitzman, B.A., et al., *The state of resting state networks.* Topics in magnetic resonance
445   imaging: TMRI, 2019. **28**(4): p. 189.
446 29. Kaiser, D.A., *Cortical cartography.* Biofeedback, 2010. **38**(1): p. 9-12.
447 30. Koessler, L., et al., *Automated cortical projection of EEG sensors: anatomical correlation via*
448   *the international 10–10 system.* Neuroimage, 2009. **46**(1): p. 64-72.
449 31. Khan, D.M., et al., *Effective connectivity in default mode network for alcoholism diagnosis.*
450   IEEE Transactions on Neural Systems and Rehabilitation Engineering, 2021. **29**: p. 796-808.

Declaration of interests

☒The authors declare that they have no known competing financial interests or personal relationships that could have appeared to influence the work reported in this paper.

☐The authors declare the following financial interests/personal relationships which may be considered as potential competing interests:

CHAPTER 9: CONCLUSIONS

9.1 Thesis summary

This study focuses on real-time EEG epilepsy seizure detection and brain connectivity analysis in complex brain disorders. The background and research problems are provided firstly, along with a comprehensive literature review and summaries. Building upon the existing knowledge and research, the thesis proposed and designed three experiments for EEG seizure detection and three experiments for brain connectivity analysis.

9.2 Conclusion

In a comprehensive analysis of recent advancements in EEG signal processing and classification, six seminal papers have been dissected to delineate key contributions to the field.

In EEG real-time seizure detection research, this thesis provides advanced methods for epilepsy seizure detection, emphasizing the synergy of diverse signal transformation techniques like DWT TQWT and STFT with cutting-edge neural network models to achieve remarkable accuracy in real-time applications. The evolution of real-time epilepsy seizure detection, rooted in EEG signals, signifies a transformative phase in neurocomputational research. Initiating with the integration of the DWT and traditional machine learning, the landscape was introduced to the profound potential of signal decomposition, shedding light on the intricate nature of EEG data. Building upon this foundation, subsequent research endeavoured to combine the adaptability of the TQWT with the architectural complexities of CNNs. This synthesis unearthed nuanced perspectives on EEG signal processing, revealing deeper layers of information. In the zenith of this progression, a groundbreakingly study emerged, harnessing the capabilities of the STFT with the advanced Google-Net CNN. The remarkable accuracy benchmarks set by this research not only attest to the methodology's efficacy but also forecast the expansive future of neural networks in EEG interpretation. In essence, this thesis chronicles a transformative journey, intertwining computational advancements with neurological insights, promising a new epoch in epilepsy management and enhanced patient care. Future avenues beckon the exploration and refinement of these methodologies, adapting them for newer challenges, and ensuring their widespread application in clinical scenarios.

In EEG brain connectivity analysis, this thesis offers invaluable insights into the realm of identifying distinct neurological conditions, particularly alcoholism and ScZ. The study identified markers of alcoholism using a meld of whole brain connectivity analysis with CNNs on EEG signals, shedding light on subtle neural deviations triggered by alcohol consumption. Its approach not only improves detection rates but also paves the way for timely therapeutic interventions. In addition, the research of this thesis journeyed into the realm of ScZ, employing a combination of dynamic functional connectivity analysis and 3D convolutional neural networks. It emphasized the potential of time-resolved connectivity patterns in diagnosing ScZ, illustrating the disorder's neural footprints with impressive accuracy. Another research also focused on ScZ but diverged by utilizing a functional brain network approach from EEG signals. Harnessing the MVAR and magnitude squared coherence algorithm, and juxtaposing it with 3D-CNN, this study showcased a comprehensive, efficient, and cost-effective methodology for ScZ detection, revealing potential neural biomarkers. Collectively, the research of this thesis underscores the transformative potential of marrying advanced neural network models with EEG-derived data in understanding and diagnosing neural disorders.

9.3   Future work

This thesis explores the areas of seizure detection and EEG connectivity analysis in alcoholism and ScZ. Despite these attempts, there is still room for further improvement and advancements.

In EEG seizure analysis, the works of this thesis is focusing on the seizure onset detection. The ability to predict seizures in advance can greatly benefit patients by providing them with timely warnings and opportunities for intervention. The use of portable EEG devices and brainwave monitors can enhance the clinical applicability of seizure prediction algorithms, allowing for real-time monitoring and intervention.

In EEG connectivity analysis, achieving high precision localization of complex brain disorders using whole brain connectivity statistics can be challenging. Future research can focus on source model reconstruction techniques to improve localization accuracy. These techniques involve mapping the EEG data to specific brain regions or sources to better understand the spatial distribution of abnormalities associated with complex brain disorders. Dynamic modelling approaches should be developed to

capture the temporal dynamics of brain activity, and allow more comprehensive understanding of the dynamic states and transitions within the brain.

REFERENCES

[1]   Shen, M., et al., An EEG based real-time epilepsy seizure detection approach using discrete wavelet transform and machine learning methods. Biomedical Signal Processing and Control, 2022. 77: p. 103820.

[2]   Shen, M., et al., Real-time epilepsy seizure detection based on EEG using tunable-Q wavelet transform and convolutional neural network. Biomedical Signal Processing and Control, 2023. 82: p. 104566.

[3]   Shen, M., et al., Detection of alcoholic EEG signals based on whole brain connectivity and convolution neural networks. Biomedical Signal Processing and Control, 2023. 79: p. 104242.

[4]   Shen, M., et al., Automatic identification of schizophrenia based on EEG signals using dynamic functional connectivity analysis and 3D convolutional neural network. Computers in Biology and Medicine, 2023: p. 107022.

[5]   Xinghua, T., et al., The clinical value of long-term electroencephalogram (EEG) in seizure-free populations: implications from a cross-sectional study. BMC neurology, 2020. 20(1): p. 1-7.

[6]   López-Caneda, E., et al., The brain of binge drinkers at rest: alterations in theta and beta oscillations in first-year college students with a binge drinking pattern. Frontiers in behavioral neuroscience, 2017: p. 168.

[7]   Perrottelli, A., et al., EEG-based measures in at-risk mental state and early stages of schizophrenia: a systematic review. Frontiers in psychiatry, 2021. 12: p. 653642.

[8]   Niedermeyer, E. and F.L. da Silva, Electroencephalography: basic principles, clinical applications, and related fields. 2005: Lippincott Williams & Wilkins.

[9]   Buzsaki, G. and A. Draguhn, Neuronal oscillations in cortical networks. science, 2004. 304(5679): p. 1926-1929.

[10]   Başar, E., et al., Gamma, alpha, delta, and theta oscillations govern cognitive processes. International journal of psychophysiology, 2001. 39(2-3): p. 241-248.

[11]   Steriade, M. and R.W. McCarley, Synchronized brain oscillations leading to neuronal plasticity during waking and sleep states. Brain control of wakefulness and sleep, 2005: p. 255-344.

[12]   Cohen, M.X., Analyzing neural time series data: theory and practice. 2014: MIT press.

[13]   Zandi, A.S., et al., Automated real-time epileptic seizure detection in scalp EEG recordings using an algorithm based on wavelet packet transform. IEEE Transactions on Biomedical Engineering, 2010. 57(7): p. 1639-1651.

[14]   Vidyaratne, L.S. and K.M. Iftekharuddin, Real-time epileptic seizure detection using EEG. IEEE Transactions on Neural Systems and Rehabilitation Engineering, 2017. 25(11): p. 2146-2156.

[15]   Kanmounye, U.S., et al., The World health organization's intersectoral global action plan on epilepsy and other neurological disorders 2022-2031. Neurosurgery, 2022. 90(6): p. e201-e203.

[16]   Milligan, T.A., Epilepsy: a clinical overview. The American Journal of Medicine, 2021. 134(7): p. 840-847.

[17]   Wu, J., T. Zhou, and T. Li, Detecting epileptic seizures in EEG signals with complementary ensemble empirical mode decomposition and extreme gradient boosting. Entropy, 2020. 22(2): p. 140.

[18]   Nielsen, S.F., et al., Whole-brain exploratory analysis of functional task response following erythropoietin treatment in mood disorders: a supervised machine learning approach. Frontiers in Neuroscience, 2019. 13: p. 1246.

[19]   Kurth, F., et al., A link between the systems: functional differentiation and integration within the human insula revealed by meta-analysis. Brain Structure and Function, 2010. 214: p. 519-534.

[20]   Pessoa, L., Understanding brain networks and brain organization. Physics of life reviews, 2014. 11(3): p. 400-435.

[21]   Stanley, M.L., et al., Defining nodes in complex brain networks. Frontiers in computational neuroscience, 2013. 7: p. 169.

[22]   Raichle, M.E., et al., A default mode of brain function. Proceedings of the national academy of sciences, 2001. 98(2): p. 676-682.

[23]   Park, Y.S., et al. Early detection of human epileptic seizures based on intracortical local field potentials. in 2013 6th International IEEE/EMBS Conference on Neural Engineering (NER). 2013. IEEE.

[24]   Chiang, S., et al., Seizure detection devices and health-related quality of life: a patient-and caregiver-centered evaluation. Epilepsy & Behavior, 2020. 105: p. 106963.

[25]   Stacey, W.C. and B. Litt, Technology insight: neuroengineering and epilepsy—designing devices for seizure control. Nature clinical practice Neurology, 2008. 4(4): p. 190-201.

[26]   Jurado-Barba, R., et al., Neuropsychophysiological measures of alcohol dependence: Can we use EEG in the clinical assessment? Frontiers in Psychiatry, 2020. 11: p. 676.

[27]   Di Lorenzo, G., et al., Altered resting-state EEG source functional connectivity in schizophrenia: the effect of illness duration. Frontiers in human neuroscience, 2015. 9: p. 234.

[28]   Kamarajan, C., et al., Random forest classification of alcohol use disorder using EEG source functional connectivity, neuropsychological functioning, and impulsivity measures. Behavioral Sciences, 2020. 10(3): p. 62.

[29]   Liu, W., et al., Functional connectivity combined with a machine learning algorithm can classify high-risk first-degree relatives of patients with schizophrenia and identify correlates of cognitive impairments. Frontiers in Neuroscience, 2020. 14: p. 577568.

[30]   Nutt, D., et al., Alcohol and the Brain. Nutrients, 2021. 13(11): p. 3938.

[31]   B Nejad, A., et al., Brain connectivity studies in schizophrenia: unravelling the effects of antipsychotics. Current neuropharmacology, 2012. 10(3): p. 219-230.

[32]   Tuncer, E. and E.D. Bolat, Channel based epilepsy seizure type detection from electroencephalography (EEG) signals with machine learning techniques. Biocybernetics and Biomedical Engineering, 2022. 42(2): p. 575-595.

[33]   Wijayanto, I., et al., Epileptic seizure detection on a compressed EEG signal using energy measurement. Biomedical Signal Processing and Control, 2023. 85: p. 104872.

[34]   Ghazali, S.M., et al., Modified binary salp swarm algorithm in EEG signal classification for epilepsy seizure detection. Biomedical Signal Processing and Control, 2022. 78: p. 103858.

[35]   Chavan, P.A. and S. Desai, Effective Epileptic Seizure Detection by Classifying Focal and Non-focal EEG Signals using Human Learning Optimization-based Hidden Markov Model. Biomedical Signal Processing and Control, 2023. 83: p. 104682.

[36]   Wijayanto, I., R. Hartanto, and H.A. Nugroho, Comparison of empirical mode decomposition and coarse-grained procedure for detecting pre-ictal and ictal condition

in electroencephalography signal. Informatics in Medicine Unlocked, 2020. 19: p. 100325.

[37]   Patidar, S., et al., An integrated alcoholic index using tunable-Q wavelet transform based features extracted from EEG signals for diagnosis of alcoholism. Applied Soft Computing, 2017. 50: p. 71-78.

[38]   Sairamya, N., M. Subathra, and S.T. George, Automatic identification of schizophrenia using EEG signals based on discrete wavelet transform and RLNDiP technique with ANN. Expert Systems with Applications, 2022. 192: p. 116230.

[39]   Oweis, R.J. and E.W. Abdulhay, Seizure classification in EEG signals utilizing Hilbert-Huang transform. Biomedical engineering online, 2011. 10(1): p. 1-15.

[40]   Hu, W., et al., Mean amplitude spectrum based epileptic state classification for seizure prediction using convolutional neural networks. Journal of Ambient Intelligence and Humanized Computing, 2019: p. 1-11.

[41]   Baser, O., et al., Automatic detection of the spike-and-wave discharges in absence epilepsy for humans and rats using deep learning. Biomedical Signal Processing and Control, 2022. 76: p. 103726.

[42]   Shri, T.P. and N. Sriraam, Spectral entropy feature subset selection using SEPCOR to detect alcoholic impact on gamma sub band visual event related potentials of multichannel electroencephalograms (EEG). Applied Soft Computing, 2016. 46: p. 441-451.

[43]   Iglesias-Tejedor, M., et al., Relation between EEG resting-state power and modulation of P300 task-related activity in theta band in schizophrenia. Progress in Neuro-Psychopharmacology and Biological Psychiatry, 2022. 116: p. 110541.

[44]   Shayeste, H. and B.M. Asl, Automatic seizure detection based on Gray Level Co-occurrence Matrix of STFT imaged-EEG. Biomedical Signal Processing and Control, 2023. 79: p. 104109.

[45]   Amiri, M., H. Aghaeinia, and H.R. Amindavar, Automatic epileptic seizure detection in EEG signals using sparse common spatial pattern and adaptive short-time Fourier transform-based synchrosqueezing transform. Biomedical Signal Processing and Control, 2023. 79: p. 104022.

[46]   Bajaj, V., et al., A hybrid method based on time–frequency images for classification of alcohol and control EEG signals. Neural Computing and Applications, 2017. 28(12): p. 3717-3723.

[47]   Buriro, A.B., et al., Classification of alcoholic EEG signals using wavelet scattering transform-based features. Computers in biology and medicine, 2021. 139: p. 104969.

[48]   Gosala, B., et al., Wavelet transforms for feature engineering in EEG data processing: An application on Schizophrenia. Biomedical Signal Processing and Control, 2023. 85: p. 104811.

[49]   Smit, D.J., et al., Heritability of "small-world" networks in the brain: A graph theoretical analysis of resting-state EEG functional connectivity. Human brain mapping, 2008. 29(12): p. 1368-1378.

[50]   Mumtaz, W., et al., An EEG-based machine learning method to screen alcohol use disorder. Cognitive neurodynamics, 2017. 11(2): p. 161-171.

[51]   Gökşen, N. and S. Arıca, A simple approach to detect alcoholics using electroencephalographic signals, in EMBEC & NBC 2017. 2017, Springer. p. 1101-1104.

[52]   Pain, S., et al., Detection of alcoholism by combining EEG local activations with brain connectivity features and Graph Neural Network. Biomedical Signal Processing and Control, 2023. 85: p. 104851.

[53]   Wang, J., et al., Discrimination of auditory verbal hallucination in schizophrenia based on EEG brain networks. Psychiatry Research: Neuroimaging, 2023. 331: p. 111632.

[54]   Prieto-Alcántara, M., et al., Alpha and gamma EEG coherence during on-task and mind wandering states in schizophrenia. Clinical Neurophysiology, 2023. 146: p. 21-29.

[55]   Adamczyk, P., M. Wyczesany, and A. Daren, Dynamics of impaired humour processing in schizophrenia–An EEG effective connectivity study. Schizophrenia Research, 2019. 209: p. 113-128.

[56]   Khan, D.M., et al., Effective Connectivity in Default Mode Network for Alcoholism Diagnosis. IEEE Transactions on Neural Systems and Rehabilitation Engineering, 2021. 29: p. 796-808.

[57]   Zhao, Z., et al., Classification of schizophrenia by combination of brain effective and functional connectivity. Frontiers in Neuroscience, 2021. 15: p. 651439.

[58]   Phang, C.-R., et al., A multi-domain connectome convolutional neural network for identifying schizophrenia from EEG connectivity patterns. IEEE journal of biomedical and health informatics, 2019. 24(5): p. 1333-1343.

[59]   Rubinov, M. and O. Sporns, Complex network measures of brain connectivity: uses and interpretations. Neuroimage, 2010. 52(3): p. 1059-1069.

[60]   Sadiq, M.T., et al., Alcoholic EEG signals recognition based on phase space dynamic and geometrical features. Chaos, Solitons & Fractals, 2022. 158: p. 112036.

[61]   Kim, J.-Y., H.S. Lee, and S.-H. Lee, EEG source network for the diagnosis of schizophrenia and the identification of subtypes based on symptom severity—A machine learning approach. Journal of Clinical Medicine, 2020. 9(12): p. 3934.

[62]   Samiee, K., et al., Long-term epileptic EEG classification via 2D mapping and textural features. Expert Systems with Applications, 2015. 42(20): p. 7175-7185.

[63]   Zarei, A. and B.M. Asl, Automatic seizure detection using orthogonal matching pursuit, discrete wavelet transform, and entropy based features of EEG signals. Computers in Biology and Medicine, 2021. 131: p. 104250.

[64]   Li, C., et al., Seizure onset detection using empirical mode decomposition and common spatial pattern. IEEE Transactions on Neural Systems and Rehabilitation Engineering, 2021. 29: p. 458-467.

[65]   Omidvar, M., A. Zahedi, and H. Bakhshi, EEG signal processing for epilepsy seizure detection using 5-level Db4 discrete wavelet transform, GA-based feature selection and ANN/SVM classifiers. Journal of Ambient Intelligence and Humanized Computing, 2021: p. 1-9.

[66]   Donos, C., M. Dümpelmann, and A. Schulze-Bonhage, Early seizure detection algorithm based on intracranial EEG and random forest classification. International journal of neural systems, 2015. 25(05): p. 1550023.

[67]   Agarwal, S. and M. Zubair, Classification of Alcoholic and Non-Alcoholic EEG Signals Based on Sliding-SSA and Independent Component Analysis. IEEE Sensors Journal, 2021. 21(23): p. 26198-26206.

[68]   de Miras, J.R., et al., Schizophrenia classification using machine learning on resting state EEG signal. Biomedical Signal Processing and Control, 2023. 79: p. 104233.

[69]   Gao, Y., et al., Deep convolutional neural network-based epileptic electroencephalogram (EEG) signal classification. Frontiers in neurology, 2020. 11: p. 375.

[70]   Cao, X., et al., Automatic seizure classification based on domain-invariant deep representation of EEG. Frontiers in Neuroscience, 2021: p. 1313.

[71]   Wang, X., et al., One dimensional convolutional neural networks for seizure onset detection using long-term scalp and intracranial EEG. Neurocomputing, 2021. 459: p. 212-222.

[72]   Mukhtar, H., S.M. Qaisar, and A. Zaguia, Deep convolutional neural network regularization for alcoholism detection using EEG signals. Sensors, 2021. 21(16): p. 5456.

[73]   Lillo, E., M. Mora, and B. Lucero, Automated diagnosis of schizophrenia using EEG microstates and Deep Convolutional Neural Network. Expert Systems with Applications, 2022. 209: p. 118236.

[74]   Supakar, R., P. Satvaya, and P. Chakrabarti, A deep learning based model using RNN-LSTM for the Detection of Schizophrenia from EEG data. Computers in Biology and Medicine, 2022. 151: p. 106225.

[75]   Hassan, F., S.F. Hussain, and S.M. Qaisar, Fusion of multivariate EEG signals for schizophrenia detection using CNN and machine learning techniques. Information Fusion, 2023. 92: p. 466-478.

[76]   Andrzejak, R.G., et al., Indications of nonlinear deterministic and finite-dimensional structures in time series of brain electrical activity: Dependence on recording region and brain state. Physical Review E, 2001. 64(6): p. 061907.

[77]   Herwig, U., P. Satrapi, and C. Schönfeldt-Lecuona, Using the international 10-20 EEG system for positioning of transcranial magnetic stimulation. Brain topography, 2003. 16: p. 95-99.

[78]   Goldberger, A.L., et al., PhysioBank, PhysioToolkit, and PhysioNet: components of a new research resource for complex physiologic signals. circulation, 2000. 101(23): p. e215-e220.

[79]   Moctezuma, L.A. and M. Molinas, EEG channel-selection method for epileptic-seizure classification based on multi-objective optimization. Frontiers in neuroscience, 2020. 14: p. 593.

[80]   Bache, K. and M. Lichman, UCI Machine Learning Repository. University of California, School of Information and Computer Science, Irvine, CA (2013). 2017.

[81]   Abenna, S., M. Nahid, and H. Bouyghf, Alcohol use disorders automatic detection based BCI systems: a novel EEG classification based on machine learning and optimization algorithms. International Journal of Information Science and Technology, 2022. 6(1): p. 14-25.

[82]   Gorbachevskaya, N. and S. Borisov, EEG data of healthy adolescents and adolescents with symptoms of schizophrenia. 2002.

[83]   Borisov, S., et al., Analysis of EEG structural synchrony in adolescents with schizophrenic disorders. Human Physiology, 2005. 31(3): p. 255-261.

[84]   Gorbachevskaya, K. and S. Borisov, Eeg of healthy adolescents and adolescents with symptoms of schizophrenia. 2019.

[85]   Abdelhameed, A. and M. Bayoumi, A deep learning approach for automatic seizure detection in children with epilepsy. Frontiers in Computational Neuroscience, 2021. 15: p. 29.

[86]   Alharthi, M.K., et al., Epileptic Disorder Detection of Seizures Using EEG Signals. Sensors, 2022. 22(17): p. 6592.

[87]   Jiang, L., et al., Seizure detection algorithm based on improved functional brain network structure feature extraction. Biomedical Signal Processing and Control, 2023. 79: p. 104053.

[88]   Malar, E. and M. Gauthaam, Wavelet analysis of EEG for the identification of alcoholics using probabilistic classifiers and neural networks. International Journal of Intelligence and Sustainable Computing, 2020. 1(1): p. 3-18.

[89]   Farsi, L., et al., Classification of alcoholic EEG signals using a deep learning method. IEEE Sensors Journal, 2020. 21(3): p. 3552-3560.

[90]   Kumari, N., S. Anwar, and V. Bhattacharjee, A deep learning-based approach for accurate diagnosis of alcohol usage severity using eeg signals. IETE Journal of Research, 2022: p. 1-15.

[91]   Li, H. and L. Wu, EEG Classification of Normal and Alcoholic by Deep Learning. Brain Sciences, 2022. 12(6): p. 778.

[92]   Baygin, M., et al., Automated accurate schizophrenia detection system using Collatz pattern technique with EEG signals. Biomedical Signal Processing and Control, 2021. 70: p. 102936.

[93]   Akbari, H., et al., Schizophrenia recognition based on the phase space dynamic of EEG signals and graphical features. Biomedical Signal Processing and Control, 2021. 69: p. 102917.